



UFBA

UNIVERSIDADE FEDERAL DA BAHIA
ESCOLA POLITÉCNICA
PROGRAMA DE PÓS GRADUAÇÃO EM
ENGENHARIA INDUSTRIAL - PEI

DOUTORADO EM ENGENHARIA INDUSTRIAL

ANDRÉ LUIZ SANTOS SÃO PEDRO

Supercritical fluid technology for development of solid
lipid particles entrapping curcumin



SALVADOR
2016



UNIVERSIDADE FEDERAL DA BAHIA
ESCOLA POLITÉCNICA
PROGRAMA DE PÓS-GRADUAÇÃO EM **ENGENHARIA**
INDUSTRIAL



**Supercritical fluid technology for development of solid
lipid particles entrapping curcumin**

by

André Luiz Santos São Pedro

Salvador, 2016

André Luiz Santos São Pedro

Supercritical fluid technology for development of solid lipid particles entrapping curcumin

Thesis presented to the Industrial Engineering Post-Graduation Program in partial fulfillment of the requirements for the degree of Doctor of Philosophy in Industrial Engineering, under supervision of Prof. Dr. Elaine C. de M. Cabral Albuquerque, Prof. Dr. Silvio A. B. Vieira de Melo, with co-supervision of Prof. Dr. Alberto Bertucco during sandwich PhD period and contribution of Prof. Dr. Rosana Lopes Fialho and Prof. Dr. Cristiane Flora Villareal.

Salvador, 2016

Modelo de ficha catalográfica fornecido pelo Sistema Universitário de Bibliotecas da UFBA para ser confeccionada pelo autor

Sao Pedro, André Luiz Santos
Supercritical fluid technology for development of
solid lipid particles entrapping curcumin / André Luiz
Santos Sao Pedro. -- Salvador, 2016.
102 f. : il

Orientadora: Elaine Christine de Magalhães Cabral
Albuquerque.

Coorientador: Silvio Alexandre Beisl Vieira de
Melo.

Tese (Doutorado - Programa de Pós-Graduação em
Engenharia Industrial) -- Universidade Federal da
Bahia, Escola Politécnica, 2016.

1. Nanopartículas Lipídicas Sólidas. 2. Micropartículas
Lipídicas Sólidas. 3. Fluido Supercrítico. 4. Particles
from Gas Saturated Solutions (PGSS). 5. Cúrcuma. I.
Albuquerque, Elaine Christine de Magalhães Cabral. II.
de Melo, Silvio Alexandre Beisl Vieira . III. Título.

SUPERCRITICAL FLUID TECHNOLOGY FOR DEVELOPMENT OF SOLID LIPID PARTICLES ENTRAPPING CURCUMIN

André Luiz Santos São Pedro

Tese submetida ao corpo docente do Programa de Pós Graduação em Engenharia Industrial da Escola Politécnica da Universidade Federal da Bahia – UFBA, como parte dos requisitos necessários para obtenção do grau de doutor em Engenharia Industrial.

Examinada por:

Prof. Dr. Miguel Angel Iglesias Duro



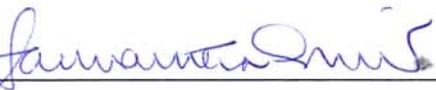
Doutor em Simulación y Control de Procesos Químicos pela Universidad de Vigo – Espanha
Universidade Federal da Bahia – UFBA - Escola Politécnica

Profa. Dra. Cristiane Flora Villarreal



Doutora em Farmacologia pela Universidade de São Paulo - Brasil
Universidade Federal da Bahia – UFBA – Faculdade de Farmácia

Profa. Dra. Samantha Cristina de Pinho



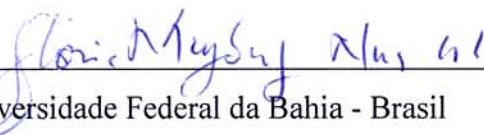
Doutora em Engenharia Hidráulica e Saneamento pela Universidade de São Paulo - Brasil
Universidade de São Paulo - USP – Faculdade de Zootecnia e Engenharia de Alimentos

Prof. Dr. Paulo de Tarso Vieira e Rosa



Doutor em Engenharia Química pela Universidade Estadual de Campinas - Brasil
Universidade Estadual de Campinas – Unicamp – Instituto de Química

Profa. Dra. Gloria Meyberg Nunes Costa



Doutora em Engenharia Industrial pela Universidade Federal da Bahia - Brasil
Universidade Federal da Bahia – UFBA – Escola Politécnica

Salvador
2016

I dedicate this work to my beloved and one of a kind mum
Rute Maria Santos São Pedro (*in memoriam*)

"Just because someone stumbles and loses their path, doesn't
mean they're lost forever."

(Prof Charles Francis Xavier)

"The glory of friendship is not the outstretched hand, not the
kindly smile, nor the joy of companionship; it is the spiritual
inspiration that comes to one when you discover that someone
else believes in you and is willing to trust you with a
friendship."

(Ralph Waldo Emerson)

Acknowledgments

During the course of this work there were so many changes and ups and downs on its own conception, as well as on its execution. To walk through a path like this without taking shortcuts or being favored in any sense demands a lot of faith, effort and mainly a bunch of help. So, gratitude is the fairest way to follow.

Firstly I dedicate all moments of resilience, all strength to stand, every little push, every single insight on the construction of this thesis to the All-love Almighty God.

Certainly I could not get at this point without the wisdom, amity and endless love of my sisters and brothers lent by God Laisse Evangelista, Suzana Moura, Lusiane Bahia, Danilo dos Anjos, Caroline Moura, Lucas Ramos, Silvia Cruvinel, Viviane Guimarães, Viviane Arrais and Berthier Alves.

I cannot thank enough to Islane Espírito Santo, Cinara Vasconcelos, Cassia Detoni, Tamara Angelo, Alice Kiperstok, Ludmila Chaves, Milena Lima, Maiana Pitombo, Paula Becerra, Shana Menezes and Fernanda Magalhães. You not only lighted up my scientific path, but also, made me a greater man.

I could never forget my beloved "awesome" worldwide fellows Maria Grazia Tremo, Jacopo Sacquegno, Gianluca Tornese, Mattia Marini, Alice Schirone, Moritz Pflutschinger, Merili Luuk, Enric Luzán, Hannah Bridle, Amaia Goienetxea, Kaisu Halonen, Belen del Rio, Asia Firek and Fabian Selamadam who made me get confidence to believe in myself to face the unknown and not fear the struggle, and the art of partying hard.

The old continent was very generous to me. To keep myself together, Federica Catena, Giovanni Rigon, Alberto Bortolami, Alessandro Simonato and Laura Decqual became true soulmates and confidants. Thanks to Sebastian Willmitzer and Metin Karaylan for support and friendship.

This thesis definitely only could come to an end thanks to dedication, patience and effort of outstand co-workers-turned good friends. I am in great debit with my hardworker intern Stefania dalla Villa, the always dedicated, gifted and patient technician Lucio Gelmi and my lab colleagues and great savers Renato Cipriani, Elia Tercero, Micol della Zassa, Alberto Biasin, Nicola Michelin and Nicola Gemo from University of Padova. In the Federal Univesity of Bahia, Tatiane Woytysiak

and Robinson Carvalho were truly angels. Not only saved my life several times as also taught me essential lessons of being a good professional. Further, my deep gratitude to Cassio Santana from Fiocruz.

To those who received the most challenging task of guiding I owe all my gratitude. Prof Elaine Cabral has been more than a supervisor, but a scientific mother. A role model of professional, scientist and person to be followed. Thank you for investing in me and believing in me. Prof. Silvio Melo, Profa. Rosana Fialho, Profa. Gloria Meyberg and Prof. Alberto Bertucco, I dedicate to you a great thank for introducing me into the tricky world of Engineering. Profa Cristiane Villareal, thanks for the wise advises. Also a great thank to Prof. Paolo Caliceti and Stefano Salmaso for co-supervising me and teach me so many things.

Finally, I would like to thank the Coordination for the Improvement of Higher Education Personnel (CAPES) for all the support in Brazil, as well as in Italy by means of Sandwich Doctoral Institutional Program Overseas (PDSE, grant number: BEX0155/12-8).

SÃO PEDRO, André Luiz Santos. Supercritical fluid technology for development of solid lipid particles entrapping curcumin. 2015. Doctoral Thesis - Escola Politécnica, Universidade Federal da Bahia, Salvador, 2015.

Abstract

Curcuma longa appears as one of the main sources of a phenolic compound with a multitarget bioactivity profile named as curcumin. As main drawbacks, the photosensitivity and high lipophilicity have limited the use of curcumin on pharmaceutical field. The encapsulation technology has been investigated as the approach of choice to overcome these limitations. Solid lipid nanoparticles (SLN®) and microparticles (SLM) have been pictured as a very interesting platforms on development of formulations for biomedical applications. Since traditional SLN®/SLM production methods possess a series of limitations, the processing by supercritical carbon dioxide (scCO₂) has been widely investigated, since scCO₂ is namely recognized by its special physicochemical features, at relatively mild operation conditions without any incremental toxicological risk to pharmaceutical manufacture chain. Concerning to this, the aim of this work was to investigate the use of scCO₂-based technology for the production of curcumin-loaded SLN®/SLM formulations. SLM were obtained by PGSS, where [tristearin+soy phosphatidylcholine (PC)+dimethylsulfoxide (DMSO)+curcumin] mixtures were processed. Samples with (tristearin+PC)/(DMSO+curcumin) w/w ratios ranging from 65.6:1 to 3:1 were prepared either in the presence or absence of helium and then processed by PGSS. The SLM size ranged from 7.8 to 70.0 µm, and the drug loading yield was found to be between 30 and 87 drug/lipid w/w%. The particles obtained from lipid mixtures with low DMSO feed were homogeneous in size. The formulation prepared with the highest DMSO feed yielded a bimodal particle size distribution with significant aggregation. Interestingly, the use of helium in the preparation of the lipid mixture was found to improve drug loading and particle dimensional features. However, by far, the most interesting result was the obtainment of a homogenous population of SLN® within the 0.5% curcumin samples. With an average size of 118.5 nm, no indication of chemical incompatibility among curcumin and SLN® excipients was found on infrared studies and *in vitro* tests demonstrated that the carrier components reduced significantly the cytotoxicity of curcumin. In addition, the preparation process was not found to degrade curcumin, indicating that PGSS can be properly set-up for the preparation of curcumin lipid particles.

SÃO PEDRO, André Luiz Santos. Supercritical fluid technology for development of solid lipid particles entrapping curcumin. 2015. Tesi di Dottorato - Escola Politécnica, Universidade Federal da Bahia, Salvador, 2015.

Riassunto

La *Curcuma longa* sorge come una delle principali fonti di un composto fenolico con un profilo bioattività multitarget conosciuto come curcumina. Come inconvenienti principali, la fotosensibilità e l'alta lipofilità limitano l'uso della curcumina nel campo farmaceutico. La tecnologia di incapsulamento è stata studiata come metodo di scelta per superare queste limitazioni. Le nanoparticelle lipidiche solide (NLS) e microparticelle lipidiche solide (MLS) sono state descritte come piattaforme molto interessanti per lo sviluppo di formulazioni per applicazioni biomediche. Poiché tradizionali metodi di produzione NLS/MLS possiedono una serie di limitazioni, il trattamento da biossido di carbonio supercritico (scCO₂) è stato ampiamente studiato, poiché scCO₂ è cioè riconosciuto dalle sue caratteristiche fisico-chimiche speciali, in condizioni operative relativamente blande senza alcun rischio tossicologico incrementale farmaceutica a catena. Riguardo a questo lo scopo di questa tesi è stato quello di esaminare l'uso della tecnologia a base di scCO₂ per la produzione di formulazione di NLS/MLS caricate con curcumina. MLS sono stati ottenuti da PGSS, dalle miscele composte di tristearina, fosfatidilcolina di soia (PC), dimetilsolfossido (DMSO) e curcumina. I campioni con i rapporti p/p (tristearin + PC) / (DMSO + curcumina) che vanno da 65,6: 1 a 3: 1 sono stati preparati sia in presenza o assenza di elio e poi elaborati da PGSS. Il diametro medio delle MLS ha oscillato fra 7,8 e 70,0 µm e la resa di farmaco carico è stato compreso fra 30 e 87 farmaco / lipidi p/p%. Le particelle ottenute dalle miscele lipidiche con basso contenuto di DMSO hanno presentato dimensioni omogenee. Le formulazioni preparate con il massimo contenuto di DMSO hanno prodotto particelle con dimensioni di distribuzione bimodale con l'aggregazione significativa. È interessante notare che l'uso di elio nella preparazione della miscela lipidica ha migliorato la resa di farmaco carico e le caratteristiche dimensionali delle particelle. Tuttavia, di gran lunga, il risultato più interessante è l'ottenimento di una popolazione omogenea di NLS nei campioni curcumina 0,5%. Con una dimensione media di 118,5 nm, non è stata trovata nessuna indicazione di incompatibilità chimica tra curcumina e gli eccipienti su studi a raggi infrarossi e i test *in vitro* hanno dimostrato che i componenti dell'NLS hanno ridotto in modo significativo la citotossicità della curcumina. Inoltre, il processo di preparazione non è stato trovato per degradare curcumina, indicando che PGSS può essere opportunamente applicata per la preparazione di particelle lipidiche di curcumina.

SÃO PEDRO, André Luiz Santos. Supercritical fluid technology for development of solid lipid particles entrapping curcumin. 2015. Tese de Doutorado - Escola Politécnica, Universidade Federal da Bahia, Salvador, 2015.

Resumo

A *Curcuma longa* é tida como uma das principais fontes do composto fenólico com um perfil de bioatividade multialvo conhecido como curcumina. Como desvantagens principais, a fotossensibilidade e elevada lipofilia têm limitado a utilização de curcumina na área farmacêutica. A tecnologia de encapsulamento tem sido investigada como a abordagem de escolha para superar essas limitações. Nanopartículas lipídicas sólidas (NLS) e micropartículas lipídicas sólidas (MLS) têm sido apresentadas como plataformas interessantes para o desenvolvimento de formulações para aplicações biomédicas. Uma vez que os métodos tradicionais de produção das NLS/MLS possuem uma série de limitações, o processamento por dióxido de carbono supercrítico (scCO₂) tem sido amplamente investigado, uma vez que scCO₂ é nomeadamente reconhecido pelas suas características físico-químicas especiais, sob condições de operação relativamente moderadas, sem qualquer risco toxicológico incremental para cadeia produtiva farmacêutica. Dessa maneira, o objetivo deste trabalho foi investigar o uso da tecnologia baseada em scCO₂ para a produção de PLS contendo curcumina. MLS foram obtidos pela técnica conhecida pelo termo em inglês "Particles Generated from Saturated Solutions" (PGSS), a partir de misturas compostas de triestearina, fosfatidilcolina de soja (PC), dimetilsulfóxido (DMSO) e curcumina. As amostras com razão m/m de (triestearina + PC) / (DMSO + curcumina) variando entre 65,6: 1 e 3: 1 foram preparadas na presença ou ausência de hélio e processadas por PGSS. MLS foram obtidas com diâmetro médio na faixa de 7,8 a 70,0 µm e uma faixa de rendimento de carga de 30 a 87 (droga / lipídio) m/m% de curcumina nas partículas. As partículas obtidas de misturas com menor teor de DMSO apresentaram tamanho homogêneo. Aquelas obtidas de misturas com maior teor de DMSO apresentaram uma distribuição de tamanho bimodal, com agregação significativa. Curiosamente, o uso do hélio levou ao aumento da carga de fármaco e redução do tamanho de partícula. No entanto, o resultado mais interessante foi a obtenção de uma população homogênea de NLS entre as amostras de MLS de curcumina a 0,5%. Com um tamanho médio de 118,5 nm, nos estudos de infravermelho, não foram encontrados sinais de incompatibilidade química entre os componentes das NLS e ensaios *in vitro* demonstraram que os excipientes reduziram significativamente a citotoxicidade de curcumina. Além disso, o processo de preparação não degradou a curcumina, indicando que PGSS pode ser adequadamente empregado para a preparação de partículas lipídicas incorporando a curcumina.

List of Figures

Figure 1. Curcuminoid structures.....	8
Figure 2. Bioactivity profile of curcumin	10
Figure 3. Possible structures of solid lipid particles according to the distribution of drug molecules (pink dots) in the lipid matrix (brown filling). (A-D) capsules; (E-F) spheres. The grouped pink dots symbolize drug molecules not soluble in the matrix, but dispersed. The single unit dispersed dots represent drug dispersed on molecular form.....	14
Figure 4. Expulsion of drug molecule after crystallizing of lipid structures into SLN®	17
Figure 5. Scheme of hot and cold homogenization techniques applied to high pressure and high shear homogenization methods, adapted from Mehnert <i>et al.</i> (2001).	18
Figure 7. Scheme of comminuting of emulsion droplets by high pressure homogenization apparatus.	19
Figure 6. Scheme of particle comminuting with a rotor-stator set of a high shear homogenizer, adapted from (Doucet <i>et al.</i> , 2005)	19
Figure 8. Scheme of SLN® formation on microchannel system (Zhang, S.-H. <i>et al.</i> , 2008).....	21
Figure 9. Scheme of SLN® formation by membrane contactor apparatus (Charcosset <i>et al.</i> , 2005).	22
Figure 10. Typical spray drying scheme for production of particulate formulations (Sonarome, 2014).	26
Figure 11. Scheme of cryogenic grinding/milling system provided by Air Products and Chemicals, Inc. (Air Products, 2016).....	27
Figure 12. Generic scheme of electrospray atomization process (Ijsebaert <i>et al.</i> , 2001)	28
Figure 13. P-T phase diagram of pure CO ₂	29
Figure 14. Schematic representation of the coating process developed by Ribeiro dos Santos <i>et al.</i> (2002). (A) Filling step: BSA crystals (white) and lipid material (black); (B) Solubilization of lipid in scCO ₂ with dispersion of insoluble BSA crystals; (C) Decompression phase with lipid deposition on BSA; (D) Coated particles are obtained.....	30
Figure 15. Extraction system used in SFEE process developed by Chattopadhyay <i>et al.</i> (2007)	31

Figure 16. A: Schematic representation of the supercritical co-injection process (1) CO ₂ cylinder (2) cooler (3) pump (4) heater (5) saturation vessel (6) high pressure vessel (7) valve (8) pneumatic conveying (9) co-injection advice (10) gas/solid separation filter; B: co-injection device (Calderone <i>et al.</i> , 2008).	33
Figure 17. Example of PGSS plant for particle formation of drug-loaded particles (Bahrami and Ranjbarian, 2007).	34
Figure 18. Variation of lipid melting point under CO ₂ at different pressures. A: monoglyceride (Knez and Weidner, 2001); B: tripalmitin (Li <i>et al.</i> , 2006); C: Gelucire® 43-01 (●), Precirol® ATO5 (○) and Compritol® 888 ATO (▼) (Sampaio De Sousa <i>et al.</i> , 2006).	35
Figure 19. Typical P-T phase diagram for CO ₂ -solid lipid system. Abbreviations: LG, liquid-gas; SL, solid-liquid; SLG, solid-liquid-gas; TP, triple point; CP1 and CP2, critical points of pure compounds (1 and 2); 1, 2, vapor pressure curves of pure compounds. 1 is stated for CO ₂ and 2 for solid lipid (Liu, 2008).	36
Figure 20. Typical P-T phase diagram for CO ₂ -solid lipid system with a proposed localization of PGSS steps.	37
Figure 21. Schematic representation of different results obtained under different operational conditions in a PGSS method for production of PEG-600 particles (Kappler <i>et al.</i> , 2003).	38
Figure 22. Lipid structures. a) Tristearin; b) 1,2-dilinoleoylsn-glycero-3-phosphocholine	50
Figure 23. DSC thermograms of lipid mixtures at different pressures.	51
Figure 24. Decrease on melting point of the lipid mixture at different compositions and different pressures.	52
Figure 25. Typical particle size distribution.	64
Figure 26. Micrographs of 0.5% curcumin-loaded SLN® obtained by TEM. Scale bar: 500nm	65
Figure 27. Chemical compatibility evaluation of curcumin and SLN® excipients by IR analysis. ...	66
Figure 28. Evaluation of the effect of free and encapsulated curcumin on cell viability. *** <i>p</i> <0.0001	68
Figure 29. Scheme of PGSS plant used in this work. V2-V14 – valves; PI - Pressure Indicator; TIC – Temperature Indicator – Controller; MC – Mix Chamber; MU – Micronization Unit; EC – Expansion Chamber; HC – Harvest Unit.	98
Figure 30. Photos of the PGSS plant used in this work.	99

Figure 31. Scheme produced by Gardella srl. under instructions and supervision of costumer.....99

Figure 32. [A]: Scheme for mixture preparation under helium atmosphere - (1) curcumin solution inlet; (2) helium outlet; (3) molten lipid mixture / [B] Photo of the system..... 101

List of Tables

Table 1. Concepts of Adverse Drug Reaction.....	4
Table 2. Half-life of curcumin after oral administration in different clinical trials	12
Table 3. Common excipients used on SLN® tailoring.....	15
Table 4. Available works with curcumin-entrapped SLN®	23
Table 5. Melting temperature of lipid mixtures at different compositions and pressures.	49
Table 6. Carbon chain pattern for free fatty acids and phospholipids in Epikuron 200	50
Table 7. Melting point of mixtures of tristearin/epikuron200/DMSO/curcumin.....	52
Table 8. Size measurement parameters 0.5% curcumin SLN®*	64
Table 9. Identification of bands found on obtained IR spectra.....	67
Table 10. Compositions tested.....	100

Outline

Abstract	VII
Riassunto	VIII
Resumo	IX
List of Figures	X
List of Tables	XIII
State of Art	3
1 Adverse Drug Reactions	4
2 Phytomedicine	6
2.1 Drug prospection	6
2.3 Synergy and biocompatibility of phytomolecules	7
3 Curcumin	8
3.1 Obtainment and chemistry	8
3.2 Pharmaceutical considerations	9
3.2.1 <i>Multi-target bioactivity</i>	9
3.2.2 <i>Pharmacotechnical concerns</i>	11
4 Encapsulation Technology	13
4.1 Particulate systems	13
4.2 Solid Lipid Nanoparticles (SLN®)	14
4.2.1 <i>Traditional methods of preparation</i>	17
4.2.2 <i>Curcumin entrapment studies</i>	22
4.3 Solid Lipid Microparticles (SLM)	24
4.3.1 <i>Traditional methods of preparation</i>	25
4.3.2 <i>Curcumin entrapment studies</i>	28
5 Supercritical Fluid Approach	29
5.1 Solid Lipid Particles (SLN® and SLM) Production by scCO ₂ Processing	30
5.1.1 <i>Supercritical Fluid-Based Coating Technique</i>	30
5.1.2 <i>Supercritical Fluid Extraction of Emulsions (SFEE)</i>	31
5.1.3 <i>Supercritical Co-Injection Process</i>	32
5.1.4 <i>Particles from Gas Saturated Solutions (PGSS)</i>	33
Aim of work	41
1 General Aim	42

2 Specific Aims	42
<u>Material and Methods</u>	<u>43</u>
1 Material	44
2 Methods	44
2.1 Solid Lipid Particle Production	44
2.2 Solid Lipid Particle Characterization	44
2.2.1 DSC measurements	44
2.2.2 Percentage of encapsulated curcumin	44
2.2.3 Size measurements and morphology	45
2.2.4 IR Spectroscopy	45
2.2.5 Cell Viability Test	45
<u>Results and Discussion</u>	<u>47</u>
Thermal investigations on Curcumin/Lipids/DMSO/CO₂ mixtures	48
1 DSC Measurements	49
1.1 System 1 lipid + CO ₂ and 2 lipids + CO ₂	49
1.2 System 2 lipids + curcumin + DMSO + CO ₂	52
SLM Production by PGSS and Characterization	54
SLN® Production by PGSS and Characterization	63
1 Size measurement	64
2 Morphology	64
3 Infrared Spectra	65
4 Cytotoxicity test	67
<u>Conclusions</u>	<u>69</u>
<u>Future Perspectives</u>	<u>72</u>
Attachment I - Method Details	97
1 Particle Production	97
1.1 PGSS plant	97
1.2 Mixture preparation	99
1.3 Particle Production	101
Attachment II - Publication List	102

Introduction .

Despite of all efforts on seeking alternatives to the current use of standard drugs by clinics, research of new options is still urgent. A large number of clinical complications derive from drug adverse effects. Also, low efficacy profile of the available drug therapy appears as one of the main causes of patient non-adherence and worsening of pathological conditions. The impacts on public health sector as well as the contribution to labor impairment reinforce the constant search for therapeutic options. In this context, the kingdom *Plantae* can offer a plethora of new therapeutic leads for drug development processes. Since ancient times, plants *in natura* and special preparations have been used as strong agents for curative purposes. Several of the commercial available medicines widely known were prospected from plant material.

Among the large range of available options, curcumin has been emerged as a really interesting molecule. Well known by its presence on spices derived from *Curcuma longa*, curcumin provides a significant antiinflammatory activity. Extensive studies have proved the action of curcumin through varied inflammatory paths and it is directly connected to a vast number of therapeutic applications. However, curcumin is highly hydrophobic, which confers a very low bioavailability and also instability in physiological conditions, as well as upon exposure to light.

In this context, one interesting alternative for these physicochemical challenges is the association of curcumin to innovative drug delivery systems. The solid lipid nanoparticles (SLN®) and microparticles (SLM) represent good options for this purpose. These particles are composed by lipids which are solids at room temperature. The term lipid includes triglycerides, partial glycerides, fatty acids, steroids and waxes. The drug incorporated into SLN®/SLM has its water solubility improved by action of lipid matrix compounds, leading to an improvement of bioavailability, and is commonly released on a prolonged profile, which can lead to the maintenance of a constant drug concentration on the organism post administration. It can imply on reduction of side effects and reduces the frequency of doses of pharmaceuticals.

In comparison with other types of encapsulation systems, SLN®/SLM offer some important advantages. Two of the most studied encapsulation systems for medical application are the polymeric and the liposomal ones. While the monomeric residues from polymeric particles can be toxic to human body metabolism, the lipids used on SLN®/SLM preparation are preferred due to the physiological nature of their lipid constituents, which prevents acute and chronic toxicity. In addition, the solid state of SLN® favors less complicated methods of sterilization than those observed for liposomal formulations, as well as, higher particle physical stability.

Currently a wide range of techniques for production of SLN®/SLM are available. Solvent emulsification/evaporation, high pressure homogenization, hot and cold homogenization have been the most cited. The choice of these processes depends on their feasibility for scaling up to industry

production and on the overall costs of operation. However, they are multi-step, generally involve high temperature and shear rates and several cycles at high pressure. These extreme process conditions lead to wider particle size distribution and degradation of the drug. Further, the high kinetic energy content of the obtained particles promotes their coalescence and the presence of organic solvent residues compromises their safety for human use.

In this context, the supercritical fluid technology appears as a great opportunity to overcome these method limitations. Specifically, supercritical carbon dioxide (scCO₂) offers a wide range of possible applications on pharmaceutical field. CO₂ reaches its critical point at 31.1 °C and 70.8 bar, which allows processing of bioactive compounds under mild operation conditions avoiding thermal degradation. Other significant advantages of supercritical fluid processing include the possibility of recycling of CO₂, the production of organic solvent-free particles, achievement of particulate systems with a narrower particle size distribution, in a single-step operation.

Besides these features, supercritical fluid techniques also have shown extreme versatility by the use multipurpose plants and operation conditions. Among the available techniques for SLN®/SM production by supercritical fluid processing, particles from gas saturated solutions (PGSS) has been shown as the most interesting. In addition to all advantages of supercritical fluid technology, PGSS can produce powder formulations directly, requires the use of small volume pressurized equipment, demands relatively low amounts of CO₂, and easily performs the recovery of the product and the gas. This process already runs in plants with capacity of some hundred kilograms per hour. Considering the endorsement granted by all afore mentioned information, this work intended to develop curcumin-solid lipid particle-based formulations by supercritical fluid technology.

This thesis is organized in chapters. The first one is composed by this *Introduction*. In order to provide a big picture background, this thesis is composed of an extensive *State of Art* (chapter II), which covers the available information concerning the importance of drug prospection from plants, curcumin and its medical applications, encapsulation technology and supercritical fluid technology linked to the production of particulate systems. Then, the *Aims* (chapter III) of this work are cleared up, followed by the *Material and Methods* (chapter IV) applied to fulfill the designed purposes. *Results and Discussion* (chapter V) are organized in three sections: the first one presents the preliminary results, the second presents the papers published with the results for SLM, while the third one comprises the complementary results for SLN®. Finally, *Conclusions* (chapter VI) sum up evaluation of the whole work and relate to the *Future Perspectives* (chapter VII). The *Reference* (chapter VIII) list shows all references in alphabetic order. The Attachment I provides the publication list of works linked to this thesis.

State of Art. II

1 Adverse Drug Reactions

The use of drugs as therapeutic tools on clinical practice is idiosyncratically associated to risks. Since every pharmacological effect is defined by affecting a physiological process, the repercussion of this phenomenon can be turned into a noxious outcome. In this context, the concept of adverse drug reaction (ADR) have been turned widely known on medical field. The Table 1 presents variations on the gold standard concepts of ADR adopted by different associations. These concepts have been commonly stated as the basis for clinical bodies, including hospitals and regulatory agencies approach on ADR management and care.

Table 1. Concepts of Adverse Drug Reaction

Association	Concept	References
Food and Drug Administration (FDA)	Adverse event means any untoward medical occurrence associated with the use of a drug in humans. An adverse event or suspected adverse reaction is considered "serious" if, in the view of either the investigator or sponsor, it results in any of the following outcomes: Death, a life-threatening adverse event, in patient hospitalization or prolongation of existing hospitalization, a persistent or significant incapacity or substantial disruption of the ability to conduct normal life functions, or a congenital anomaly/birth defect. Important medical events that may not result in death, be life-threatening, or require hospitalization may be considered serious when, based upon appropriate medical judgment, they may jeopardize the patient or subject and may require medical or surgical intervention to prevent one of the outcomes listed in this definition.	(FDA, 2015)
World Health Organization (WHO)	A response to a medicine which is noxious and unintended, and which occurs at doses normally used in man.	(WHO, 2002)
American Society of Health-System Pharmacists (ASHP)	Any unexpected, unintended, undesired, or excessive response to a drug that: <ul style="list-style-type: none"> ▪ Requires discontinuing the drug (therapeutic or diagnostic); ▪ Requires changing the drug therapy; ▪ Requires modifying the dose (except for minor dosage adjustments); ▪ Necessitates admission to a hospital; ▪ Prolongs stay in a health care facility; ▪ Necessitates supportive treatment; ▪ Significantly complicates diagnosis; ▪ Negatively affects prognosis; ▪ Results in temporary or permanent harm, disability, or death. 	(ASHP, 1995)

Briefly, any noxious and unintended effect derived from drug treatment is considered as an ADR. An ADR or a combination of multiple ADRs can lead to treatment failure, as well as, to the development of new medical problems which can be as harmful or even worse than the previous condition (Pérez Menéndez-Conde *et al.*, 2011). A 3-month observational study on New Somerset Hospital in Cape Town, South Africa, revealed that 6.3% of patients were admitted as a result of an ADR (Mehta *et al.*, 2008). An 1-year investigation of patients admitted to the Geriatric Unit of the Casa Sollievo della Sofferenza Hospital, San Giovanni Rotondo in Italy, revealed that around 6% were ADR-related (Franceschi *et al.*, 2008). A cross-sectional study performed by 4 months on

Bellvitge University Hospital, Spain, showed that 4.2% of hospital admissions were caused by ADRs (Pedrós *et al.*, 2014). In a tertiary care teaching hospital from North India, a rate of 3.5% was found for severe ADRs (Tandon *et al.*, 2014).

Some other works have collected data of adverse drug events (ADE) which are composed of both ADRs and consequences from medication errors. An ADE prevalence of 4.2% was found among the patients after a 5-day cross-sectional study in Ibn Sina general teaching hospital in Rabat, Morocco (Benkirane *et al.*, 2009). A 4-month prospective observational cohort study conducted in the pediatric, neonatal intensive care unit, and postnatal wards of a university hospital in Dunedin, New Zealand found an alarming rate of 12.9% of ADE among patient admissions (Kunac *et al.*, 2009). Stausberg (2014) has found an overall prevalence rate of ADE among hospitalizations of 3.22% for England, 4.78% for Germany and 5.64% for USA. In this context, the incidence of ADR has been stated as a major public health care problem direct linked to an impact on the overall costs and decrease of patient productivity that cannot be ignored (Alomar, 2014).

In addition to this scenario, the mortality rates associated to ADRs is a significant issue. The Institute of Medicine from USA estimates around 7,000 deaths related to ADRs annually (Alomar, 2014). A study performed on North India relates around 3,000 deaths related to ADR per year (Tandon *et al.*, 2014). The rates of hospital admissions and mortality caused by ADRs in different countries confirm the relevance of reinforcement of pharmacovigilance routines, continuous education of clinicians, pharmacists, nurses and all clinical supportive staff, as well as, the research for safer therapeutic alternatives (Ivanov *et al.*, 2015; Marquez *et al.*, 2015).

2 Phytomedicine

One of the earliest findings on use of medicinal plants date from 60,000 years ago with the discovery of pollen and flower fragments of different medicinal plants in a grave of a Neanderthal man. Other investigations have found pieces of birch fungus, presumably used as a laxative and antibiotic with 5,300-year-old 'iceman' discovered in 1991 in the Italian Alps (Hart, 2005). Since then, the application of plant material with prophylactic and therapeutic purposes have been largely reported.

Over the Earth's surface 250,000 to 350,000 plant species have been accounted. From this amount, around 35,000 species have been reported to be therapeutically (Khan and Rauf, 2014). Ethnopharmacologic studies have described a wide range of medicinal plants and their preparations selected as a pivotal part of folk ancient knowledge transferred from generation to generation. A great part of these medicinal expertise is deeply linked to religious practices. The phytomedicine, commonly cited as "traditional medicine" due to its ancestry, is often characterized by use of recommend complex herbal mixtures and multi-compound extracts (Leonti and Casu, 2013; Papp *et al.*, 2014). Currently the WHO estimates that around 80% of world's population chooses herbal products as therapeutic leads or as adjuvant of purified molecules-based drugs (Kutama *et al.*, 2015).

2.1 Drug prospection

Considering all knowledge on traditional medicine supported by centuries of practice, it has been used as a guide for prospection of new drugs. On 19th century the characterization of pure molecules in medicinal and toxic plants took place on the pharmaceutical scenario. On the first decades of the same period, some of the compounds in current use on medical practice were first isolated from their original plant matrices, such as morphine from *Papaver somniferum* L., quinine from *Cinchona* spp., caffeine from *Coffea arabica* L., and atropine from *Atropa belladonna* L. (Heinrich, 2013).

One of the most traditional approaches on drug discovery researches is known as Phenotypic Drug Discovery. On this approach, synthetic or isolated compounds are tested in different cell types in order to evaluate changes on phenotypic features, such as cellular viability or protein expression modulation. In order to reduce the number of experiments, a new approach, the Target Drug Discovery has been implemented. On this one, a certain biological target is selected and a screening of compounds is performed and the modulation of this target is evaluated. However, some recent data have demonstrated that most of first-in-class drugs with innovative mechanisms of action have

come from phenotypic screening (Kotz, 2012; Moffat *et al.*, 2014) . So, currently, the selection of a route on drug prospection can be a not so clear task for the research centers.

Despite all the effort on the research of alternative therapeutic drugs, most of them are classified as me-too drugs, i.e. molecules structurally very similar to already known drugs or possess a very similar mechanism of action and efficacy comparable to commercially available medicines. Due to this failure the interest on natural product research has been increased (Lahlou, 2013). In this context herbs, botanicals, herbal medicines and phytopharmaceuticals have returned as a trend for pharmaceutical research.

2.3 Synergy and biocompatibility of phytomolecules

Characteristics from phytoproducts draw up some advantages when compared to synthetic drugs. The plant-derived crude materials commonly known as herbal products as well as the pharmacologically standardized plant-based products (phytopharmaceuticals) present a complex mixture of components. Several studies have demonstrated in different plant preparations a synergic activity among their biological active constituents. Also, the association to structural primary metabolites, such as glycosides, proteins or lipids, can enhance the pharmacologic effect of active molecules (Ulrich-Merzenich *et al.*, 2010; Lewandowska *et al.*, 2014; Wang *et al.*, 2014). Furthermore, taking into account the biological synthesis route of active phytomolecules they commonly present a significant biocompatibility which improves their safety profile contributing to a relatively fewer occurrence of adverse reactions.

3 Curcumin

3.1 Obtainment and chemistry

First isolated by Vogel and Pelletier (1815), curcumin, also designated by the official chemical name [1,7-bis(4-hydroxy-3-methoxyphenyl)-1,6-heptadiena-3,5-dione], is an orange-yellow coloured polyphenol prospected from roots and stalk of the herb *Curcuma longa* L. (Simanjuntak *et al.*, 2010). The chemical structure depicted on Figure 1 was firstly elucidated by Kostanecki and colleagues (1910). Curcumin is found as a crystalline powder, with melting point of 183°C, molecular formula of C₂₁H₂₀O₆ and molecular weight of 368.37 g/mol. The core structure of curcumin consists of a feruloylmethane skeleton composed of phenolic rings connected by unsaturated carbonyl groups that form a diketone. Further, it is common the occurrence of tautomeric transition from the ketone form to a enolic form which is more energetically stable due to formation of hydrogen bond (Lin and Lin, 2008; Akram *et al.*, 2010).

Curcuma longa L. is a typical rhizomatous herbaceous plant perennial plant of the ginger family, Zingiberaceae. Turmeric is derived from tropical South Asia and demands temperatures between 20° C and 30° C, and a considerable amount of annual rainfall to thrive. Once harvested, the turmeric root is boiled, dried, and ground to obtain the powder used as spice in curries, as well as a folk medicine for wide range of applications (Li, S. *et al.*, 2011; Revathy *et al.*, 2011).

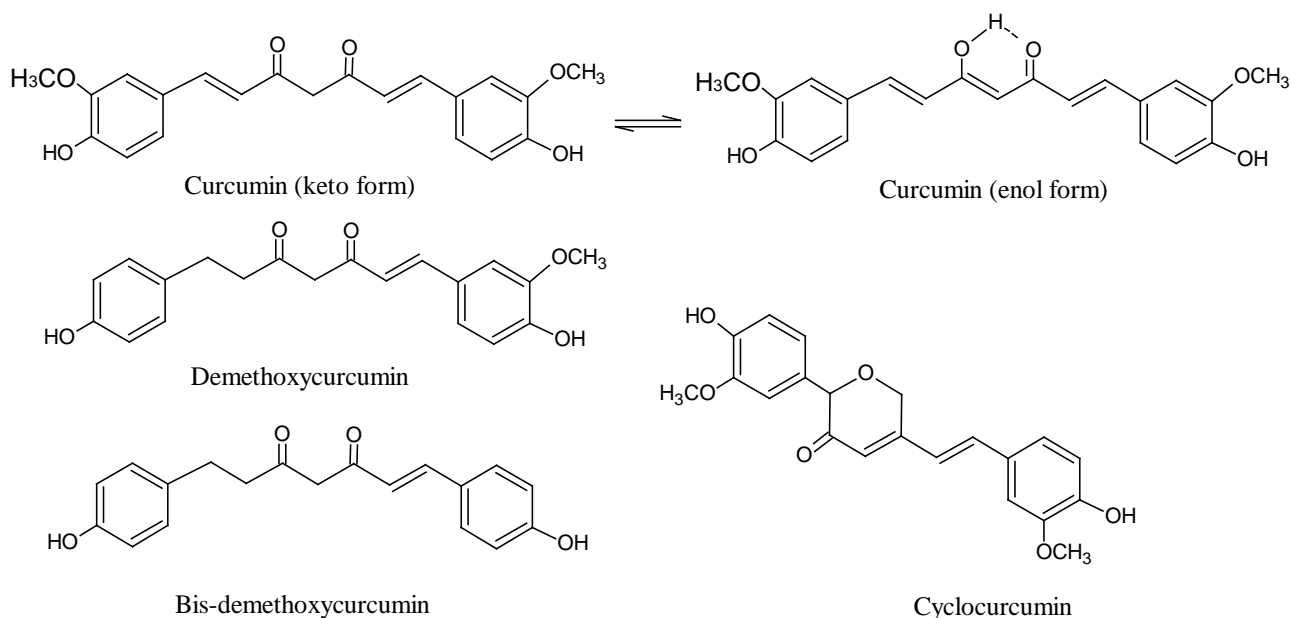


Figure 1. Curcuminoid structures

The main polyphenolic secondary metabolites extracted from turmeric rhizomes are usually named as curcuminoids. The literature has described three major curcuminoids comprising about 75-80% curcumin, 15-20% demethoxycurcumin, 3-5% bis-demethoxycurcumin. More recently the cyclocurcumin has been described as a fourth major turmeric constituent (Lin and Lin, 2008; Shieh

et al., 2013). This curcuminoid complex is popularly referred as Indian saffron, yellow ginger, yellow root, kacha haldi, ukon, or natural yellow 3. In comparison to the others curcuminoids, curcumin presents the most prominent biological activities. However, taking into account that isolation of pure compounds from turmeric is considered a difficult and high cost procedure, curcumin is usually marketed associated to other curcuminoids as minor impurities (Revathy *et al.*, 2011).

3.2 Pharmaceutical considerations

3.2.1 Multi-target bioactivity

Curcumin has been widely recognized by its antiinflammatory properties. It has been largely proved the action of curcumin on acute inflammation by blockage of the inflammatory cascade pathways derived from arachidonic acid metabolism. Both lipoxygenase and cyclooxygenase enzymes are inhibited by curcumin which prevents the production of molecules responsible for the cardinal symptoms of inflammation, in a similar way to traditional nonsteroidal antiinflammatory drugs (Basnet and Skalko-Basnet, 2011). Further, curcumin has been also found as an effective alternative for chronic inflammation conditions. Some studies have attributed this outcome to the action of curcumin at gene expression level. It has been found curcumin to down-regulate the expression of pro-inflammatory genes, such as those that codify the inducible nitric oxide synthase (iNOS) enzyme (Kaewsamut *et al.*, 2007; Telles *et al.*, 2014), tumor necrosis factor alpha (TNF- α), interleukins 1 β and 6 (Aggarwal *et al.*, 2013; Das and Vinayak, 2014). This is a consequence of the suppression performed by curcumin of a transcription factor essential for expression of proinflammatory genes, the nuclear factor kappa-B (NF- κ B) (Cho *et al.*, 2007; Jurenka, 2009; Zhang *et al.*, 2010).

Along with the antiinflammatory profile, the antioxidant activity is the most attributed to curcumin and its analogues, where different mechanisms have been cited (Guo *et al.*, 2011). Curcumin has been described to be capable of inducing the biosynthesis of endogenous antioxidant enzymes which are physiologically in charge of protecting macromolecules from free radicals. This induction is promoted by an up-regulation of gene expression of synthases that produce these endogenous antioxidants, which includes glutathione-S-transferase, glutathione peroxidase and superoxide dismutase (Biswas *et al.*, 2005; Jagetia and Rajanikant, 2015). On the other hand, some authors have pointed out the direct radical scavenging ability of curcumin as its main antioxidant mechanism. The hydrogen atom transfer (HAT), one of the most accepted mechanisms for that, attributes an electron donation from curcumin molecule to the free radical through a hydrogen atom abstraction as an explanation for radical elimination. This abstraction can occur from the central

active CH₂ group in the heptadienone link of curcumin keto form or from phenolic hydroxyl group on the enol form (Aggarwal *et al.*, 2007; Galano *et al.*, 2009; Guo *et al.*, 2011).

Beyond its two main properties - antiinflammatory and antioxidant - curcumin has further acquired a large range of potential biomedical applications. Taking into account that curcumin interacts to a wide spectrum of cell types and chemical signals in the organism, it has shown a really varied bioactivity profile which makes it a multi-functional or pluri-pharmaceutical substance as can be noted on Figure 2. Sometimes, curcumin has been referred as the "spice of life" (Gargeyi *et al.*, 2011).

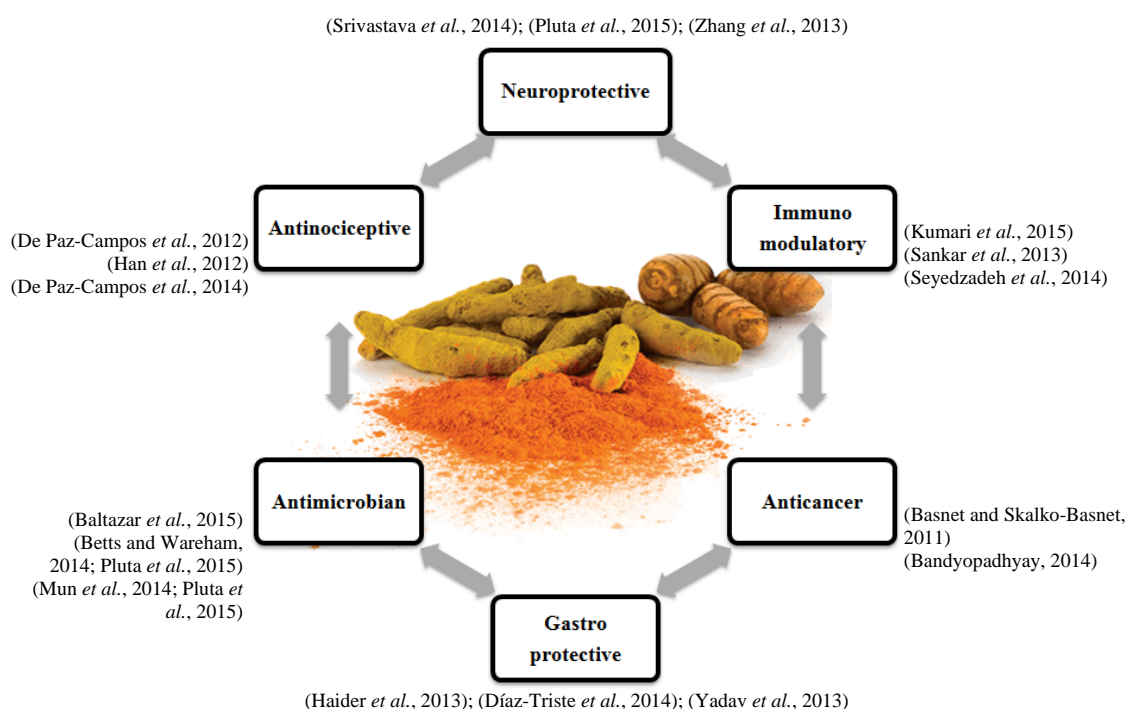


Figure 2. Bioactivity profile of curcumin

Works have highlighted a pronounced anticancer activity associated to multi-varied cancer-linked targets combining specific apoptotic activity by down-regulation of highly varied enzymatic pathways to inhibition of tumor-demanded angiogenesis and other mechanisms (Hasima and Aggarwal, 2012). Beyond its intrinsic antimicrobial activity, curcumin is also found to modulate drug-resistance against pathologic bacteria (Mun *et al.*, 2013). Further, a combination of antiinflammatory and antioxidant activities is directly associated with gastroprotective properties (Irving *et al.*, 2011). Antiapoptotic features associated with the inhibition of neurotoxic inflammatory mediators confers to curcumin also neuroprotective properties (Wu *et al.*, 2013). The blockage of nociceptive receptors, neuro-recovery and once more the inhibition of inflammatory mediators is also connected to the antinociceptive profile of curcumin (Tajik *et al.*, 2007; Zhao *et al.*, 2012).

3.2.2 Pharmacotechnical concerns

Curcumin presents a very poor solubility in water at acidic and physiological pH, ranging about 0.2mg/mL (Sreenivasan *et al.*, 2010). Despite the presence of highly polar enolic and phenolic groups on curcumin structure, this curcuminoid possesses a logP value of 2.5 conferred by the strongly hydrophobic aliphatic bridge in the core of the molecule that connects the polar domains (Balasubramanian, 2006). Curcumin is soluble in DMSO (>11mg/mL), acetone and ethanol (1mg/mL). Taking into account that only solubilized drug molecules can be absorbed by the cellular membranes to subsequently reach the site of drug action, the poorly water soluble drugs, as curcumin, present a low and variable bioavailability leading to low efficacy pharmacological profile (Chaudhary *et al.*, 2012).

As stated for all class II drugs, i.e. low solubility and high permeability, the research of strategies for improving solubility properties and consequently bioavailability parameters is pivotal for improving efficacy and safety of the formulation (Kawabata *et al.*, 2011). This statement justifies the plenty of studies on curcumin with different approaches, such as nanonization (Moorthi and Kathiresan, 2013), water soluble analogues synthesis (Anand *et al.*, 2008; Pandey *et al.*, 2011), and association with varied pharmaceutical carriers applied as drug delivery systems (Yallapu *et al.*, 2012). The latter approach represents an advantageous alternative also for protection of the curcumin molecule from degradation by oxidation reactions. Curcumin is a known photo sensitive molecule. High degradation rates are found for curcumin upon UV-Vis light exposure leading to a production of mainly phenolic compounds derived from the breakdown of the carbon chain connecting the two aromatic rings of the molecule. This reaction is enhanced under oxygen-rich atmosphere (Singh *et al.*, 2010).

In regard of the lipophilic nature of curcumin, parenteral routes of administration have been avoided and the association with biocompatible solubilizers has been faced as the alternative of choice for favoring oral delivery. In this manner, the stability of curcumin through gastrointestinal tract is also another concern. The presence of a highly reactive β -diketone moiety in the curcumin structure leads to a high instability at pH above 6.5, what makes it highly unstable on intestinal tract (Jantarat, 2013). The β -diketone moiety acts a specific substrate of a series of aldo-keto reductases and can be decomposed in human body rapidly. In addition, the phenolic hydroxyl groups facilitate the glucuronidation process leading to rapid metabolism of curcumin (Jantarat, 2013). Still, the bare solubility rate on gastric fluid leads it has been described that most part of orally administered curcumin is excreted through the feces (Jäger *et al.*, 2014). These facts correlate with the clinical trial data listed on Table 2. Only formulations with solubilization enhancers on the composition,

could lead to readable concentrations of curcumin on plasma and even in this condition, short half-life times ($t_{1/2}$) were obtained for curcumin.

Table 2. Half-life of curcumin after oral administration in different clinical trials

Formulation	Composition	Intake scheme	Total Cu dose	$t_{1/2}$ (h)	Volunteers	Reference
Curcumin capsules	crude curcumin extract	single intake	500mg	N.D.	healthy male volunteers (20-26 y.o.)	(Shoba <i>et al.</i> , 1998)
Sabinsa C ³ complex® capsules	187 mg curcumin, 58mg demethoxycurcumin, 5 mg bisdemethoxycurcumin, microcrystalline cellulose, magnesium stearate, silicone dioxide	single intake	7.48g	10.30	healthy male and female volunteers (12-60 y.o.)	(Vareed <i>et al.</i> , 2008)
			8.98g	8.80		
Curcuminoid capsules	95% curcuminoid extract	single intake	650mg	N.D.	male and female volunteers (18-65 y.o.) with metastatic high-grade osteogenic sarcoma	(Gota <i>et al.</i> , 2010)
Longvida®	turmeric root extract, pure phosphatidylcholine, vegetable stearic acid, ascorbic acid palmitate		650mg	7.46		
Theracurmin® capsules	10% curcumin, 2% other curcuminoids, 46% glycerin, 4% gum ghatti, 38% water	single intake	150mg	9.70	healthy male and female volunteers (38-51 y.o.)	(Kanai <i>et al.</i> , 2012)
			210mg	13.00		

Cu - curcumin; y.o. - years old; N.D. - no detectable, i.e. the trace values of curcumin found on plasma were under detectable ability of applied method, which impeded the $t_{1/2}$ calculation.

These data ratify the suitability of association studies of curcumin to drug delivery systems as an essential approach for bioavailability and safety enhancement of curcumin-based formulations. Further, the association with varied drug delivery systems commonly lead to a prolonged release of drug molecules which favors the prolongation of their plasmatic levels and consequently its therapeutic effect, which means a considerable suitability for application on chronic treatments.

4 Encapsulation Technology

4.1 Particulate systems

For several years, the research on development of drug formulations has focused on tailoring of delivery systems which are capable of delay and sustain the drug release after administration (Maderuelo *et al.*, 2011). These kinds of formulations, commonly known as modified drug delivery systems, take several advantages when compared with the conventional pharmaceutical forms. Their capability of maintaining constant drug blood levels confers to them improved efficacy, reduced toxicity, improved patient compliance and convenience (Kumar, 2000). In addition, intending the optimization of the delayed drug release from these formulations, controlled release systems have been widely studied. Controlled release may be defined as a method which allows controlling time and the site of drug release at a specific rate (Pothakamury and Barbosa-Canovas, 1995).

Among the controlled drug release systems, colloidal systems have played a prominent role on pharmaceutical research field. Colloidal particles possess average size ranging on nanometric scale, also known as nanoparticles (Kamble *et al.*, 2010). Taking in consideration the concept of controlled release, the major aims on designing nanoparticles have included the control of particle size, morphology and release of bioactive chemicals in order to achieve site-specific action of the drug at a therapeutically rate and dose regimen (Mohanraj and Chen, 2006).

Nanoparticles were first developed around 1970 for carrying of vaccines and anti-cancer drugs (Kumar, 2000) and up to date they are related to both nanospheres and nanocapsules. Nanospheres have a matrix type constitution where the entrapped molecule may be distributed on the sphere surface or inside de particle. Nanocapsules are vesicular systems in which the drug is retained into a core with different composition of the outer membrane (Reis *et al.*, 2006). Besides controlling the release of drug molecule, these nanoparticle carriers also protect themselves against possible thermal or photo degradation which assures more stability and consequently an extended shelf life to the final product.

Futhermore, considering some disadvantages of nanoparticles when compared to microparticles (>1,000nm), microparticulate systems also have being a significant alternative for drug delivery. Due to their tight diameter, nanoparticles generally possess a low payload, leading to a necessity of using large amounts of the formulation to achieve desirable therapeutic response. In addition, the small size confers less physical stability, related to a higher tendency to undergo chemical reactions by means of oxidative and hydrolytical pathways, elicited by the higher surface area. This can also facilitate their aggregation and also penetration of release media favoring a faster release of the drug

molecules. Also, the production of nanoparticles commonly demands high energy methods in order to confer to thermodynamic unstable systems a long term kinetic stability (Kohane, 2007; Macdonald, 2015).

However the main aspect that will rule the choice of the formulation it is its application. Microparticles and nanoparticles show different uptake pathways by immunologic system, as well as, possess important differences on their pharmacokinetic profiles, due to their different tendencies to plasmatic protein-binding, capacities of penetrating membranes and accumulation rates, as well as, drug release mechanisms (Chakravarthi *et al.*, 2010; Hardy *et al.*, 2013)

4.2 Solid Lipid Nanoparticles (SLN®)

The efforts for discovering some alternatives to overcome the limitations of conventional particulate systems resulted on the development of the solid lipid nanoparticles, typically named as SLN® (Figure 3). First introduced in 1991 (Müller, 1991), SLN® are colloidal particles composed by lipids which are solids at room temperature (Siekmann and Westesen, 1992). The term lipid includes triglycerides, partial glycerides, fatty acids, steroids and waxes. The drug incorporated into SLN® is released on a prolonged profile after administration and as a consequence a constant concentration of the drug molecule can be maintained on blood stream. The literature has been shown that beyond the composition of lipid matrix, the method of preparation seems to have an important role on the definition of the release mechanism of drug molecule (Müller *et al.*, 2000; Mehnert and Mader, 2001; Wissing *et al.*, 2004).

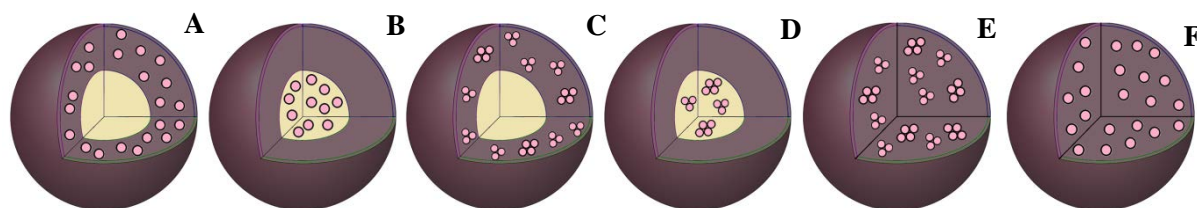


Figure 3. Possible structures of solid lipid particles according to the distribution of drug molecules (pink dots) in the lipid matrix (brown filling). (A-D) capsules; (E-F) spheres. The grouped pink dots symbolize drug molecules not soluble in the matrix, but dispersed. The single unit dispersed dots represent drug dispersed on molecular form.

High encapsulation rates are obviously desirable, since they can reduce the number of particles to achieve therapeutic levels. The encapsulation performance is mainly governed by chemical nature of the drug molecule, i.e. according to its lipophilicity or hydrophilicity. Therefore, to achieve a high entrapping efficiency, it is preferable the selection of a drug molecule with high solubility in lipids (Wissing *et al.*, 2004). Considering the high lipophilicity of lipid matrix constituents in SLN®, hydrophilic molecules are hardly incorporated into these particles. Most

methods of SLN® preparation involves the melting of constitutive lipids with subsequent solidification by cooling and after this step the interaction of hydrophilic compounds with SLN® matrix significantly decreases leading to a phase separation that facilitates the burst release of the drug (Almeida and Souto, 2007).

Surfactant molecules also present a key role on SLN® production. Considering that most of processes of production of SLN® are composed of a pre-O/W emulsion preparation step, surfactants acting as emulsifiers have been applied. Further, in order to enhance the encapsulation efficiency of active substances with different chemical nature from the selected solid structural lipids, surfactants can be used. Taking into account that not all surfactants are capable to form a stable film at the interface between the inner and outer phase of an emulsion, i.e. act as an emulsifier, the selection of the suitable surfactant is critical on SLN® preparation (Vaclavik and Christian, 2007). The Table 3 summarizes valuable information for SLN® excipient selection.

Table 3. Common excipients used on SLN® tailoring

Structural Lipids (melting point)					
<u>Triglycerides</u>		<u>Fatty acids</u>		<u>Waxes</u>	
Tricaprin	(32.0°C)	Decanoic acid	(31.0°C)	Carnauba wax	(82-86°C)
Trilaurin	(45.5°C)	Myristic acid	(54.4°C)	Bee wax	(62-64°C)
Trimyristin	(57.0°C)	Palmitic acid	(62.6°C)	Cetyl palmitate	(55.0°C)
Tripalmitin	(66.0°C)	Stearic acid	(69.6°C)	Cetyl alcohol	(49.3°C)
Tristearin	(68.0°C)	Behenic acid	(80.0°C)	Stearyl alcohol	(56-5°C)
<u>Glyceride mixtures</u>		<u>Pure Glycerides</u>			
Witepsol®	(33-44°C)	Glyceryl monostearate		(81.5°C)	
Precirol® ATO5	(53-57°C)	Glyceryl behenate		(83.0°C)	
Gelucire® 50/13	(47-53°C)				
Surfactants (HLB value)					
<u>Sorbitan fatty acid esters</u>		<u>Ethylene oxide/propylene oxide copolymers (Pluronics)</u>		<u>Polyoxyethylene sorbitan fatty acid esters (Tweens)</u>	
Span 20	(8.6)	Poloxamer 188	(29.0)	Polysorbate 20	(16.7)
Span 60	(4.7)	Poloxamer 407	(21.5)	Polysorbate 60	(14.9)
Span 85	(1.8)			Polysorbate 80	(15.0)
<u>Phospholipids</u>		<u>Salts</u>			
Soybean Lecithin	(7.0) ^a	Sodium glycocholate		(23.1)	
Egg Lecithin	(4.0) ^a	Sodium cholate		(25.0)	
		Taurocholic acid sodium salt		(22.1)	

Witepsol®: mixtures of glycerides of C10-C18 fatty acids, glycerol and fatty acids C10-C18 / Precirol® ATO5: mixture of mono-, di- and triglycerides and contains mainly a diglyceride (51.6 wt%) with one C16 (48.9%) and one C18 (48.8%) fatty acid saturated chains/ Gelucire®: mixture of mono, di and triglycerides of saturated fatty acids C8-C18.

^aThese values can variate according to the composition of the natural phospholipid.

In comparison with other types of particles, SLN® possesses some important advantages. Taking into account its evaluation of potential cytotoxicity, SLN® has a broad acceptance owing to physiological nature of its lipid constituents, preventing acute and chronic toxicity. This is ratified by the fact that SLN® excipients generally possess the GRAS (Generally Recognized as Safe)

status conferred by FDA (Mehnert and Mader, 2001; Rahman *et al.*, 2010). Moreover, the solid state of SLN®, similar to polymeric particles, favors less complicated performing of sterilization and higher particle stability by avoiding of aggregation, resulting in a larger shelf-life, when compared to liposomal or microemulsion formulations.

These features make SLN® a good option for different pharmaceutical and cosmetic applications considering their relatively easy manipulation in various kinds of formulations which enables their use in a large range of sites for drug delivery, such as oral cavity and gastrointestinal tract (Holpuch *et al.*, 2010; Aji Alex *et al.*, 2011; Gao *et al.*, 2011; Luo *et al.*, 2011), brain (Kaur *et al.*, 2008; Wong *et al.*, 2010), ocular tissues (Attama *et al.*, 2008; Del Pozo-Rodriguez *et al.*, 2008; Gokce *et al.*, 2008), respiratory tract (Liu *et al.*, 2008; Nassimi *et al.*, 2010), skin (Puglia *et al.*, 2008; Bhaskar *et al.*, 2009; Kuchler *et al.*, 2009; Lv *et al.*, 2009), as well as systemic through parenteral routes including subcutaneous (Lu *et al.*, 2006), intramuscular (Xie *et al.*, 2011) and intravenous (Gao *et al.*, 2008; Joshi and Muller, 2009; Del Pozo-Rodriguez *et al.*, 2010; Jain *et al.*, 2010).

Additionally to all these characteristics, SLN® still have the inherent advantages of every lipid-based formulations linked to the modulation on uptake of drugs by oral as well as by parenteral routes (Martins *et al.*, 2007; Joshi and Muller, 2009). In particular, in the oral route the lipidic excipients enables avoiding of first-pass effect due to their capacity of enhancing drug solubilization in the intestinal milieu, recruit intestinal lymphatic drug transport and alter enterocyte-based drug transport and disposition (Porter *et al.*, 2007). Notably, in parenteral applications, the highly judicious control of particle size and pyrogen presence are imperative. Beyond the intrinsic biologic risks associated to pyrogens, SLN® can interact with them causing gelation leading to potential embolism problems. In addition, any particulate formulations with large polydispersity index also present a high risk of embolism events (Martins *et al.*, 2007)

A crucial issue to assure the SLN® stability is monitoring the crystalline behavior of the structural lipids of the particle. Polymorphism is commonly found in lipids and depending on the crystallization conditions, various crystalline states called subcell structures are generated, among which the lateral packing of the hydrocarbon chains is remarkably different. Into the SLN® the lipid matrix recrystallizes at least partially in the α -form (unstable polymorphic form) where the carbon chains assume a hexagonal disposition, or in the β' -form (metastable polymorphic form) with an orthorhombic perpendicular packing. The lipid as a bulk tends to recrystallize preferentially in the β' -form, which transforms quickly into the β -form, with a triclinic parallel disposition. During storage, the crystalline lipid structures migrate to more stable polymorphic forms, i.e., from α -form to β' -form and subsequently to β -form. In this process the hydrocarbon chain packing

increase enormously with consequent reduction of imperfections in the lipid lattice. The packing of hydrocarbon chains becomes less dense in the order β , β' , and α and is accompanied by melting point depression. Generally, the transformation is slower for long-chain than for short-chain triacylglycerols (Takechi *et al.*, 2007; Da Silva *et al.*, 2009; Souto and Müller, 2010).

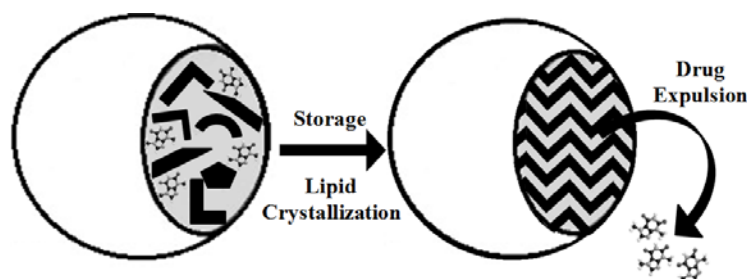


Figure 4. Expulsion of drug molecule after crystallizing of lipid structures into SLN®

As depicted in Figure 4, this physical transition of lipids to highly crystalline state into SLN® matrix lead to expulsion of hydrophilic and lipophilic drug molecules (Pietkiewicz *et al.*, 2006). In case of suspensions, the active compound is expelled to the dispersing media while the SLN® shrinks in the solid powdered preparations. Both processes prevent the safe and efficient action of SLN® formulations. Considering that mixture of lipids containing fatty acids of different chain length forms less perfect crystals with many imperfections, its use on SLN® preparation offers more space to accommodate guest molecules, preventing expulsion of drugs.

4.2.1 Traditional methods of preparation

High Pressure and High Shear Homogenization

The high pressure and high shear homogenization techniques are commonly preceded by intermediate homogenization steps to produce a coarse emulsion or solid particle suspension to be subsequently comminuted. In the hot homogenization step the process is entirely conducted under temperatures above the melting point of the lipid. The drug is dispersed or homogenized on molten lipid with subsequent mixture with hot aqueous phase. This system is maintained hot in order to enable the reduction of oily droplets by application of a disruption force generated in a high shear homogenizer or high pressure homogenizer. The main disadvantage of this method is related to the tendency to degradation of the drug molecule, as well as the lipid material, mainly if it possesses unsaturations on its carbon structure (Sinha *et al.*, 2010).

The cold homogenization was created to overcome the temperature-induced limitations of hot emulsification. However, the thermal exposure for obtainment of a homogenous primary mixture remains an issue. The freezing of oily droplets leads to a decrease on physical strength of

the obtained micrometric solid particles which can be disrupted by homogenizers. However, in this method a broader particle size distribution is commonly achieved when compared to the hot homogenization (Mehnert and Mader, 2001). The Figure 5 depicts a scheme with possible ways of SLN® production by these methods.

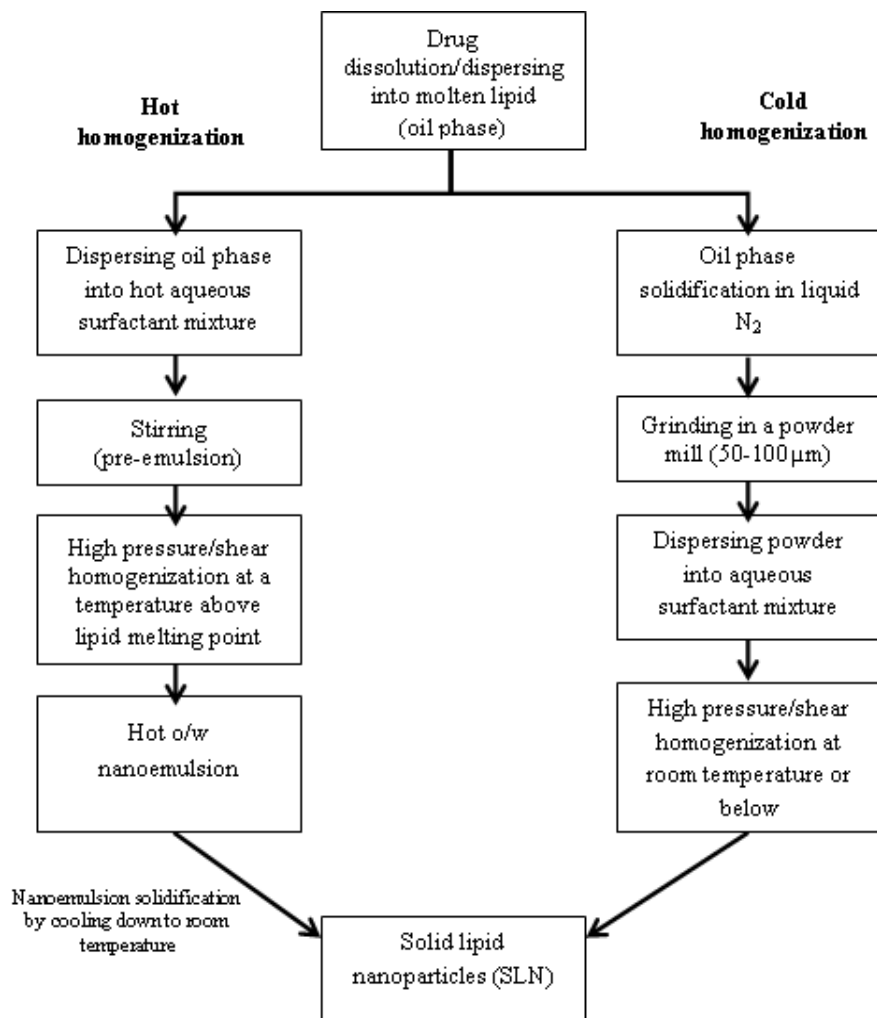


Figure 5. Scheme of hot and cold homogenization techniques applied to high pressure and high shear homogenization methods, adapted from Mehnert *et al.* (2001).

High shear homogenizers have represented some of the equipment of choice for producing SLN® suspensions. (Hou *et al.*, 2003; Chen *et al.*, 2010; Hsu *et al.*, 2010). The stator-rotor type is the favorite homogenizer for SLN® production, where the melted lipid droplets from the emulsion are broken along the rotation axis of the stator mediated by impacts into the annular chamber between stator and rotor as depicted in Figure 6 (Jamison, 1990). The SLN® size is highly dependent of shear rate. In general the primary emulsion is formulated by hot emulsification intending to maintain the melted form of the lipid and allows the comminuting of droplets up to a nanometric scale. Although this method is relatively rapid, with easy handling and scale up, it presents relevant disadvantages. The high shear homogenization demands the use of high

temperatures that compromises the stability of thermo-labile drugs. Further, it has been detected the partial distribution of the drug during the two homogenization steps and the deep concern is the presence of micron-sized particle subpopulations in the obtained SLN® suspension (Mehnert and Mader, 2001).

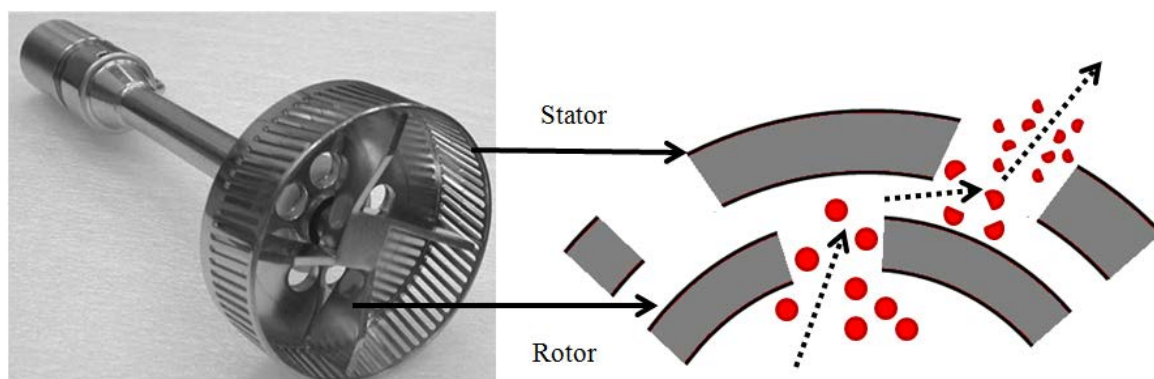


Figure 6. Scheme of particle comminuting with a rotor-stator set of a high shear homogenizer, adapted from (Doucet *et al.*, 2005)

With broad application on pharmaceutical field, the high pressure homogenizers offer several options on making ready of diverse preparations (Liedtke *et al.*, 2000). The scale up of high pressure homogenization techniques is achieved without relevant problems and, in addition, it is possible to run preparations at large range of temperatures, which allows processing of thermostable and termolabile drugs (Saupe and Rades, 2006). In these advices homogenization is achieved by a nozzle head made from ruby, sapphire, or diamond. In the nozzle setup, homogenization pressure is determined by the high pressure pump, being controlled by the force exerted over the needle blocking the fluid flow (Figure 7). The pressure driving pump (up to 400 MPa) promotes a high speed at crossover of the two flows which results in high shear, turbulence, and cavitation over the single outbound flow stream leading to reduction of particle size present into primary emulsion or suspension (Ut, 2011).

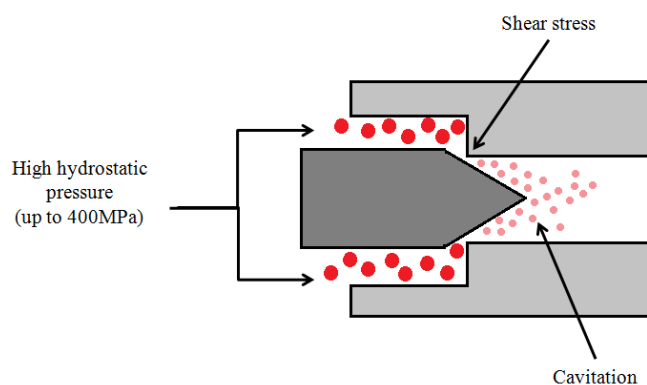


Figure 7. Scheme of comminuting of emulsion droplets by high pressure homogenization apparatus.

Despite all cited advantages, the high temperature achieved into high pressure homogenizer, as well as the high pressure and various cycles, lead to formation of particles with high kinetic energy content which results in a high coalescence tendency (Mehnert and Mader, 2001; Mäder, 2006).

Ultrasonication

This method uses ultrasound to reduce the particle size of oily droplets on a primary emulsion usually prepared by high shear equipment. The temperature above the melting point of the lipids enables the particle disruption. The process is performed by ultrasound probe or a bath. For both advises, the obtained particles carry a high energy content leading to a high aggregation tendency. The metal contamination can be a specific disadvantage related to use of a probe (Ekambaram *et al.*, 2012).

Microemulsion

This is an organic solvent-free method based on the dilution of microemulsions. The primary microemulsions are prepared by dispersion of molten lipid associated with drug substance. This hot microemulsion is diluted into cold aqueous water leading to precipitation of nano lipid drops. High-temperature gradients facilitate rapid lipid crystallization and prevent aggregation (Ekambaram *et al.*, 2012). Various works have demonstrated the use technique, however thermal exposure of drug compound remains as a significant issue (Lu *et al.*, 2008; Ma *et al.*, 2009; Kheradmandnia *et al.*, 2010).

Solvent Injection

This technique is based on precipitation of lipid particles originated from primary solution in a pharmaceutical acceptable organic solvent. This factor makes this method more preferred for drug formulation. Briefly, the solid lipid is solubilized into a water-miscible solvent, such as acetone, ethanol. Then, this solution is pumped through an injection need into an aqueous phase causing the immediate lipid precipitation. The pumping flow and inner diameter of injection micro-sized needle, as well as solubility of the lipid on primary solvent are the most important factors to determinate the SLN® size (Mishra *et al.*, 2010; Parhi and Suresh, 2010).

Solvent Emulsification-Diffusion

In this method an emulsion is prepared by solubilization of the lipid and active compound with subsequent heat in a temperature above the melting point of the lipid. This oil phase is dropped

into an aqueous phase containing emulsifiers heated at the same temperature of oil phase (Zhang, X. G. *et al.*, 2008; Subedi *et al.*, 2009; Urban-Morlan *et al.*, 2010). After continuous stirring the emulsion is refrigerated with consequent formation of SLN®. The literature relates that only solvents that show a rapid distribution into aqueous media is capable of forming nanoparticles, e.g., acetone (Mehnert and Mader, 2001). It is possible to identify clear limitations, such as the use of organic solvents that present recognized toxic potential, large polydispersity index of the obtained particles, as well as the use of high temperatures that can also lead to oxidation of lipids (Mäder, 2006).

Coacervation

The method developed by Battaglia and colleagues (2008) is based on slowly interaction between a salt of fatty acid and an acid solution (coacervating solution) in the presence of different stabilizing agents, usually polymers. This method is performed by modulation of kraft point which is coefficient solubility of monomers and micelles. Briefly, the kraft point of fatty acid sodium salts is reduced by electrolytic solution with quick cooling of the system leading to precipitation of solid particles (Corrias and Lai, 2011).

Microchannel emulsification

As depicted on Figure 8 the microchannel emulsification technique is capable of producing SLN® by promoting the interaction of an organic phase and an aqueous phase through a cross-junction system in a continuous mode. Briefly, a solution constituted by a solid lipid solubilized into a water-miscible solvent is injected into the inner capillary, while an aqueous phase with surfactant is injected into the outer capillary at the same time. When these two fluids meet in the outer capillary the water acts as an antisolvent, leading to lipid supersaturation and finally precipitation of SLN®s (Zhang, S.-H. *et al.*, 2008; Zhang, S. *et al.*, 2008).

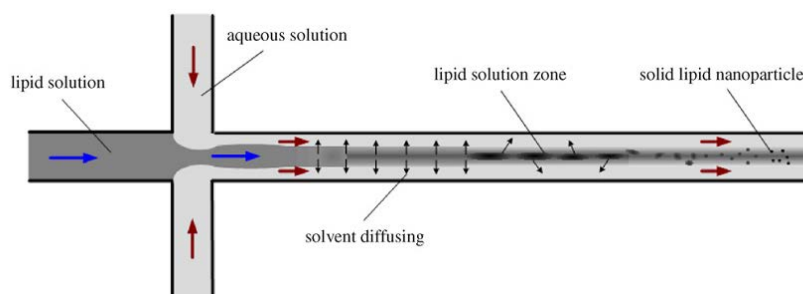


Figure 8. Scheme of SLN® formation on microchannel system (Zhang, S.-H. *et al.*, 2008).

To enhance the mass transfer of solvent from lipid solution stream into the aqueous stream Yun and colleagues (2009) added a T-junction to the microchannel system that provides a N₂ flow

at the downstream of the cross-junction into the main flow streams upward to form gas–liquid slug flow. Due to relatively more stable fluid field, efficient mass transfer and uniform concentration distribution in these microsystems, the obtained SLN® always have narrow size distribution. Problems with obstruction of microchannels during SLN® formation are commonly reported.

Membrane Contactor

The SLN® production is performed by a membrane contactor module as depicted on Figure 9. An organic solvent-lipid phase is heated in a pressurized vessel above the lipid melting point conveyed through a tube to the module and pressed through the membrane pores, allowing the formation of small droplets, which are detached from the membrane pores by tangential water flow. SLN® are formed after cooling of the obtained suspension. The water phase is generally applied at temperatures below the lipid melting point in order obtain smaller SLN® due to the sudden solidification of lipid droplets in contact with cooler aqueous stream. Usually, ceramic membranes ranging from 0.1 to 0.45 μm pore size (Charcosset *et al.*, 2005; Corrias and Lai, 2011).

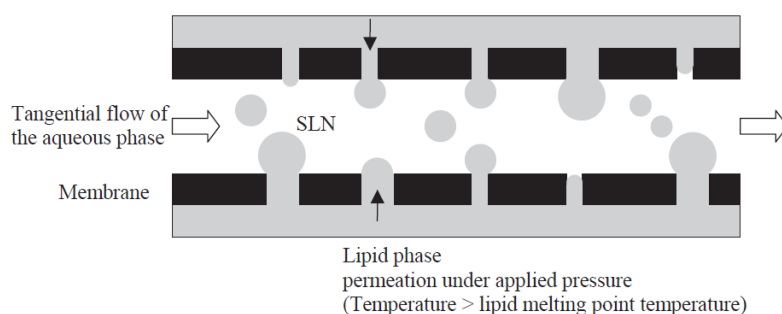


Figure 9. Scheme of SLN® formation by membrane contactor apparatus (Charcosset *et al.*, 2005).

4.2.2 Curcumin entrapment studies

Several works have been developed entrapping isolated curcumin and its analogues, as well as curcumin-rich extracts, in SLN® formulations. The Table 4 shows the works available in literature. Most of them describe the use of glyceryl monostearate, tristearin and soybean phosphatidylcholine as structural lipids associated to tween80 as main emulsifier. Due to its large acceptance as pharmaceutical excipient in several formulations by FDA, European Medicines Agency (EMA) and other Regulatory Agencies, ethanol is the organic solvent of choice in various works with curcumin entrapment into SLN®. All the works listed on Table 4 describe the use of traditional methods, among which the microemulsion technique is the most exploited. Furthermore, the anticancer activity is the most investigated biomedical application for curcumin-loaded SLN®, with a few other pharmaceutical applications and only physicochemical characterizations. Since

curcumin has a huge spectrum of bioactivities, there is a clear lack of studies investigating the biomedical potential of curcumin entrapped into SLN®.

The comprehension of the importance involved on development of curcumin-based controlled release formulations is already a reality. However, taking into account the limitations of traditional methods of production, alternative methods must be exploited intending the achievement of more efficient, innovative and safer products.

Table 4. Available works with curcumin-entrapped SLN®

Method of preparation	SLN® composition	Organic solvent	Application	Reference
Solvent injection	curcumin (150mg); stearic acid (200mg); soy PC (100mg); polyoxyethylene(40)stearate	Chloroform	Pharmacokinetic studies and asthma treatment	(Wang <i>et al.</i> , 2012)
Hot emulsification / high shear homogenization	0.1% curcuminoid extract; 5-12.5% stearic acid; 4% glyceryl monostearate; 5-15% poloxamer 188; 5-15% dioctyl sodium sulfosuccinate	Ethanol	Formulation and physicochemical studies	(Tiyaboonchai <i>et al.</i> , 2007)
	0.1% curcuminoid extract; 5-12.5% stearic acid; 4% glyceryl monostearate; 5-15% poloxamer 188; 5-15% dioctyl sodium sulfosuccinate	Ethanol	Anti-aging (cream base)	(Plianbangchang <i>et al.</i> , 2007)
	2% curcuminoids; tristearin, trimyristin, glyceryl monostearate (various ratios); 1% soy PC; 4% poloxamer 188; 3% tween 80	-	Antimalaria activity	(Nayak <i>et al.</i> , 2010)
	0.6% curcumin; 5% gelucire 50/13®; 8% poloxamer 407	-	Buccal delivery	(Hazzah, Farid, Nasra, El-Massik, <i>et al.</i> , 2015)
	curcumin (75 or 150mg); compritrol 888 ATO® (7.5g); pluronic F68 (3.75g)	-	Oral administration studies	(Righeschi <i>et al.</i> , 2016)
Hot emulsification / high pressure homogenization	0.1% curcuminoids; 10% tristearin, trimyristin, or medium chain triglycerides; 2.5% poloxamer188; 0.05% sodium azide	-	Formulation and physicochemical studies	(Noack <i>et al.</i> , 2012)
	curcumin; HSPC; DSPE; cholesterol; triolein (1.5:1:1.2:1 w/w)	Ethanol	Anticancer activity	(Mulik <i>et al.</i> , 2010)
	curcumin (8mg); glyceril trimyristate (630mg); propylene glycol caprylate (70mg); pluronic F-68 (300mg)	Ethanol	Anticancer activity	(Sun <i>et al.</i> , 2013)

	curcumin (600 mg); cholesterol (600 mg); tween 80 (0.1 g)	Ethanol/Acetone	Formulation and physicochemical studies	(Jourghanian <i>et al.</i> , 2016)
Ultrasonication	curcuminoids (900mg); stearic acid (1.8g); soy PC (3.5g); tween 80	Acetone / Dichloromethane	Pharmacokinetic and anticancer studies	(Li, R. <i>et al.</i> , 2011)
	curcumin (60mg); solid lipid (gelucire 39/01®, gelucire 50/13®, compritol 888 ATO® or precirol ATO5®) (various ratios); poloxamer 407	-	Antimicrobial activity	(Hazzah, Farid, Nasra, Hazzah, <i>et al.</i> , 2015)
	curcumin (10mg); N-hexadecylpalmitate (430mg); 1.6% tween40	-	Oral administration studies	(Kim <i>et al.</i> , 2016)
Microemulsion	curcumin; 7.27% glyceryl behenate; 0.58% soy PC; 45.45% tween80	-	Pharmacokinetic studies	(Kakkar <i>et al.</i> , 2010)
	curcumin; 0.58% soy PC 45.45% tween 80; 7.27% glyceryl behenate	-	Study on interference on brain physiology	(Kakkar and Kaur, 2011)
	curcumin; 7.27% glyceryl behenate; 0.58% soy PC; 45.45% tween80	-	Formulation, physicochemical and pharmacokinetic studies	(Kakkar <i>et al.</i> , 2011)
	curcumin; 7.27% glyceryl behenate; 0.58% soy PC; 45.45% tween80	-	Anticancer activity	(Kakkar <i>et al.</i> , 2012)
	curcumin; 7.27% glyceryl behenate; 0.58% soy PC; 45.45% tween80	-	Assessment of brain delivery	(Kakkar, Vandita <i>et al.</i> , 2013)
	curcumin; 7.27% glyceryl behenate; 0.58% soy PC; 45.45% tween80	-	Cerebral ischemic reperfusion injury treatment	(Kakkar, V. <i>et al.</i> , 2013)
Coacervation	curcumin; myristic acid, palmitic acid, stearic acid or behenic acid; varied polymeric stabilizers; citric acid, lactic acid or NaH ₂ PO ₄	Ethanol	Anticancer activity	(Chirio <i>et al.</i> , 2011)

* DSPE: distearoylphosphatidylethanolamine; HSPC: hydrogenated soya phosphatidylcholine; soy PC: natural soya phosphatidylcholine; pluronic F68®: poloxamer 188; compritol ATO 888®: glyceryl behenate; precirol ATO 5®: glyceryl distearate; dynasan 114®: trimyristin; gelucire®: mixture of mono, di and triglycerides of saturated fatty acids C8-C18.

4.3 Solid Lipid Microparticles (SLM)

The solid lipid microparticles, also referred as SLM, could be stated as the micron-sized version of SLN®. The advent of nanotechnology knowledge to biomedical field has brought a lot of attention to nanoparticles, and in counterpart, microparticulate systems have been loosen the

preference upon research matters. Among the main intrinsic drawbacks of microparticles, the limited permeation through endothelium of blood vessels has been highlighted, since the normal endothelium pore size is around 6 nm and hepatic/splenic sinusoidal endothelium have 50 and 150 nm respectively. This is not a complete disadvantage, since this endothelium impermeability also reduces the side effects risks of microparticles administered intravenously. On the other hand, tumor tissue blood vessels present larger endothelium pores, ranging from 200 to 600nm, however it still hinders the access of microparticles to malignant cells limiting the efficacy of anticancer formulations (Wang *et al.*, 2011).

Also, it has been stated that formulations composed of particles greater than 5 μm are often related to pulmonary embolism events after intravenous injections, so submicron-sized particles are indicated for this route of administration. The same concern is seen on ophthalmic route, since microparticles which size ranges around 5 μm can cause a scratchy feeling in the eyes, which justifies the recommendation of a optimal particle size less than 1 μm (Jill *et al.*, 2016). Furthermore, it has been considered a consensus that significant increases on solubility is typically achieved with particles measuring less than 200nm (Tadros, 2016). However, when oral administration is considered, even possessing micron-sized dimensions, the SLM contributes to an enhancement of drug water solubility, due to the action of pancreatic lipase and bile emulsifiers upon the lipid matrix leading to a emulsified lipid environment with subsequent solubilization of the drug (Porter *et al.*, 2007).

Despite all these limitations, the SLM still present a series of advantages when compared to SLN®. Among them, the SLM production methods commonly demand milder operational conditions, and in some cases a fewer steps. Further, the larger amount of carrier material per particle unit leads to a more extended drug release profile from SLM structures, as well as to a higher drug entrapment capability. On the other hand, the lower drug loading capacity of SLN® generally demands a concentration step of final product to reach the minimum therapeutic doses. Additionally, the micron-sized dimensions show a better fit for nasal, pulmonary and skin delivery better than nanoparticles. SLM dimensions also hinder their permeation across biological membranes which reduces their potential toxic adverse reactions when compared to nanoparticles, also typically a lower amount of surfactants is required for SLM production methods contributing to a lower toxicity profile (Scalia *et al.*, 2015)

4.3.1 Traditional methods of preparation

Most of methods applied for production of SLN® can be applied for production of SLM. The result will depend on the operational conditions, the individual characteristics of formulation

components, as well as the interaction among them. In this context, this topic will focus the methods exclusively or mostly applied for SLM manufacturing.

Spray Drying

The first patent describing the spray drying process dates from 140 years ago. Commonly performed with only one step, the spray drying technique converts a liquid mixture into dried powder. Briefly, as depicted on Figure 10 a solution or suspension is pumped into a drying chamber through a nozzle where the fluid is simultaneously atomized and quickly heated by a gas flow (generally air) at high temperatures leading to rapid solvent evaporation and collection of fine powdered material. The SLM can be produced directly by this technique. For SLN®, this technique is generally used only as a drying step, which means that it demands the processing of preformed SLN® by some of the methods discussed on topic 4.2.1. (Battaglia *et al.*, 2014; Singh and Van Den Mooter, 2016). In order to avoid pumping issues and produce small sized droplets during atomization, it is commonly required the use of solutions with low solid concentration, which means the use of large amounts of organic solvents. It explains why spray drying processes hardly produce samples with residual solvent content under Pharmacopeial limits, demanding additional drying steps (Patel *et al.*, 2015).

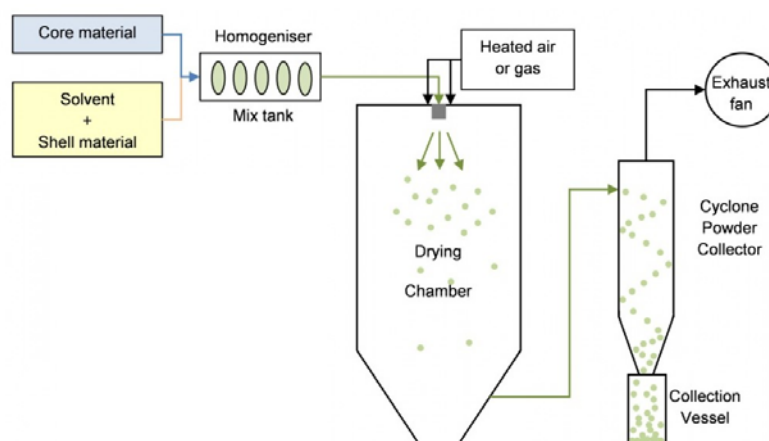


Figure 10. Typical spray drying scheme for production of particulate formulations (Sonarome, 2014).

Spray Congealing

This method is generally applied for lipids with melting point lower than 90°C. Briefly, the lipid or mixture of lipids are melted and the drug is solubilized or dispersed in this molten mass. This fluid system is then rapidly channeled to another chamber maintained under room temperature or refrigerated by dry ice or liquid nitrogen. During this channeling between the two chambers, the

molten mass is forced to pass through a atomization nozzle that generates lipid droplets that rapidly solidifies forming the SLM. This method cannot be applied for thermo-labile drugs. Primarily, the result depends on the atomization properties of the molten mixture, as well as its thermodynamic behavior and ultimately on the atomization device design (Jaspart *et al.*, 2005; Scalia *et al.*, 2015) .

Cryogenic Micronization

Also named as cold homogenization as highlighted on topic 4.2.1, this method is commonly applied as a preliminary step of SLN® production, demanding a further high shear method for particle comminuting. Shortly, a solution formed by the lipid/drug pair dissolved in an organic solvent or a melt mixture composed of molten lipid containing the drug dispersed or dissolved is stored under -80°C . After this, the frozen mixture is micronized in customized apparatus supplied with liquid N_2 (Figure 11) during the process to avoid heating and thus, any fusion which would lead to large (Del Curto *et al.*, 2003; Battaglia *et al.*, 2014).

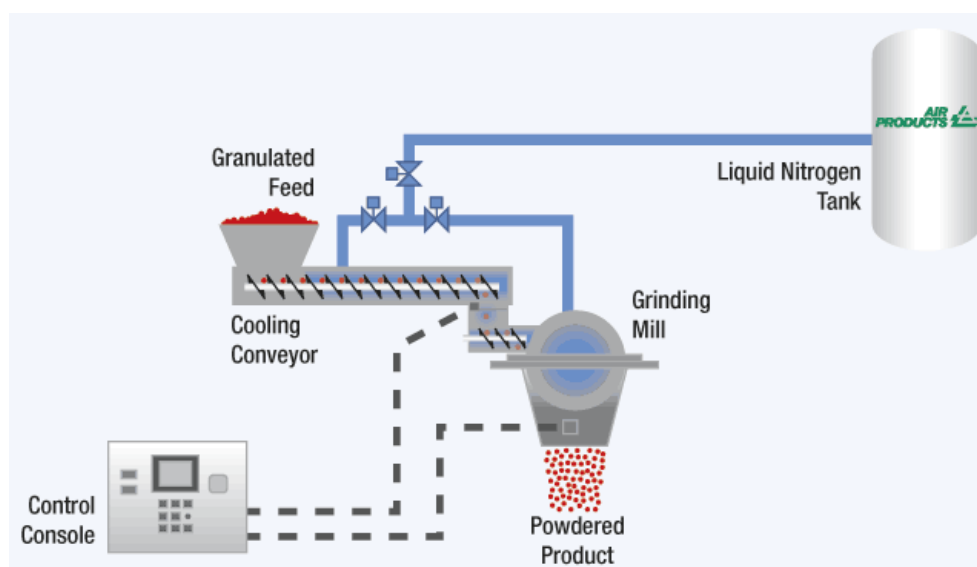


Figure 11. Scheme of cryogenic grinding/milling system provided by Air Products and Chemicals, Inc. (Air Products, 2016)

Electrospray atomization

The electrospray setup can be summarized by a metallic nozzle supplied with a high voltage power fed by a drug-containing lipid solution, working as an electrode. On the opposite site of this nozzle, a metal foil collector is placed working as a counter electrode. The compartment where the spray tower is formed is kept heated, so the solvent is evaporated and the solid particles are retained onto the collecting plate (Figure 12). Properties of the solution, flow rate and voltage applied define the mode of atomization, as well as the droplet size and shape (Trotta *et al.*, 2010; Bussano *et al.*, 2011).

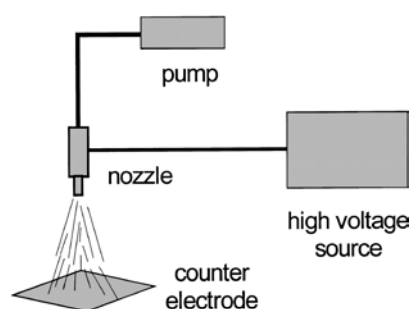


Figure 12. Generic scheme of electrospray atomization process (Ijsebaert *et al.*, 2001)

4.3.2 Curcumin entrapment studies

Yadav *et al.* (2009) investigated curcumin-loaded SLM prepared with different lipids, including palmitic acid, stearic acid and soya lecithin. Briefly a mixture of curcumin (1% w/w) and the lipid (1-10% w/w) heated at 45°C was added to heated aqueous phase containing poloxamer 188 (0.5% w/w) for obtainment of microemulsion with subsequent cooling down. It was found that the obtained curcumin-loaded SLM proved to be potent angio-inhibitory formulation. More recently, in an international conference, Geremias-Andrade *et al.* (2016) presented the study of the influence of curcumin-loaded SLM on xanthan gum gels. SLM were produced with babacu (*Orbignya speciosa*) oil (2.8 % w/w) and tristearin (1.2 % w/w), with mixtures of tween 60 and span 80 at different concentrations (2 and 4% w/w) encapsulating 0.03 % w/w of curcumin. By comparing these few data with the whole bunch of works listed on Table 4, it is obvious the preference on scientific field for researching of SLN® platform for curcumin encapsulation. It is clear a huge lack of studies focusing the association of curcumin to SLM, which makes this theme even more attractive.

5 Supercritical Fluid Approach

Supercritical fluid is defined as the state of a substance at which both temperature and pressure are above its critical values. Specifically, supercritical carbon dioxide (scCO₂) offers a wide range of applications in the pharmaceutical field (Sekhon, 2010). The use of CO₂ as a solvent or raw material has been investigated in academia and/or industry since 1950 and has intensified thirty years later with implementation of large-scale plants using online systems (Beckman, 2004). The approaches for processing bioactive compounds include mainly the particle size reduction of bulk products to nanometer scale (Martín and Cocero, 2008) and association of drug molecules to particulate carriers (Cocero *et al.*, 2009; Reverchon *et al.*, 2009).

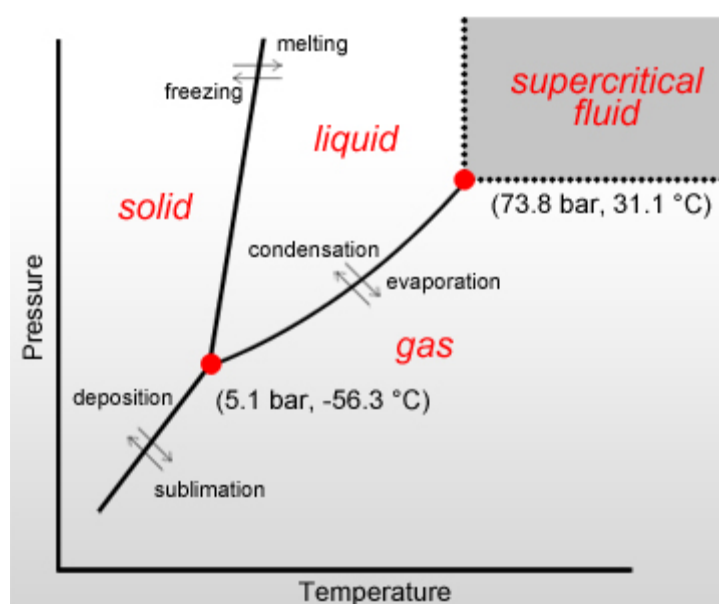


Figure 13. P-T phase diagram of pure CO₂

For wide range of supercritical carbon dioxide applications, several techniques are available due to the high versatility of scCO₂, which may be explained by the *sui generis* behavior common to supercritical fluids. At the supercritical state, CO₂ is neither a gas nor a liquid but has intermediate properties of both. It presents viscosity and diffusivity values typical of a gas and density values of a liquid. These characteristics provide to scCO₂ appreciable solvent power and facilitate mass transfer processes. Indeed, scCO₂ is dense but highly compressible, allowing easy modulation of its solvent power by few adjustments of temperature and pressure (Barry *et al.*, 2006; Moribe *et al.*, 2008; Pasquali; *et al.*, 2008). Thus, the fine modulation of scCO₂ physical chemical properties allows its use as a solvent, anti-solvent or solute according to specific operation conditions and physic-chemical features of the bulk material, which generates a relevant variety of processes (Yeo and Kiran, 2005; Bahrami and Ranjbarian, 2007; Badens, 2010).

CO₂ reaches its critical point at 31.1 °C (304.15 K) and 73.8 bar (7.38 MPa) (Figure 13), which allows processing of bioactive compounds under mild operation conditions avoiding their degradation (Barry *et al.*, 2006). scCO₂ is a good solvent for several non polar, and some polar, low molecular weight compounds and some few polymers, such as amorphous fluoropolymers and silicones (Davies *et al.*, 2008). Also, scCO₂ presents a non negligible solubility on some polymers and lipids, typical drug carriers. The solubilization of scCO₂ promotes the decrease on viscosity of the molten drug carrier making possible their pumping through the plant (Nalawade *et al.*, 2006). Other significant advantages of scCO₂ processing include the non-flammability, its relative low cost, the possibility of its total recycling, the production of organic solvent-free particles, the achievement of particulate systems with a narrow distribution of particle size and single-step operation. Furthermore, all process runs into a closed system facilitating the establishment of ascetical production of sterile formulations (Beckman, 2004).

5.1 Solid Lipid Particles (SLN® and SLM) Production by scCO₂ Processing

5.1.1 Supercritical Fluid-Based Coating Technique

Benoit *et al.* (2000) developed a relatively rapid, simply and totally solvent-free technique for coating drug particles with solid lipid compounds. The same group demonstrated the performance of its proposed method by encapsulation of bovine serum albumin (BSA) crystals with trimyristin and Gelucire® 50-02, a commercial mixture of glycerides and fatty acid esters (Ribeiro Dos Santos *et al.*, 2002). The scheme of the apparatus used is depicted in Figure 14. The mechanism of coated particle formation is composed by the total solubilization of the solid lipid into scCO₂ in a thermostated high pressure mixing chamber loaded with BSA crystals. After 1h of mixing the chamber was depressurized and scCO₂ turned to the gaseous state with consequent precipitation of the lipid on the crystals surfaces. This work was described with more details in other three articles (Ribeiro Dos Santos, Richard, *et al.*, 2003; Ribeiro Dos Santos, Thies, *et al.*, 2003; Thies *et al.*, 2003).

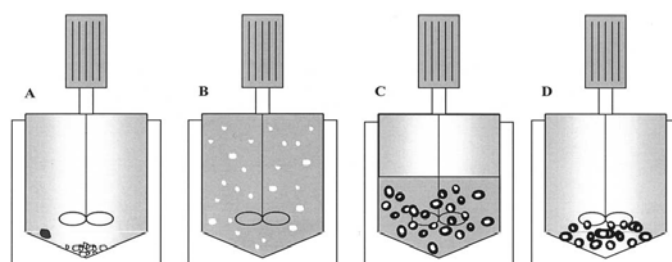


Figure 14. Schematic representation of the coating process developed by Ribeiro dos Santos *et al.* (2002). (A) Filling step: BSA crystals (white) and lipid material (black); (B) Solubilization of lipid in scCO₂ with dispersion of insoluble BSA crystals; (C) Decompression phase with lipid deposition on BSA; (D) Coated particles are obtained.

Since Gelucire is a mixture, it does not crystallize, allowing a uniform coating of BSA, while trimyristin crystallizes and forms a needle-like structure around BSA crystals leading to a burst release from the particles. However, this method is restricted to lipids with considerable high solubility into scCO_2 and the particle size is dependent on the size of the original BSA crystals. Thus, to obtain solid lipid particles with a narrow particle size distribution, the bulk drug has to be processed by an additional technique, which rises the total cost of the process.

5.1.2 Supercritical Fluid Extraction of Emulsions (SFEE)

The SFEE technique developed by Chattopadhyay and co-workers (2006) was conceived by coupling of a conventional method for oil in water (o/w) emulsion with a subsequent scCO_2 extraction process. The emulsion is typically prepared by dissolution of a solid lipid and a drug into an organic solvent, which is dispersed into the aqueous phase by an homogenizer equipment, using a certain surfactant for stabilization. Further, the emulsion is pumped through an atomization nozzle and submitted to an extraction of the organic solvent by scCO_2 in countercurrent flow. As a consequence, solidification of lipid droplets occurred and SLN® precipitated from the aqueous suspension (Mantripragada, 2003; Chattopadhyay, Pratibhash *et al.*, 2006).

Compared to traditional methods, this technique brings the advantage of enhancing the removal of the internal organic phase without affecting the emulsion stability, with shorter processing time, and innocuous residual solvent concentration in the final product. Furthermore, due to the diffusivity of scCO_2 , mass transfer for solvent removal is more efficient in comparison to conventional methods, which leads to a more efficient particle size distribution, avoiding aggregation (Chattopadhyay *et al.*, 2005; Shekunov *et al.*, 2006; Obeidat, 2009). Figure 15 illustrates the extraction plant used by Chattopadhyay *et al.* (2007) for production of SLN® constituted by tripalmitin, tristearin or Gelucire 50-13.

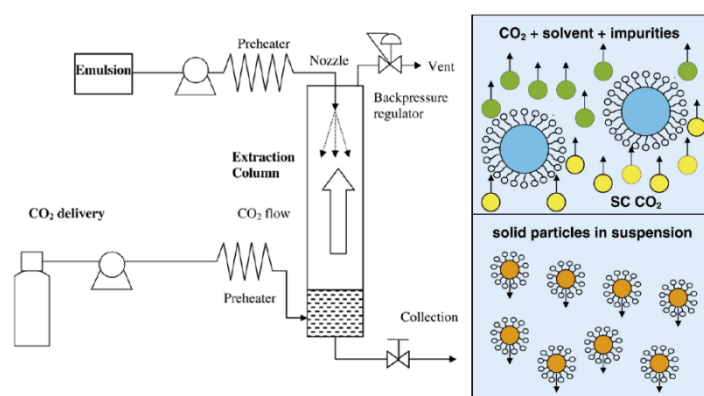


Figure 15. Extraction system used in SFEE process developed by Chattopadhyay *et al.* (2007)

After preparation of an o/w emulsion with oil phase composed by the drug and lipid dissolved into chloroform, the solvent was extracted with a scCO₂ counter-current at a flow rate of 40g.min⁻¹. SLN® with a mean diameter of 30 nm were obtained, but with a bimodal population composed by a primary peak ranging from 20 to 60 nm and a secondary one (<10%) of about 200 nm. A residual chloroform concentration of less than 20 ppm was detected, which is in accordance with the International Conference on Harmonization (ICH) guidelines that established the limit for this solvent is 60ppm (Grodowska and Parczewski, 2010).

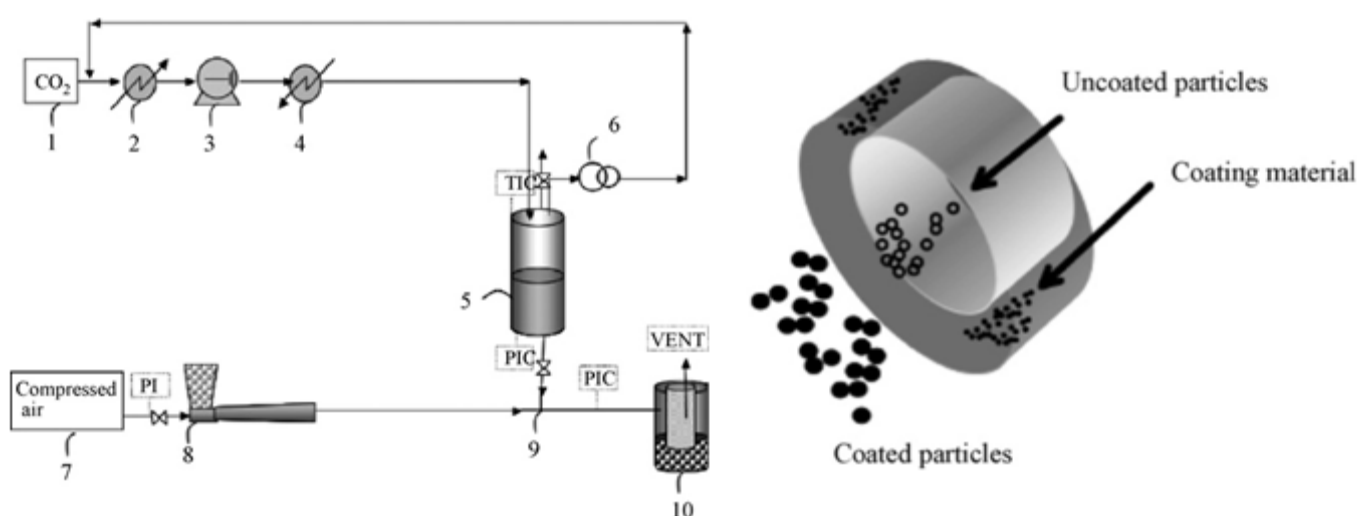
Earlier, by using the SFEE apparatus shown in Figure 15, Shekunov *et al.* (2006) performed micronization studies of cholesterol acetate and griseofulvin and evaluated some important factors for definition of particle size that can be taken in consideration for SLN® production. It was observed that the droplet size, drug concentration and solvent content are the major factors with significant influence on particle size. Naturally, as lower is the size of o/w emulsion droplets, smaller are the particles obtained. Thus, the stabilization of the emulsion by using a surfactant is highly important owing to its capability to assure the maintenance of small droplets and avoid aggregation events (Chung *et al.*, 2001). On the other hand, the partial interaction of the drug molecule with the aqueous media may promote the interaction among droplets that aggregate and form larger particles. In addition, considering that supersaturation in emulsion droplets is important for formation of small particles, increasing the solvent content promotes an increase on the growth rate. These conclusions also agree with studies conducted with PLGA nanoparticles (Chattopadhyay, P. *et al.*, 2006).

Despite the benefits of this technique, it is important to emphasize its remarkable disadvantages, such as the demand of multiple steps and the use of organic solvents. Moreover, the first step of SFEE keeps all the disadvantages associated to conventional methods of SLN® production.

5.1.3 Supercritical Co-Injection Process

Developed by Calderone and coworkers (2006), the co-injection process was presented as a new way for obtaining of solid lipid microparticles. As described in Figure 16, first a solid lipid is melted under its normal melting point due to the plasticizing effect exerted by solubilization of a pressurized gas. Second, the expansion of the gas-saturated melted lipid phase causes its pulverization, which occurs in a custom-designed co-injection device, where particles of uncoated drug are conveyed by a Venturi system at the same time. The co-injection provides the coating of the drug particles (Calderone *et al.*, 2008).

This method presents the advantage of maintaining the active principle ingredient in a different reservoir of that used for coating the material, in a way that the drug component may be exposed to room temperature avoiding its degradation. By using of Precirol® ATO5 for coating pseudoephedrine chlorhydrate (PE) and bovine serum albumin (BSA) the method was tested by Calderone *et al.* (2008). It was shown an effective coating of the particles, with significant delay of the drug release in aqueous media. Meanwhile, the observed drug release cannot be classified as prolonged due to the relatively short time for release of 100% of entrapped PE (50min) and BSA



(30min). SLM ranging from 16.4 to 65.4 μm were obtained. In pre-tests carried out with glass beads for validation of this method, it was found that for beads smaller than 20 μm aggregation events were very common.

Figure 16. A: Schematic representation of the supercritical co-injection process (1) CO₂ cylinder (2) cooler (3) pump (4) heater (5) saturation vessel (6) high pressure vessel (7) valve (8) pneumatic conveying (9) co-injection advice (10) gas/solid separation filter; B: co-injection device (Calderone *et al.*, 2008).

5.1.4 Particles from Gas Saturated Solutions (PGSS)

Among the available techniques for SLN® and SLM production by supercritical fluid processing, particles from gas saturated solutions (PGSS) has been shown as the most interesting. PGSS is a process where a solid is melted in a high pressurized vessel. Figure 17 shows a generic scheme of a PGSS plant used for drug-loaded polymer and lipid particles. Briefly, a gas-saturated polymeric or lipidic solution is expanded through a nozzle and the rapid cooling of the gas leads to quasi-instantaneous solidification of the fresh droplets formed in the upcoming spray from the nozzle, which constitutes the SLN® (Weidner *et al.*, 1995). This rapid cooling of the gas during the

expansion process is due to the Joule-Thomson effect. In few words, since an expansion of a gas from high to low pressure through a throttle valve is an isenthalpic process, it leads to a significant temperature drop.

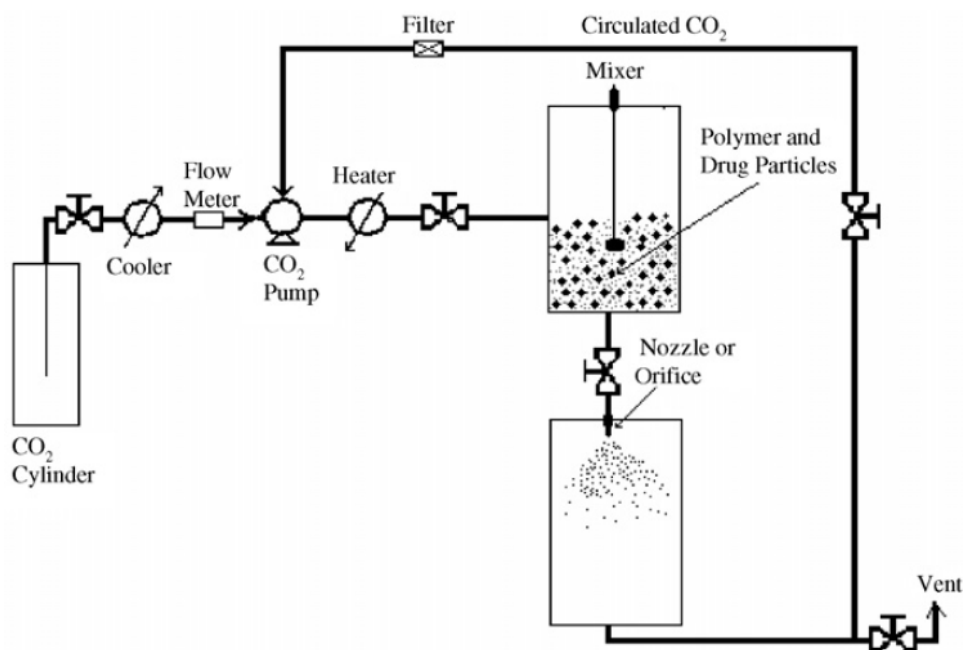


Figure 17. Example of PGSS plant for particle formation of drug-loaded particles (Bahrami and Ranjbarian, 2007).

The pressure change occurs so fastly that no significant heat transfer occurs, so the Joule-Thomson coefficient (μ) is enough suitable to describe the relation between pressure and temperature variations. Since μ relates pressure and temperature variations according to the Equation 1, a significant drop of pressure leads to a significant decrease of temperature. That is exactly what occurs on PGSS. The expansion of CO₂ from the supercritical state to the atmospheric pressure leads to a huge temperature drop that rapidly solidifies the atomized molten lipid droplets formed by the nozzle.

$$\mu = \left[\frac{\partial T}{\partial p} \right]_h \quad (1)$$

In addition to all advantages of supercritical fluid technology, PGSS can produce directly powdered formulations, requires the use of small volume pressurized equipment, demands relatively low amounts of CO₂, and easily performs the recovery of the product and the gas. This process already runs in plants with capacity of some hundred kilograms per hour (Knez and Weidner, 2001). Other great advantage of PGSS technique resides on the plasticizing effect of scCO₂ when diffused into polymer or lipid matrix, which allows their melting under mild temperatures, becoming feasible for thermolabile drug processing (Alessi *et al.*, 2003; Pasquali *et al.*, 2008). The high diffusivity of scCO₂ allows its penetration in the lipid matrix, reducing the

intermolecular interactions, increasing the chain separation and enhancing the mobility of lipid segments, acting as a molecular lubricant (Samyuktha *et al.*, 2014). Further, the saturation of bulk lipid with scCO₂ favors the formation of CO₂-lipid complexes through van der Waals interactions (Ekambaram and Abdul Hasan Sathali, 2011).

The group of Weiner *et al.* (2001) was the first one to demonstrate this plasticizing effect with a lipid as can be noted in Figure 18, where the melting point of a monoglyceride was monitored under increase of pressure in a CO₂ environment. However, it is also noted that over 200 bar, the melting point increases. González-Arias *et al.* (2015) defend that in the pressure range where a melting point decrease is noted, there is a predominant effect of the solubility of the gas in the solid lipid. Above this range, the hydrostatic pressure takes place and makes the melting temperature rising. In the same Figure it is depicted a very similar behavior for tripalmitin (Li *et al.*, 2006), Precirol® ATO5 (Sampaio De Sousa *et al.*, 2006; Calderone *et al.*, 2007), Compritol® 888 ATO (Sampaio De Sousa *et al.*, 2006) and Gelucire® 43-01 (Sampaio De Sousa *et al.*, 2006).

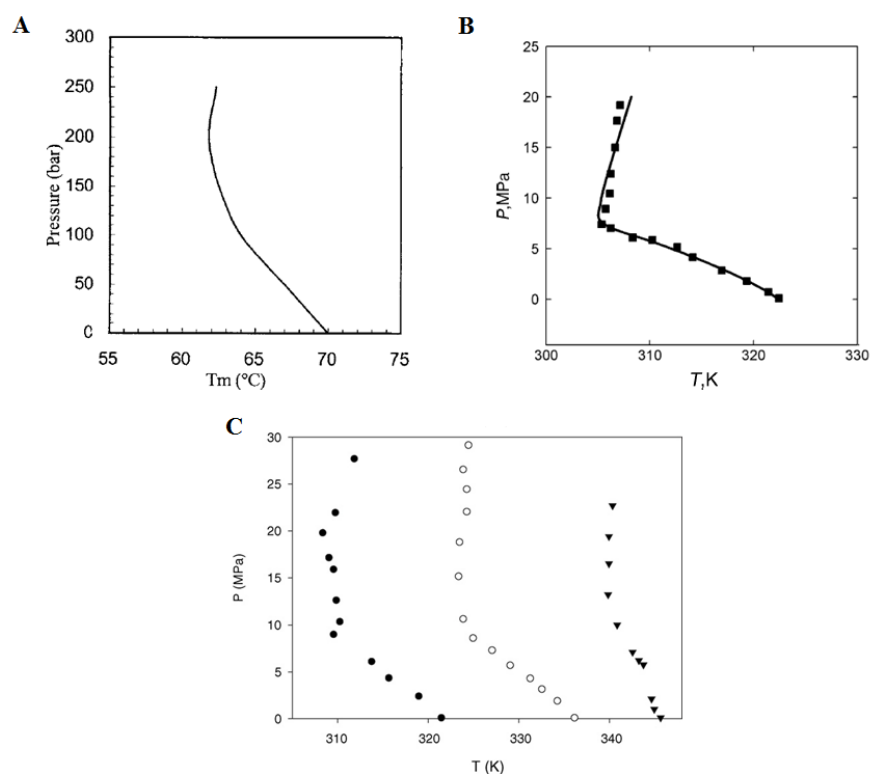


Figure 18. Variation of lipid melting point under CO₂ at different pressures. A: monoglyceride (Knez and Weidner, 2001); B: tripalmitin (Li *et al.*, 2006); C: Gelucire® 43-01 (●), Precirol® ATO5 (○) and Compritol® 888 ATO (▼) (Sampaio De Sousa *et al.*, 2006).

The pressure-temperature (P-T) phase diagram for the binary mixture solid-supercritical fluid can show varied behavior. Figure 19 depicts the typical P-T phase diagram for scCO₂-solid lipid mixture (Schmidts *et al.*, 2012). These plots are commonly seen for mixtures whose

components are not chemically similar and differ considerably in size and shape. In other words, this diagram would be the most suitable to describe the phase behavior of a system designed for production of SLN®/SLM by PGSS.

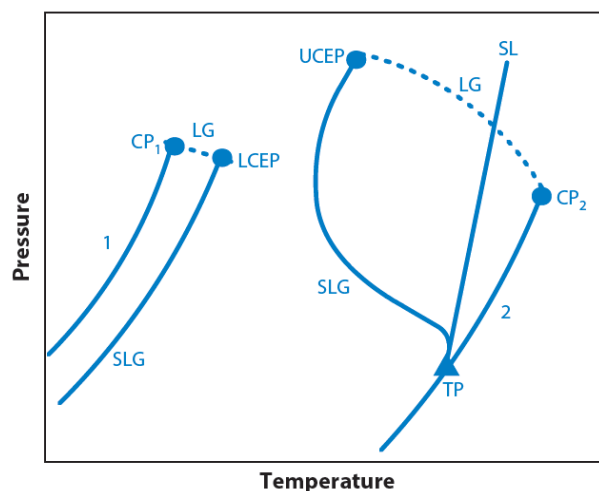


Figure 19. Typical P-T phase diagram for CO₂-solid lipid system. Abbreviations: LG, liquid-gas; SL, solid-liquid; SLG, solid-liquid-gas; TP, triple point; CP1 and CP2, critical points of pure compounds (1 and 2); 1, 2, vapor pressure curves of pure compounds. 1 is stated for CO₂ and 2 for solid lipid (Liu, 2008).

In this kind of system, there is no common range of temperature, in which both compounds are in the liquid state. Also, the critical mixture curve represented by the dotted liquid-gas (LG) equilibrium line and the solid-liquid-gas (SLG) equilibrium curve are not continuous. The lower temperature branch of the SLG curve describes the solubilization of lipid molecules into CO₂ dense gas phase until the intersection with the critical mixture curve at the lower critical end point (LCEP), where the lipid solubility increases rapid but still slight. Simply, the LCEP is the lowest temperature and pressure in which gas and liquid phases become a single phase in the presence of a solid phase, while the upper critical end point (UCEP) represents the highest conditions where this equilibrium phenomenon occurs. At the higher temperature branch of the SLG curve, the solubility of dense or supercritical CO₂ into lipid matrix is incremented which leads to a modulation of the S-L transition, i.e. melting point, of the lipid (Griffin, 1949; Liu, 2008; González-Arias *et al.*, 2015) This SLG curve branch has been experimentally demonstrated as depicted on Figure 18.

All these thermodynamic equilibrium phenomena is occurs during the saturation step of PGSS procedure, where the lipid matrix is mixed with CO₂ under high pressure conditions. After, under room conditions of temperature and pressure, the rapid expansion step leads to the quasi-instantaneous flash composed of a solid phase represented by the particles and a gas phase represented by the CO₂. The Figure 20 correlates regions of the typical P-T phase diagram for CO₂ and solid lipid system with corresponding steps on PGSS procedure.

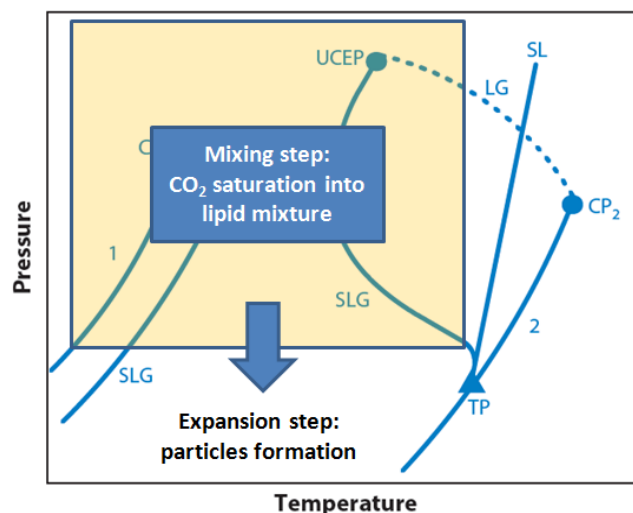


Figure 20. Typical P-T phase diagram for CO₂-solid lipid system with a proposed localization of PGSS steps.

However, the mechanisms of particle formation are not completely understood. Several studies have been conducted for modeling of particle formation in PGSS and it was found that expansion process is composed by atomization and nucleation/crystallization phenomena (Li *et al.*, 2005; Strumendo *et al.*, 2007). Briefly, the atomization can be defined as the disruption of a liquid jet in fine particles during expansion (Reitz and Bracco, 1982). Further, the nucleation describes the formation of CO₂ bubbles inside the fresh droplets of the mixture constituted of the molten lipid and drug due to the transition of the supercritical fluid to the gaseous state on the expansion chamber and the crystallization evolves the solidification of the particle surface and subsequently the inner lipid matrix under abrupt decrease of temperature due to Joule-Thompson effect (Kappler *et al.*, 2003).

Studies have indicated that nozzle diameter, pre-expansion pressure and temperature, and flow rate of carbon dioxide represent the most important factors for defining size, shape and physical state of the particles (Brion *et al.*, 2009). It has been found that as higher the saturation pressure as higher carbon dioxide diffusion is achieved into polymer or lipid matrix, while there is an inverse relationship between scCO₂ solubilization and saturation temperature (Mandzuka and Knez, 2008). The high content of scCO₂ favored by high saturation pressure leads the nucleation process to occur faster than crystallization of surface during the expansion step resulting in the formation of small particles. However, as higher scCO₂ content more abrupt is the disruption of the lipid matrix with potential formation of particles of highly varied shape. This is not a desirable effect considering that particles of varied shape commonly present a burst release of the active compound (Kappler *et al.*, 2003).

For the temperature the opposite effect on particle size is observed, i.e., the particle size increases with increasing temperature above the melting point of the carrier material. This can be explained by the decrease of scCO₂ solubility upon increasing temperature. Thus, with lower fluid content into the particles, the crystallization of the particle surface occurs faster than CO₂ bubbles formation which leads to retention of the gas and less disruption events resulting in larger particles. This phenomenon is readily observed when the selected saturation temperature is already below the lipid or polymer melting point (Nalawade *et al.*, 2007). Figure 21 presents a scheme with different particles obtained with different operation conditions in a work performed by Kappler and coworkers (2003).

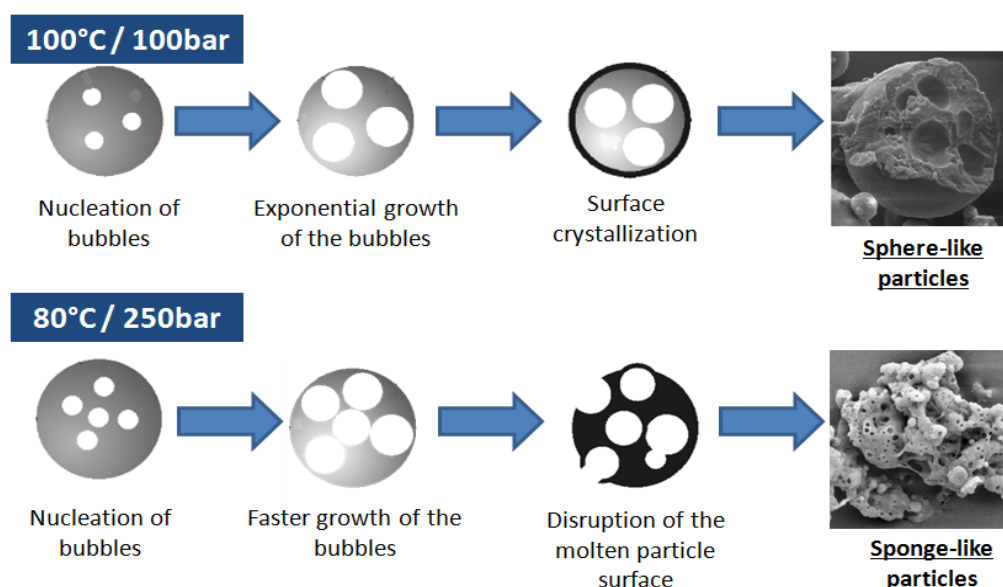


Figure 21. Schematic representation of different results obtained under different operational conditions in a PGSS method for production of PEG-600 particles (Kappler *et al.*, 2003).

Despite the wide range of available lipids and drug molecules, the operational conditions are unique depending upon the specific system. Rodrigues *et al.* (2004) produced microcomposite lipid particles composed by hydrogenated palm oil entrapping theophylline by PGSS. Solid lipid particles of about 3µm were obtained for a mixing step at 333 K and a pressure range of 12-18 MPa, and a nozzle diameter of 25 µm. It was also observed that an increase in the pre-expansion pressure leads to the formation of more spherical and larger particles. On the other hand, burst release of theophylline from the particles was detected. In a similar PGSS apparatus and for the same pre-expansion operational conditions Wang *et al.* (2008) achieved trimyristin and tripalmitin particles loaded with ibuprofen of about 2 µm diameter. However, a 100 µm diameter nozzle was used, indicating that the type of lipid and saturation time also have a significant role on the particle size distribution. Equipped with an 80 µm diameter nozzle and under the same pre-expansion

conditions, these authors showed less attractive results from lipid particles synthesized with beeswax and menthol. A multimodal population of particles ranging from 45 to 180 μm was obtained (Zhu *et al.*, 2010).

By application of similar conditions, Sampaio de Sousa and coworkers (2007) achieved glyceryl monostearate microparticles loaded with caffeine of about 5 μm diameter. However, due to the hydrophilicity of caffeine, it was necessary to use water as co-solvent. Further studies under 13 MPa and 345 K with the addition of Cutina® HR and titanium dioxide (an anticaking additive) in the formulation showed that the low affinity of the hydrophilic compounds like caffeine and glutathione resulted in a low payload and a burst release. Otherwise, a lipophilic compound, ketoprofen, presented a high entrapment rate and sustained release ($t_{2h} = 20\%$) (García-González *et al.*, 2010). The same group, trying to improve the physicochemical features of solid lipid particles, associated solid lipids to polymers to produce hybrid particles by PGSS. The first work associated a hydrophilic polymer PEG4000 (HLB=18) to a hard fat Gelucire® 43/01 (HLB=1) by mixing, both molten, in the high pressure chamber of PGSS apparatus. Since these components have no chemical affinity their mixing leads to the formation of an emulsion, where CO_2 was dissolved. Temperature and pressure employed had no clear influence on particle shape, while more sphere-like particles were obtained when nozzle diameter was reduced from 600 to 300 μm . Among the different ratios of Gelucire/PEG4000, some of them presented a core-shell structure where the outer layer was proved to be formed by PEG4000 (Rodríguez-Rojo *et al.*, 2010). Later, in order to improve the stability of the particles and guarantee the formation of a core-shell structure, the emulsion was prepared with an emulsifier Inwitor® 600 (HLB = 4). As the best result spherical multicore hybrid particles were obtained from the expansion of a CO_2 saturated O/W macroemulsion at 12 MPa and 323 K, with a PEG:Gelucire mass ratio of 3:1. They presented 227 μm ($d_{0.5}$) with a structure composed by PEG outer layer with multiple Gelucire cores (Gonçalves *et al.*, 2015).

Intending the successful achievement of solid lipid particles in nanometric scale, Bertuccio *et al.* (2007) developed a modified PGSS method in which the particle formation is assisted by an auxiliary gas (synthetic air, nitrogen or the combination of both). This modification enabled the formation of submicron-sized lipid particles. Based on this method, with pre-expansion conditions set at 150 bar and 40 °C and a 100 μm nozzle diameter, SLN® loaded with insulin or human growth hormone (HGH) were produced with a lipid matrix composed of phosphatidylcholine and tristearin. Spherical shape particles were obtained with a mean diameter of 197 nm and a mean loading efficiency of 57 % and 48 % for insulin and HGH, respectively (Salmaso, Bersani, *et al.*, 2009). Taking into account that insulin is a hydrophilic protein, other work using DMSO as co-solvent

promoted an increase in the loading efficiency to 80 %, with values of residual solvent below 20 ppm (Salmaso, Elvassore, *et al.*, 2009). By using the same saturation conditions, SLN® based on tristearin and magnetite nanoparticles (Fe_3O_4) of about 200 nm were also produced and the loading capacity was slightly increased with addition of phosphatidylcholine (Vezzù *et al.*, 2010).

The good results obtained by Bertucco and coworkers in entrapping hydrophilic compounds in SLN®, keeping a sustained release, reveals the need of selecting the correct emulsifier and/or co-solvent. Otherwise, a low encapsulation rate is achieved and also a segregation of the drug from the lipid matrix may occur during particle formation in the expansion unit. This condition favors the deposition of the drug on the particle surface generating a burst release (García-González *et al.*, 2010).

More recently other group used a PGSS apparatus for production of solid lipid microparticles constituted of fully hydrogenated canola oil (FHCO) entrapping spearmint essential oil (Ciftci and Temelli, 2016). After evaluating different nozzle diameters (0.1, 0.3 and 14.3 mm) and pressures (122, 211 and 300 bar), the best results were obtained for a 0.1 mm nozzle diameter at 122 bar, providing particles with 1.27 μm diameter and 96 % of encapsulation efficiency. Taking into account that essential oils are composed of volatile components, part of the spearmint essential oil solubilized in the supercritical phase was carried away during the expansion step leading to a decrease on EE%.

Thus, facing the limitations of SFEE and supercritical coating techniques, PGSS has been extensively investigated. Furthermore, the successfully generation of submicrometric particles by Bertucco and coworkers show that plant adaptations have a central role in PGSS optimization. Due to the particular features of each system, there is no standard fixed condition for production of SLN®. Therefore, an adequate knowledge about physicochemical characteristics of the lipid carrier and the drug molecule is pivotal for the correct choice of optimum operational conditions. The versatility of scCO_2 -based systems provides various alternative solutions. As a consequence, complementary studies have to be conducted to optimize the production of submicron sized solid lipid particles, with high loading efficiency, low polydispersity and controlled drug release.

This vast summary serves as a guide to choose suitable operational conditions, mainly structural set plant arrangements, for particle production by PGSS. Also, based on these data, it can be suggested that the utilization of scCO_2 technology in the production of SLN® and SLM entrapping pharmaceuticals and biopharmaceuticals is a promising field under intense investigation. The encapsulation of curcumin in SLN® and SLM produced by scCO_2 is an interesting and innovative process and there is no patent registered so far.

Aim of work .

1 General Aim

The general aim of this work is the investigation of curcumin entrapment into SLN® and SLM by PGSS process.

2 Specific Aims

- Investigation of operational conditions of particle production by PGSS;
- Study of the particle engineering related to supercritical fluid technology processes;
- Comprehension of physicochemical interactions among lipid carriers, curcumin and CO₂;
- Improvement of PGSS particle production by optimization of curcumin entrapment rate;
- Physicochemical and cytotoxicity profile characterization of curcumin-loaded SLN® and SLM.

Material and Methods **IV**

1 Material

Tristearin with purity higher than 99%, dimethylsulfoxide, dichloromethane and citric acid were purchased from Sigma-Aldrich (St. Louis, MO). Epikuron 200 was a kind gift from Cargill Inc. (Minneapolis, MN). The 98% pure curcumin, HPLC grade methanol, ethanol and acetonitrile were acquired from Merck (Darmstadt, Germany). CO₂, synthetic air and N₂ were purchased from Rivoira (Padova, Italy).

2 Methods

2.1 Solid Lipid Particle Production

The production of solid lipid particles was performed as described on the article published on The Journal of Supercritical Fluids which the full text can be found on the Chapter V of this thesis. For more details, go the Attachment I of this thesis.

2.2 Solid Lipid Particle Characterization

2.2.1 DSC measurements

Differential Scanning Calorimetry was performed using a TA Instruments calorimeter (model Q10P). This instrument is equipped with a high pressure cell that enables measurements to be performed in the presence of CO₂ up to a maximum operating pressure of 7 MPa. An amount of 1-5 mg of mixture (or pure lipid) was weighted into an aluminum pan and placed in the calorimeter. Lipid mixtures with different ratios of tristearin and phosphatidylcholine comprising 0, 25, 31, 40, 57, 67 and 100% were analyzed. For experiments involving CO₂, the cell was pressurized to the desired operating pressure prior to heating of the sample. A continuous flow of CO₂ was maintained through the cell during the heating cycle. The sample was heated from 40 to 300 °C at a rate of 10°C/min. DSC measurements for a given sample were performed at least three times.

2.2.2 Percentage of encapsulated curcumin

The entrapment efficiency (EE%) of curcumin into the lipid particles was determined by a RP-HPLC method using a Phenomenex Luna C18 column isocratically eluted at 1 mL/min with 0.5 % citric acid (pH 3.0)/ acetonitrile 48:52 ratio. The UV detector was set at 429 nm. 5 mg of particles were disrupted in 1 mL of methanol by vortexing for 1 min and centrifuged at 14,462 xg for 15 min. The clear supernatant was diluted in mobile phase and analyzed by HPLC. All the samples were analyzed in triplicate.

2.2.3 Size measurements and morphology

Particle size measurements were carried out by static light scattering analysis using a mastersizer 2000 equipment (Malvern, UK). Around 10 milligrams of solid material were dispersed under vortexing in 15 mL deionised water, sonicated for 30 min, and analyzed. The samples were then centrifuged upon 2.500 rpm for 3 min in order to investigate the presence of nanoparticles. The obtained supernatants were analyzed by the dynamic light scattering method in a zetasizer nano ZS apparatus (Malvern, UK) after the same sample treatment.

The morphology of micronized particles was assessed by scanning electron microscopy (SEM) directly on the dry particle samples mounted on metal stubs and after 20 nm-thick gold-coating treatment. The micrographs were obtained by a JSM-6390LV digital scanning electron microscope (JEOL, Peabody, USA) using an acceleration voltage of 10 kV at different magnifications. For those samples with readable sign on nanosizer, negative stain micrographs were prepared on copper grids covered with a formvar film. The vesicle dispersion was pipetted into the grids and stained with 2 % phosphotungstic acid and were then viewed and photographed with a JEOL 1230 transmission electron microscope (JEOL, Peabody, USA) at an accelerating voltage of 60 kV.

2.2.4 IR Spectroscopy

Infrared spectra from free curcumin, empty solid lipid particles, as well as those curcumin-loaded particles were recorded by a FTIR spectrometer (Shimadzu, Quioto, Japan). The samples were analyzed after mixing with dried KBr powder and compressing to a disc by a beam splitter. All data were collected over the spectral range 4000 to 400 cm^{-1} , with a nominal resolution of 4 cm^{-1} .

2.2.5 Cell Viability Test

Due to limitations presented by specific characteristics of samples, only those with 0.5 % curcumin composition were submitted to the cytotoxicity test. More details concerning this topic is explained on the third section of chapter V of this thesis. The cytotoxicity of curcumin-loaded lipid particles against C2C12 myoblasts, obtained from skeletal muscle of mice, was measured by MTT assay. The cells were seeded in a 96-well plate in a density of 2×10^3 cells/well and incubated for 24 h. The medium was then replaced with increasing concentrations of curcumin, drug-loaded lipid particles and drug-free lipid particles. Incubation was continued for 72 h. All media were then removed and 100 μL of MTT solution at 0.5 mg/mL in PBS were added to the wells. The cells were incubated for 3 h. MTT was removed and 100 μL was added to dissolve the formazan crystals. The optical density at 570 nm was determined using a microplate reader. Untreated cells were taken as

control with 100 % viability and cells without MTT were used as blank to calibrate the spectrophotometer to zero absorbance. Triton X-100 at 1% (v/v) was used as positive control of cytotoxicity. All experiments were performed in triplicate. Statistical analysis was performed by one-way ANOVA followed by Newman Keuls multiple comparison test.

Results and Discussion.

Thermal investigations on Curcumin/Lipids/DMSO/CO₂ mixtures

1 DSC Measurements

1.1 System 1 lipid + CO₂ and 2 lipids + CO₂

Experimental data from thermal behavior of the mixture tristearin-epikuron200 in different compositions at different pressures was assessed. These data are important for predicting the behavior of the chosen excipients in the mix chamber of the PGSS plant and consequently assist the selection of the best lipid mixture composition for the solid lipid particle production. The melting point values of the mixtures were collected as summarized in Table 5.

Table 5. Melting temperature of lipid mixtures at different compositions and pressures.

Pressure	Components	Tristearin content						
		0.0	0.25	0.31	0.40	0.57	0.67	1.00
1 bar	Tristearin form 1	-	63.88 ±0.01°C	63.28 ±0.10°C	-	-	-	-
	Tristearin form 2	-	71.57 ±0.43°C	71.33 ±0.21°C	72.48 ±0.21°C	72.40 ±0.46°C*	71.88 ±0.24°C*	72.93 ±0.09°C*
	Epikuron 200	231.87 ±0.14°C	136.36 ±0.37°C	119.99 ±4.55°C	114.08 ±4.12°C	-	-	-
20 bar	Tristearin form 1	-	61.65 ±0.59°C	-	-	-	-	-
	Tristearin form 2	-	70.07 ±0.29°C	69.58 ±0.12°C*	70.90 ±0.51°C*	71.71 ±1.45°C*	70.36 ±0.34°C*	69.83 ±0.21°C*
	Epikuron 200	233.79 ±0.83°C	118.15 ±5.79°C	-	-	-	-	-
40 bar	Tristearin form 1	-	-	-	-	-	-	-
	Tristearin form 2	-	67.30 ± 0.32°C*	66.57°C*	68.54 ±1.39°C*	69.00°C*	69.55°C*	68.42 ±0.21°C*
	Epikuron 200	234.11°C	-	-	-	-	-	-

Values showed as average ± standard deviation; *Values attributed to homogenous mixture with no distinguishable melting of pure solid phases.

At 1 bar a decrease of tristearin melting point was observed with an increase of the phosphatidylcholine content. Generally, the natural-derived phosphatidylcholines present unsaturated bonds on their carbon chains, as those found for 1,2-dilinoleoylsn-glycero-3-phosphocholine (DLPC), the main component of Epikuron200 depicted in Figure 22. The double bonds confer to these compounds a natural fluid state, i.e. the transition from a rigid to a fluid state, known as glass-transition, occurs under 0 °C. The glass-transition temperature of DLPC is -53 °C (Capitani *et al.*, 1996). So, the fluid DLPC can act as a dispersant of crystalline tristearin as well as the other lipid compounds of epikuron200, and as a consequence its melting demands less energy.

Furthermore, as depicted in Figure 23, two peaks for tristearin were identified at the highest concentrations of phosphatidylcholine. Taking into account the crystalline nature of triglycerides, it was hypothesized that these peaks refer to intermediate crystalline forms of tristearin. The mixture preparation requires the melting of both compounds, so it was thought that at large amounts of

phosphatidylcholine there is a prevention of homogeneous formation of a highly symmetrical crystal lattice during the solidification step, which leads to maintenance of intermediate crystalline forms. Only detailed X-Ray Diffraction (XRD) analysis could confirm both identity and crystalline nature of these intermediate forms.

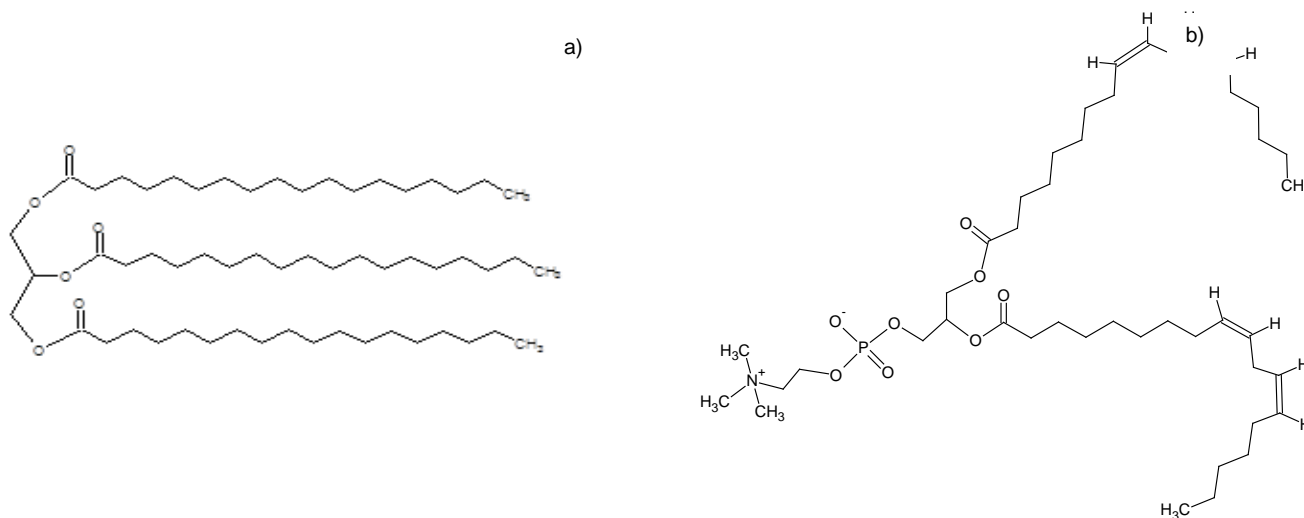


Figure 22. Lipid structures. a) Tristearin; b) 1,2-dilinoleoylsn-glycero-3-phosphocholine

Figure 23 also shows how remarkable is the effect of pressurized CO₂ on the thermal behavior of the mixture. An increase of pressure leads to the diffusion of CO₂ molecules into the solid lipid structure. The presence of CO₂ molecules in the interstice of the solid facilitates the displacement of lipid molecules during melting event reducing the melting temperature, as well as the melting enthalpy. This explains the concept of plasticizing effect of CO₂, which favors the decrease of melting point of lipids. The fluidizing power of CO₂ also contributes to the disappearance of intermediary crystalline polymorphs during melting process leading to the achievement of a homogenous mixture with only one fusion peak.

Taking into account the complex composition of natural lecithin, or even the structural complexity of pure phospholipids, several secondary melting transitions can occur below the normal temperature of fusion. Because of this, a relatively high heat rate was chosen (10 °C/min) for the DSC runs in order to avoid the intermediate transitions and detect a distinguishable peak of the main melting event. These secondary events are linked to movements of carbon chains and displacement of polar heads not only of DLPC but also of the other components of Epikuron200 as listed on Table 6.

Table 6. Carbon chain pattern for free fatty acids and phospholipids in Epikuron 200

C ₈	C ₁₆	C _{16:1}	C ₁₈	C _{18:1}	C _{18:2}	C _{18:3}
0.8%	12.2%	0.4%	2.7%	10.7%	67.2%	6.0%

Adapted from Bergenståhl (1983).

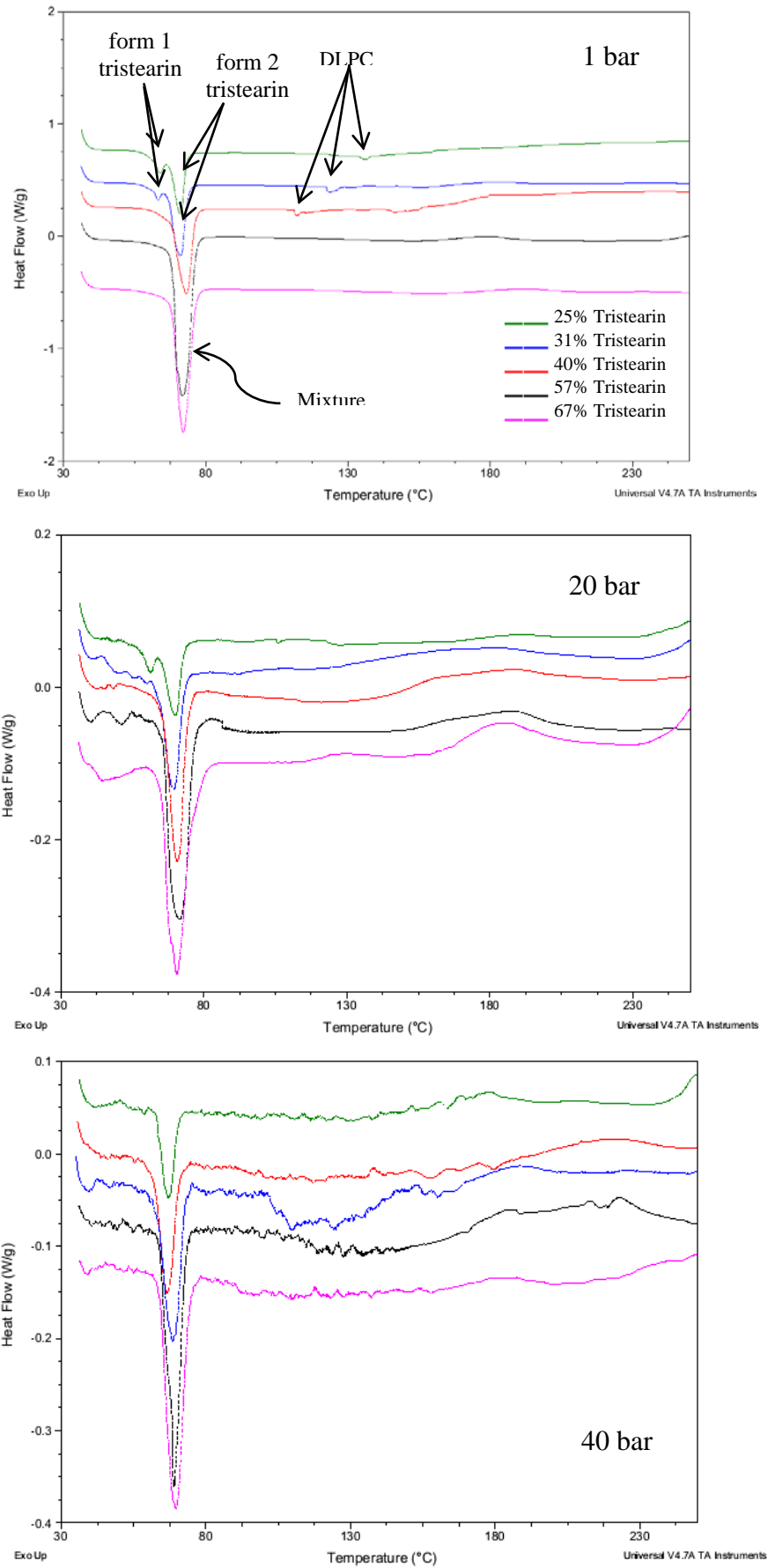


Figure 23. DSC thermograms of lipid mixtures at different pressures.

At high pressures, the DSC equipment shows interference noise on the measurements that can affect the detection of low enthalpy events. Considering that no reproducible peak within the replicates of each condition was found, into the noise zone, only one peak of the mixture was registered for all compositions at 40 bar.

1.2 System 2 lipids + curcumin + DMSO + CO₂

The behaviour of the lipid mixture with curcumin at different compositions for different pressure conditions was also evaluated. As summarized on Table 7 and Figure 24, a clear influence of the curcumin content was observed. The larger curcumin amount, the larger the decrease on the melting point. This can be explained by the DMSO content in the mixture, used for an homogenous dispersing of curcumin into lipid mixture. Taking into account that all the components of the mixture can be solubilized by DMSO, it can act as a solvent and facilitate the fluidization of the lipid matrix in a synergic way with the plasticizing phenomenon produced by CO₂ molecules.

Table 7. Melting point of mixtures of tristearin/epikuron200/DMSO/curcumin

Composition				Pressure		
Tri	PC	DMSO	Cu	1bar	20bar	40bar
49.5	24.7	17.5	8.3	69.30 ±0.26°C	68.01 ±0.57°C	65.58 ±0.07°C
54.2	31.7	9.6	4.5	70.54 ±0.17°C	69.51 ±0.54°C	67.51 ±0.20°C
57.6	36.5	4.0	1.9	70.13 ±0.15°C	69.86 ±0.36°C	68.12 ±0.07°C

Values showed as average ± standard deviation.

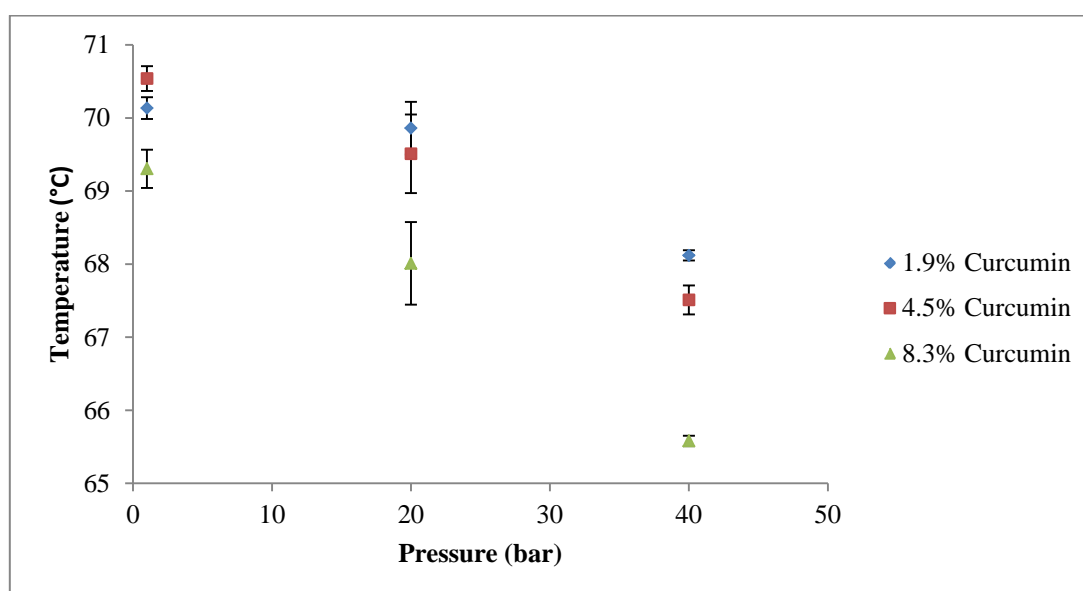


Figure 24. Decrease on melting point of the lipid mixture at different compositions and different pressures.

The detection of only one peak of fusion on DSC thermograms indicates the achievement of a homogenous mixture in which the components are molecularly dispersed. The tristearin/Epikuron200/CO₂ mixtures showed to be dependent on the lipids ratio. However, the use of curcumin and DMSO in the mixtures facilitated homogenization of the components in all compositions tested. This is very important for the PGSS process. Considering that the first step of the PGSS technique is the melting of the lipid mixture followed by rapid solidification during expansion, processing of homogenous mixtures leads to homogenous solid products, i.e. the state transitions during PGSS processing would not affect the homogeneity of the final powder product. A heterogeneous mixture could favor different fusion/solidification rates leading to powder lumps formation or clogging problems in tubing and valves.

SLM Production by PGSS and Characterization

(Paper published in the Journal of Supercritical Fluids, 107 (2016) 534-541)



Contents lists available at ScienceDirect

The Journal of Supercritical Fluids

journal homepage: www.elsevier.com/locate/supflu

Curcumin-loaded solid lipid particles by PGSS technology



André São Pedro^{a,b}, Stefania Dalla Villa^b, Paolo Caliceti^c, Silvio A.B. Vieira de Melo^a, Elaine Cabral Albuquerque^a, Alberto Bertucco^b, Stefano Salmaso^{c,*}

^a Programa de Engenharia Industrial, Escola Politécnica, Universidade Federal da Bahia, Salvador-Bahia, Brazil

^b Department of Industrial Engineering, Università degli Studi di Padova, Padova, Italy

^c Department of Pharmaceutical and Pharmacological Sciences, Università degli Studi di Padova, Padova, Italy

ARTICLE INFO

Article history:

Received 7 May 2015

Received in revised form 8 July 2015

Accepted 8 July 2015

Available online 18 July 2015

Keywords:

Curcumin

Supercritical CO₂

Solid lipid particles

Formulation

Particles from a gas saturated solution

ABSTRACT

Curcumin is a poorly water-soluble and fragile compound that, by virtue of its biological activities, has been considered for a variety of therapeutic applications. In this work, a novel process based on supercritical fluid technology has been used for encapsulating curcumin in solid lipid particles (SLP) to yield curcumin formulations with enhanced biopharmaceutical properties. SLP were obtained by a Particles Generated from Gas Saturated Solution technique (PGSS), where [tristearin+soy phosphatidylcholine (PC)]/[dimethylsulfoxide (DMSO)+curcumin] mixtures were processed. The effects of operative conditions were investigated in order to identify the main parameters that affect the biopharmaceutical properties of the final product. Samples with (tristearin+PC)/(DMSO+curcumin) w/w ratios ranging from 65.6:1 to 3:1 were prepared either in the presence or absence of helium and then processed by PGSS. The drug loading yield was found to be between 30 and 87 drug/lipid w/w%. The particles obtained from lipid mixtures with low DMSO feed were homogeneous in size. The formulation prepared with the highest DMSO feed yielded a bimodal particle size distribution with significant aggregation. Interestingly, the use of helium in the preparation of the lipid mixture was found to improve the biopharmaceutical properties of the SLP, namely drug loading and particle dimensional features. The preparation process was not found to degrade curcumin indicating that PGSS can be properly set-up for the preparation of curcumin lipid particles.

© 2015 Elsevier B.V. All rights reserved.

1. Introduction

In the last decades, pharmaceutical research has devoted many efforts in order to generate new, more potent and highly selective drugs. However, many newly designed molecules failed to access the market due to low clinical acceptability, namely poor biopharmaceutical properties and pharmacokinetic profile. Molecules of natural origin have raised the pharmaceutical industry interest since they are regarded as valuable alternatives to new chemical entities for their intrinsic molecular selectivity toward biological targets and limited toxicity. Accordingly, over the years, traditional medicine has inspired the research of innovative therapeutic options.

Curcuma longa, a herbaceous perennial plant from Zingiberaceae family, commonly cited as "turmeric", has been used for over 4000 years by Asian medicine for treating gastrointestinal irritation, liver disorders, microbial infections, skin wounds, arthritic pain, stress,

and mood disorders [1]. The therapeutic activity of turmeric is ascribed to curcumin, the main biologically active molecule so far isolated from turmeric root. Curcumin, which has been proved to possess potent anti-inflammatory activity, interferes with a variety of pathways regulating the inflammation process by a multi-target mechanism that results in many biological activities, including antioxidant, anticancer, analgesic and gastro-protective activity.

The curcumin molecule contains phenol moieties connected by an unsaturated bond, which confers low polarity, poor solubility in water and high sensitivity to photo and thermal degradation [2,3]. These features greatly limit the development of suitable formulations. The low chemical stability of curcumin, which is responsible of the short shelf life of curcumin-based products, and the poor water solubility dramatically affects the absorption and bioavailability of this active molecule with consequent unsatisfactory pharmacokinetic profile and reduced efficacy [4–6].

Encapsulation techniques have been largely studied in order to overcome the poor biopharmaceutical features of many compounds with high pharmacological activity. Micro- and nano-encapsulation can provide a useful mean to enhance the physico-chemical stability of bioactive molecules while improving

* Corresponding author. Tel.: +39 0498271602.

E-mail address: stefano.salmaso@unipd.it (S. Salmaso).

the drug absorption through physiological barriers [7,8]. Several papers report the investigation of solid lipid nanoparticles (SLN) as carriers of choice for curcumin [9,10]. SLN are composed of solid lipids, usually “Generally Recognized as Safe” (GRAS) status conferred by the FDA [11], that endow these vehicles with relatively higher physical stability than that of other lipid-based particulate systems, namely liposomes.

Particle size and composition are the key factors dictating the oral absorption of particulate systems. It is a consensus that particles smaller than 100 nm can be absorbed after oral administration through the intestinal endothelium, which leads to enhanced drug bioavailability [7,12]. Lipid particles of micrometric scale were also found to enhance the absorption of molecules across the intestinal endothelium as a result of the lipid component effect on drug dissolution and mucosae permeability alteration [12,13]. Thus, solid lipid particles (SLP) with a broad size range have been studied for pharmaceutical applications.

SLP have been prepared using a variety of excipients including glycerides, waxes and fatty acids. However, one of the main issues associated to the use of these materials is the loss of the encapsulated active molecules from SLP due to crystallization of the lipid matrix through their shelf life [14,15]. Once the lipid components self-organize in a crystal lattice, the bioactive molecule is forced to phase-separate from the matrix. To delay the crystallization of the lipid matrix and promote the homogeneous dispersion of the active molecules within the matrix, amorphous lipid molecules, such as natural phosphatidylcholines, have been included in the lipid mixtures [16,17]. Accordingly, 1,2-dilinoleoyl-*sn*-glycero-3-phosphocholine, the main component of Epikuron200®, was widely used for this purpose. The unsaturation on the two linoleoyl moieties reduces the crystallization of this soybean derived lecithin.

The traditional methods for SLP production present significant drawbacks, such as the use of relevant volumes of organic solvents, residual solvent contamination in the final product, harsh conditions, namely high temperatures. Furthermore, these methods include a number of time consuming steps, which further complicate the SLP preparation [11]. Supercritical fluid (SCF) technology has emerged as an interesting alternative for the production of particulate formulations for a wide range of applications. Carbon dioxide (CO₂) is a non-toxic and non-inflammable fluid and possesses a relatively low critical temperature and pressure. CO₂ is the gas of choice for supercritical processes, including chromatographic methods for enantioselective separation [18,19], chemical extraction from natural sources [20], pharmaceutical and cosmetic tailoring [21], food processing [22], as well as for processing of pharmaceuticals that can be degraded under harsh conditions. Furthermore, depending on the nature of the biologically active compound, supercritical CO₂ can be used as solvent, anti-solvent or solute [23,24].

In the “Particles Generated from Gas Saturated Solutions” (PGSS) process, CO₂ is employed as a solute. A molten mixture composed of the lipid matrix forming materials and the bioactive molecule is saturated by CO₂ at supercritical conditions. This remarkably reduces the viscosity of the molten mass allowing for its outflow to the expansion chamber through a micrometric nozzle. Curcumin loaded SLP have been mainly prepared by hot homogenization [10,25,26] and microemulsion [27,28] techniques. According to the preparation conditions, namely materials and process parameters, these techniques have been found to produce either nanoparticles with size below 100 nm or microparticles with size of a few hundred μm , while the curcumin loading was usually below 5%, w/w [10,29]. With respect to these methods, SCF-based technologies can operate under mild conditions as it may avoid high temperatures and the use of organic solvents or co-excipients, namely emulsifiers. Furthermore the SCF processes result in straightforward

powder production, which limits the number of the overall steps for particle preparation, namely solvent elimination and particle recovery. Therefore, the use of SCF technology can yield beneficial outcomes for the formulation of SLP. For example, curcumin loaded nanoparticles with size below 100 nm and 38%, w/w, drug loading were obtained by anti-solvent supercritical methods [30]. Precipitation by PGSS technique has been found to be an interesting approach for the encapsulation of fragile drugs in SLP [31–33]. Recent interesting studies showed that PGSS can be successfully used to prepare curcumin/PEG fine powders without drug degradation [34].

In order to exploit the advantages of PGSS in the production of SLP, we investigated for the first time the exploitation of this process for preparation of curcumin loaded SLP for pharmaceutical applications. This work was aimed at investigating the process feasibility and at providing a first preliminary assessment of the effect of the operative conditions, namely DMSO feed and the use of helium in the lipid mixture preparation on the particulate product features by the physical characterization of the particles. At our best knowledge, no study has been reported so far in the available literature describing curcumin loaded lipid particles using PGSS.

2. Materials

Tristearin ($\geq 99\%$), dimethylsulfoxide (DMSO, 99%), dichloromethane (DCM, $\geq 99.5\%$) and citric acid (99%) were purchased from Sigma-Aldrich (St. Louis, MO, USA). Epikuron 200 (soy phosphatidylcholine PC) was a kind gift from Cargill Inc. (Krefeld, Germany). The 98% pure curcumin, HPLC grade methanol, ethanol and acetonitrile were obtained from Merck (Darmstadt, Germany). The CO₂ (99.99%), synthetic air (99.99%) and N₂ (99.99%) were purchased from Rivoira (Padova, Italy). All chemicals were used as received.

3. Methods

3.1. PGSS bench-scale unit

The preparation of SLP microparticles was carried out using the system shown in Fig. 1 according to a batch process. Liquid CO₂ stored in a main reservoir kept at 5 °C by a chiller (Lauda, Würzburg, Germany) was pumped by a piston pump (DOXE Office Meccaniche Gallaratesi, Milan, Italy) to feed the mix chamber and a secondary reservoir. The secondary reservoir worked as a back-pressure chamber to keep the pressure constant inside the mix chamber during the expansion step. The bottom of the mix chamber was connected to the micronization unit by a needle valve (Swagelok, Lengnau, Switzerland) (V9). Valve V9 and the inlet pipe were heated by the same heating device. A 180 μm capillary nozzle was installed at the bottom of the micronization unit, which was heated by ceramic cartridges inserted in cylindrical cavities placed at 120° each other, in order to control its temperature around 60 °C. The gas-saturated material flowing from the mix chamber was coaxially intercepted by a high pressure N₂ beam in the micronization unit, fed just before the nozzle to improve the lipid mixture atomization. Further, a low pressure stream of synthetic air was provided to promote a streamline flow upon the expansion chamber walls in order to avoid the adhesion of the lipid droplets. The micronization chamber was a 0.2 L volume plexiglass tube, including two parts of different diameter, and working as a spray tower. This tube was screwed to the divergent section of the collection chamber made in PVC. A metallic filter located in the cross section of the collection chamber and sealed by a neoprene O-Ring gasket retained the solid lipid particles.

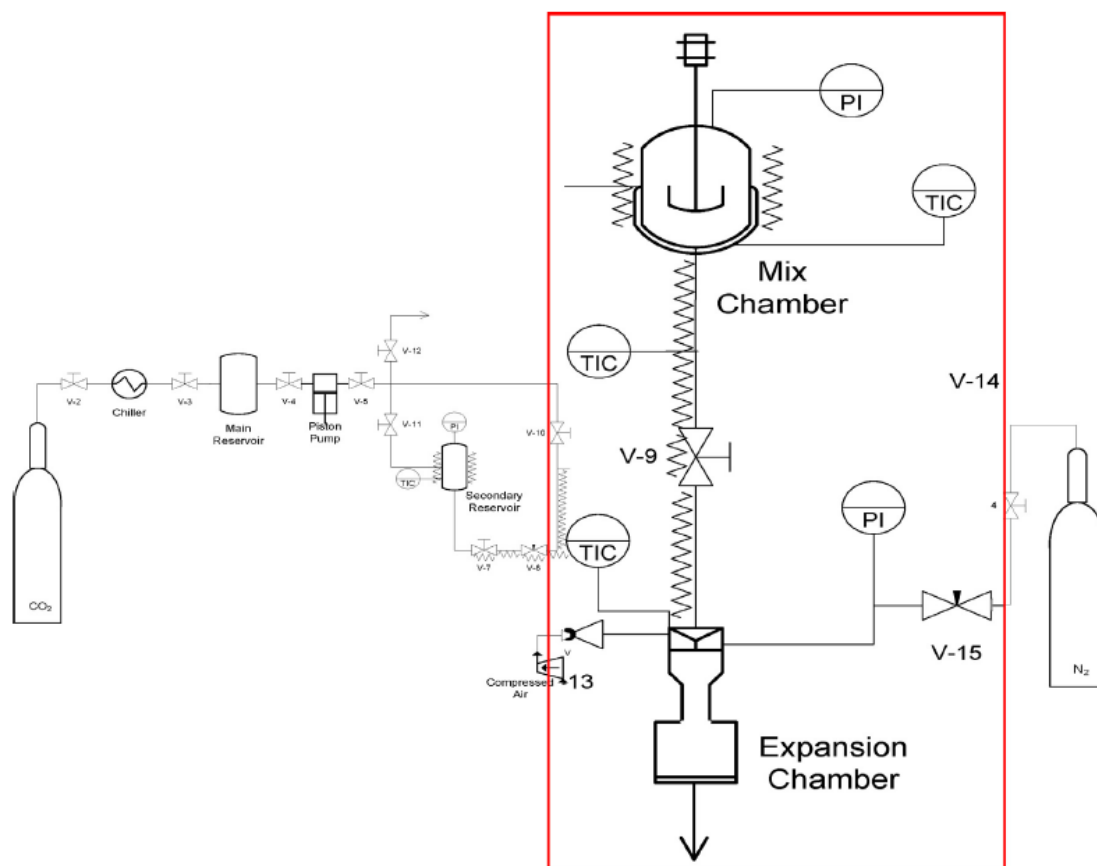


Fig. 1. Scheme of PGSS plant used in this work. V2–V15—valves; PI—pressure indicator; TIC—temperature indicator—controller.

3.2. Mixture preparation

In an amber glass flask, lipid mixtures were prepared by dissolving 0.45–0.6 g soy PC in dichloromethane (DCM) (1.7:1 PC/DCM w/v). The solutions were dispersed in 0.9 g of melted tristearin at 60 °C and the lipid mixtures were stirred until complete homogenization and DCM evaporation [35]. The lipid mixtures were heated to 65 °C and mixed with increasing volumes of DMSO solutions of curcumin (375 mg/mL). The mixtures were stirred while the temperature slowly decreased until complete solidification. The lipid/drug mixtures were prepared either under room atmosphere or under helium. The solid material was maintained overnight under vacuum and then processed by PGSS.

3.3. Particle production

Tristearin/soy PC/DMSO/curcumin mixtures (1.5 g) were loaded into the mix chamber of the PGSS plant (Fig. 1) thermostated at 75 °C and processed according to batch process. The system was pressurized with CO₂ to 150 bar and the temperature was decreased to 55 °C. The lipid mixture was maintained under stirring at 500 rpm and pressurized at 150 bar by using CO₂ of the secondary reservoir. The expansion valve, the secondary reservoir and the micronization unit were thermostated at 60 °C. After achieving the steady state of temperature and pressure (30 min), valve V9 connecting the mixer chamber with the micronization chamber was opened to allow the melted lipid mixture to be sprayed in the micronization unit. N₂ at 140 bar and synthetic air at 5 bar were simultaneously co-axially injected into the micronization unit. The pressure in the mixing chamber was maintained at 130 bar

throughout the preparation process. The particle precipitation process occurred in 15 s. At the end of the run, the dry material was collected from the metallic filter placed on the bottom of the collection chamber. The CO₂ flow was maintained for 5 min at constant rate. The dichloromethane content in the final product was assessed according to the protocol reported elsewhere [32].

3.4. DSC analysis

DSC analyses were performed using a Q10P calorimeter (TA Instruments, New Castle, DE, USA) equipped with a high pressure cell that enables measurements in the presence of CO₂ up to a maximum operating pressure of 7 MPa. Amounts of 1–5 mg of tristearin, soy PC, curcumin and lipid particles were weighted and placed in the calorimetric chamber. For experiments performed by using CO₂, the cell was pressurized to the desired operating CO₂ pressure prior to heating the sample. A continuous flow of CO₂ was maintained through the cell during the heating cycle. The samples were heated from 40 to 300 °C at a rate of 10 °C/min. Three DSC analysis replicates were performed for each sample.

3.5. SLP curcumin loading capacity and degradation of processed curcumin

The curcumin loading yield percentage was assessed by reverse-phase HPLC (RP-HPLC) using a 250 × 4.6 mm Phenomenex Luna C18 column (Phenomenex, Torrance, CA, USA) isocratically eluted with a 48:52 v/v% of 0.5% w/v citric acid (pH = 3.0)/acetonitrile mixture at 1 mL/min flow rate. The UV detector was set at 429 nm. Lipidic mixtures (5 mg) before PGSS processing and freshly prepared

particles were dispersed in 1 mL of methanol, vigorously vortexed for 1 min and centrifuged at $14,462 \times g$ for 15 min. The clear supernatant was diluted with the mobile phase and analysed by RP-HPLC. Samples were analysed in triplicate and the curcumin loading yield percentage was calculated by:

$$\text{Loading yield \%} = \left[\frac{\text{curcumin loaded in SLP}}{\text{curcumin in the starting mixture}} \right] \times 100 \quad (1)$$

The effect of the PGSS process on the stability of curcumin was assessed by comparing the chromatographic profile of non-processed curcumin dissolved in methanol with the one of the curcumin recovered from lipid mixtures before PGSS treatment and that recovered from particles after PGSS.

3.6. Particle size and morphology analyses

Particle size analysis was carried out by static light scattering (SLS) using a Malvern mastersizer 2000 equipment (Malvern, Worcestershire, UK). Particles (10 mg) were dispersed under vortexing in 15 mL of mQ water, sonicated in ice bath for 30 min and finally analysed.

The morphology of micronized particles was assessed by scanning electron microscopy (SEM) directly on the dry particle samples mounted on metal stubs and after 20 nm-thick gold-coating treatment. The micrographs were obtained by a JSM-6390LV digital scanning electron microscope (JEOL, Peabody, USA) using an acceleration voltage of 10 kV at different magnifications.

4. Results

The pharmaceutical ingredients used for the SLP preparation, namely lipids and phospholipids, were selected on the basis of their regulatory status and physicochemical properties. All materials are in fact approved by the main regulatory agencies (FDA and EMA) for oral formulations. Furthermore, these materials possess proper fluidity in a large range of combinations suitable for processing the matrixes under supercritical or near-critical conditions.

DMSO was added to the mixture to homogeneously disperse curcumin in the lipid phase as it is poorly soluble in the soy PC/tristearin mixture. In a preliminary study, ethanol and acetone were used to produce a homogeneous lipid/curcumin matrix. However, the rapid evaporation of these solvents yielded curcumin precipitation and segregation within the lipid matrix. DMSO has lower toxicity as compared to other organic solvents, namely dichloromethane and chloroform, frequently used in the preparation of lipid particles and vesicles. For such a reason, DMSO is widely applied in pharmaceutical formulations thanks to its ability to solubilize a wide array of organic compounds. It is worth to note that Food and Drug Administration (FDA) classifies DMSO as a class 3 solvent, i.e. with low toxic potential [36]. The high solubility of curcumin in DMSO was the key to select it as vehicle for curcumin in various studies. Furthermore, there are a few reports claiming that supercritical processes allow for the extensive removal of this solvent from formulations [37–39].

DMSO was found to affect the viscosity of the lipid matrix. The lower the amount of DMSO in the tristearin/PC/DMSO mixture, the more viscous was the final mixture. Therefore, DMSO promotes the homogenous dispersion of curcumin in the lipid mixture and enhances the fluidity of the final mixtures that facilitates the lipid mixture atomisation during the supercritical processes. On the other hand, previous studies showed that DMSO promotes the particle aggregation and increases the particle size [30]. Therefore, a set of preparations were carried out by using increasing DMSO feed in the lipid mixture to evaluate the effects of this solvent on the produced particles.

Table 1

Composition of mixtures prepared for PGSS processing, in w/w%.

Mixture	Tristearin (%)	Soy PC (%)	DMSO (%)	Curcumin (%)
Mix 1	59.4	39.1	1.0	0.5
Mix 2	58.7	38.2	2.1	1.0
Mix 3	57.6	36.5	4.0	1.9
Mix 4	54.2	31.7	9.6	4.5
Mix 5	49.5	24.7	17.5	8.3

Various lipid/curcumin mixtures (Table 1) were processed to evaluate the effect of the composition of the mixture and the mixture preparation method on the physicochemical and biopharmaceutical properties of the final formulation. The mixtures were prepared by simple mixing the curcumin solution in DMSO into the fused lipid mixture at 65 °C. In another set of experiments, curcumin/lipid mixtures with the same compositions reported in Table 1 were prepared under a helium stream to guarantee an inert environment to prevent curcumin oxidation.

Helium was initially selected among inert gasses because it is commonly used as eluent in gas-chromatography for analyses of both lipids and curcumin derivatives [40,41]. Furthermore, helium was reported to have very low solubility in lipids compared to other inert gasses, which have been demonstrated to penetrate into the lipid masses altering the lipid matrix [42,43]. Therefore, helium was expected to have low effect on the curcumin/lipid structure. According to its chemical and physical inertness, helium was considered the gas of choice for the preparation of lipid/curcumin mixtures.

4.1. Dimensional analysis

The PGSS process yielded yellow-coloured fine powders of curcumin loaded SLP. The dichloromethane content in the final products was always below 5 ppm, which is significantly lower to the value admitted by the United States Pharmacopoeia and the European Pharmacopoeia (400 ppm and 600 ppm, respectively).

Studies carried out processing lipid mixtures containing either DMSO/curcumin or DMSO only showed that the DMSO feed in the processed mixture has a significant effect on the dimensional properties of the particles while curcumin does not affect the particle size of the processed material. The light scattering analyses showed that all formulations presented a bimodal size distribution profile corresponding to two particle size populations. It is worth to note that studies reported in the literature showed that bimodal profiles were obtained with curcumin loaded tristearin and trimyristin nano/microparticles [10]. However, in the case of curcumin loaded tristearin and trimyristin nano/microparticles it was demonstrated that the bimodal profiles were an artefact of the Laser Diffraction analysis. Indeed, Photon Correlation Spectroscopy showed that the product did not contain the microparticle fraction. Therefore, in order to investigate whether the fraction with higher size was ascribed to aggregates, the dimensional analyses were performed after mild sonication of the samples, which was performed in ice bath to promote particle disaggregation without particle fusion and coalescence due to heat increase. In all cases, the dimensional profiles showed a decrease of the relative content of the population attributed to aggregates. Fig. 2 shows an example of the dimensional profiles of two formulations obtained with low and high DMSO feed in the processed mixture. The mixture with low DMSO feed resulted in homogenous size distribution while the mixture with the higher DMSO feed showed a particle population with both small and large size particles. The dimensional profiles obtained after sonication were elaborated in order to calculate the content of aggregates and the size, size distribution and population homogeneity of the non-aggregated particles. No

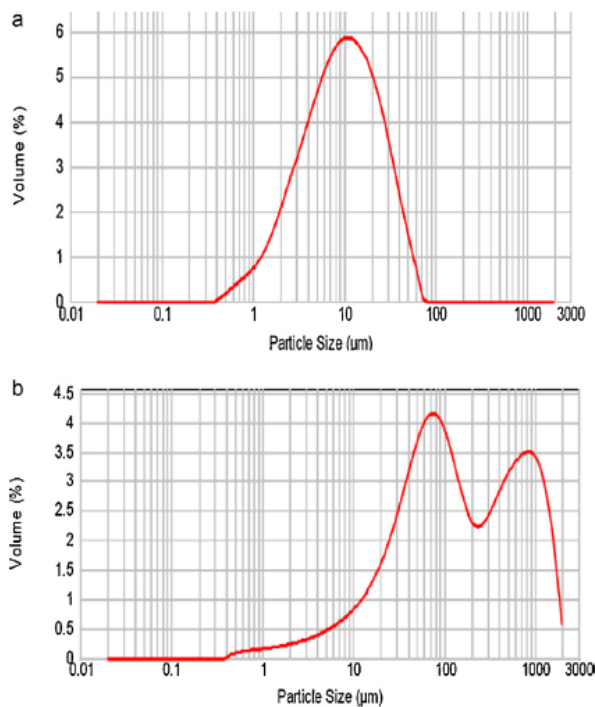


Fig. 2. Particle size distribution from light scattering analysis of samples prepared with different DMSO feed in the processed mixture: (a) Mix 1, Table 1; (b) Mix 5, Table 1.

aggregation was observed up to 4% of DMSO in the mixture. The mixture containing 9.6% and 17.5% of DMSO resulted in 5% and 40% by volume sub-population of large particles, respectively. The large particles obtained when high feed of DMSO was used are reasonably the result of fused aggregates that did not disaggregate under sonication.

Fig. 3 reports the particles size corresponding to the non-aggregated population obtained with samples containing increasing feed of DMSO in the lipid mixture and prepared under room atmosphere and under helium. The figure shows that the mean particle size of the non-aggregated particle population linearly increases as the DMSO feed in the processed mixture increases. The span values of the non-aggregated particle population were in the range of 3.02–3.92, indicating that all mixtures yielded similar size distributions. The particle size increase obtained by increasing the DMSO feed in the curcumin/lipid mixture may be ascribable to

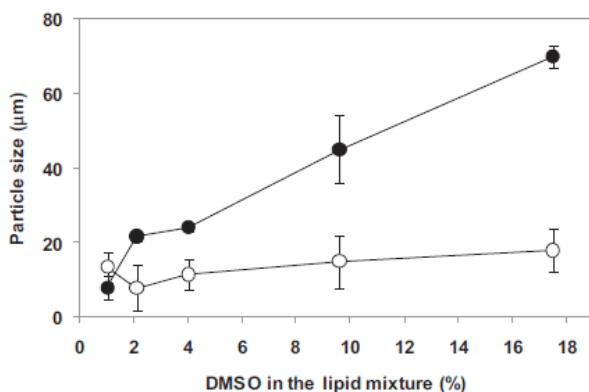


Fig. 3. Size of particles obtained by processing curcumin/tristearin/PC/DMSO mixtures prepared under room atmosphere (●) and under helium atmosphere (○). Effect of the DMSO feed in the initial mixture on the particle size.

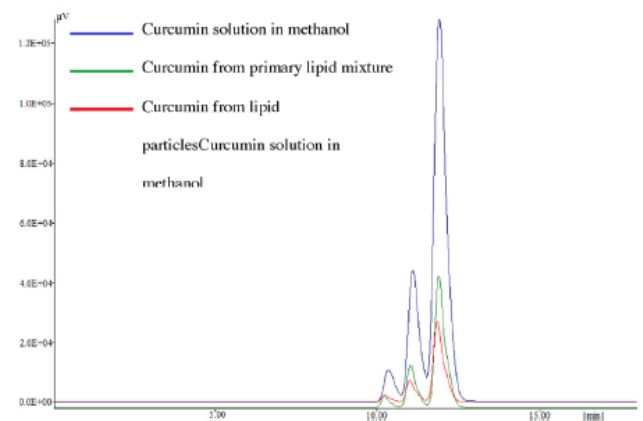


Fig. 4. RP-HPLC profiles of curcumin: freshly prepared curcumin methanolic solution, curcumin from lipid matrix before and after PGSS processing.

the formation of the lipid/solvent sub-gel structures described in the literature [44] that generate large particles during the atomization process and particle formation. To note that the formation of these sub-gel structures seems to be confirmed by the DSC profiles discussed below.

The mixtures prepared by using helium during the curcumin dispersion in the lipids showed a similar behaviour of the preparations obtained under room atmosphere: the higher the DMSO feed in the lipid mixture, the higher the mean particle size and aggregation tendency. However, Fig. 3 shows that in this case the particle size and the aggregation were significantly lower than those obtained with the mixtures prepared in the absence of helium. This result seems to indicate that the helium plays a role in the curcumin/lipid/DMSO mixture formation. Even though helium does not easily disperse in lipids and lipids are not soluble in helium [42,43], this gas has a certain affinity for lipids being used in gas chromatography for lipid analysis [40,41]. Accordingly, the helium interaction with the melted materials and adsorption on lipids could favour the dispersion of DMSO in the lipids forming more homogeneous mixtures. Therefore, helium has a double beneficial effect on the preparation of the curcumin loaded SLP; on one side it guarantees an inert environment that preserves curcumin from oxidation and on the other it favours the generation of lipid mixtures easily and homogeneously sprayable.

4.2. Curcumin loading and stability

RP-HPLC analyses were performed to evaluate the effect of the process and the formulation on the curcumin loading in the SLP, the loading yield and stability. Curcumin is in fact known to undergo rapid photo- and thermal-degradation, which represent a significant issue in the formulation and pharmaceutical use of this drug [45].

Fig. 4 reports the RP-HPLC profiles of the curcumin product from a freshly prepared methanolic solution, from one of the primary lipid mixture (Mix 2) obtained in the absence of helium, and the corresponding freshly prepared particles. The RP-HPLC chromatographic profile of the as-received unprocessed curcumin showed the presence of three chemical entities. The three products correspond to the three major curcuminoids extracted from the *Curcuma longa* and described in the literature [46,47]. The peak eluted at 11.94 min refers to curcumin while the other two peaks correspond to bi-demethoxycurcumin and demethoxycurcumin.

The area ratios of the three peaks referred to curcumin used for the SLP preparation were unchanged after lipid mixing and PGSS process, indicating that neither the formulation composition nor the supercritical process affect the chemical stability of curcumin.

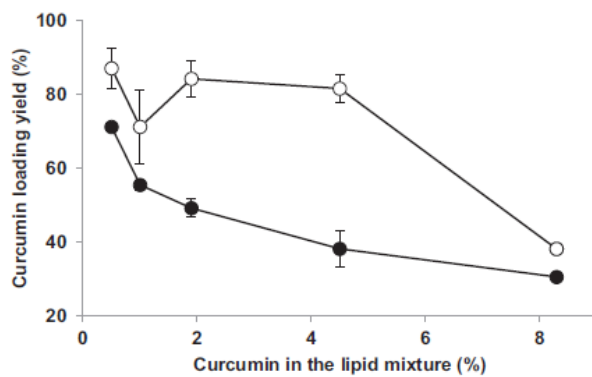


Fig. 5. Curcumin loading yield obtained with samples prepared under room atmosphere (●) or under helium (○), as a function of the curcumin in the initial mixture.

Fig. 5 displays the loading yield (%) obtained with the various formulations. The results reported in the figure show that the curcumin loading yield decreases as the drug feed in the lipid mixture increases either in the case of the mixtures prepared in the absence or in the presence of helium. This could be due to a lower dispersion of curcumin in the lipid mixture as the drug feed increases, which results in the formation of drug agglomerates that are not sprayed in the precipitation chamber. Indeed, due to the relatively high solubility of DMSO in CO₂, the DMSO in the lipid mixture can be extracted by CO₂ [32,48] yielding precipitation of curcumin not homogeneously dispersed in the lipids [49]. Curcumin precipitation

in the mixer chamber might increase as the curcumin feed ratio in the lipid mixture increases as a consequence of the increased relative partition of DMSO in the CO₂ phase. Formulations prepared with helium resulted in higher drug loading yield compared to the preparations obtained without helium. This result seems to confirm the effect of helium on the lipid matrix already discussed above to explain the dimensional data. The helium adsorption to the lipids can alter the physicochemical properties of the lipid matrix and favour the homogenous dispersion of curcumin in the lipid mass, which prevents its precipitation and segregation in the melting chamber during the PGSS process.

4.3. Morphology

The SEM analyses provided information about the morphology and dimension of the product obtained by PGSS. The images reported in Fig. 6 show the typical morphologies obtained with low and high DMSO feed in the processed mixtures and reflect the product features obtained with homogeneous or non-homogeneous lipid mixtures.

SEM micrographs show that the particles have an irregular shape. To note that similar particle size and morphology were obtained by PGSS processing of poloxamer, gelucire and glyceryl monostearate [50].

The images corresponding to the formulations obtained with 2.1% DMSO feed in the absence and in the presence of helium (Fig. 6A and B, respectively) show the presence of small microparticles and large aggregates. Actually, aggregates were not observed by light scattering because the samples were previously

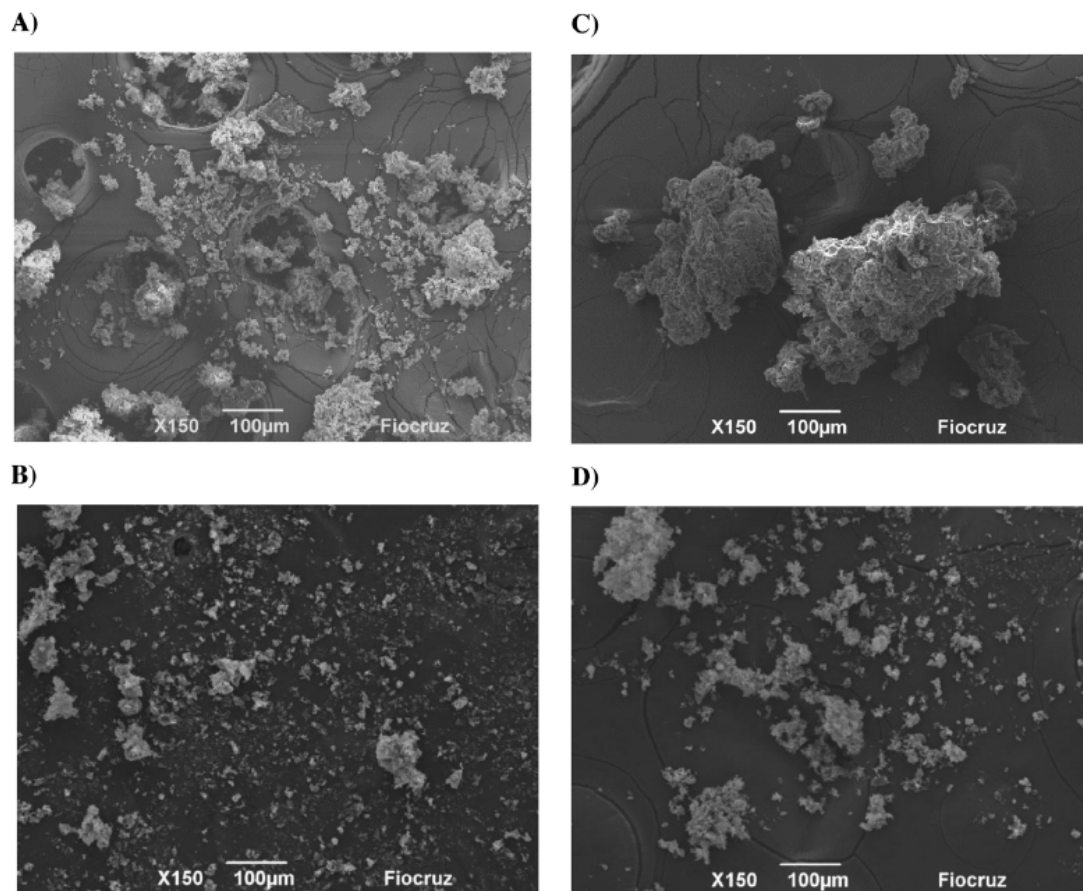


Fig. 6. SEM micrographs: (A) Mix 2 obtained under room atmosphere; (B) Mix 2 obtained under helium; (C) Mix 5 obtained under room atmosphere; (D) Mix 5 obtained under helium.

sonicated to disaggregate whilst in the case of SEM the products were analysed without disaggregation. Therefore, the large particles observed by light scattering were mainly aggregated non-fused particles as mild sonication was sufficient to disaggregate them. Particle aggregation observed by SEM can be mostly attributed to the electrostatic forces commonly present in powdered materials, due to electron transfer occurred on the sudden change in surface area during particle precipitation. As the atomization/crystallization time is very short in the PGSS process, the lipid mixtures lack time to generate newly formed particle with homogeneous surface charge leading to non-uniform charges distributions. Therefore, these charged particles undergo aggregation by electronic attraction [51,52].

The solidification rate of the newly produced particles is also pivotal for the formation of aggregates/coalescence during the expansion step. The slower the solidification rate, the larger the aggregation/coalescence rate. The not completely solidified particles can aggregate or undergo coalescence upon deposition on filter or along the expansion chamber walls just after the spraying nozzle. This can be controlled by modulating the mixture composition. Also the saturation temperature in the mix chamber is decisive on this matter: if too high temperatures are applied, an overheated molten lipid mixture is expanded forming amorphous agglomerates [53,54]. In this work, a coaxial nitrogen flow was applied in the atomization device, in order to reduce aggregation and coalescence phenomena right after the spraying nozzle. In addition, the selected saturation temperature (55 °C) was the lowest one at which no obstruction was observed at the nozzle. According to the static light scattering data Fig. 6C shows that the product obtained with higher DMSO feed (17.5%) in the absence of helium contain large agglomerates. These agglomerates present in fact a continuous matrix characterized by high irregular surface and porosity, which indicates that they were formed by partial fusion of smaller particles as revealed by light scattering analysis. On the contrary, Fig. 6D shows that the product obtained with high DMSO feed in the presence of helium is mainly formed by small particles.

DSC analyses were performed to evaluate the physical state of the components of the matrix and curcumin and the homogeneity of the final product.

The thermograms reported in Fig. 7 indicate that all formulations, except the one obtained with high DMSO feed, present a single endothermic peak that further confirms the homogeneity of the lipid matrix, while the peaks ascribable to the single components of the particles, namely the crystalline curcumin, were not visible. This confirms that the solid lipid matrix is homogeneous,

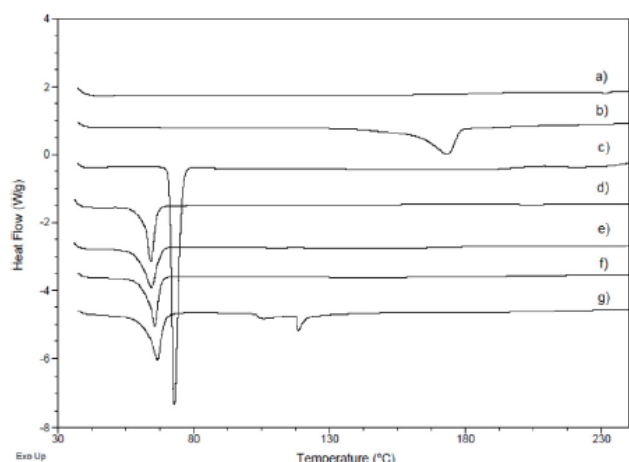


Fig. 7. DSC thermograms of raw material and curcumin-loaded solid lipid particles (a) soy PC; (b) curcumin; (c) tristearin; (d) Mix 2; (e) Mix 3; (f) Mix 4; (g) Mix 5.

Table 2

Experimental values of melting point temperatures from DSC analyses.

Sample	Melting point (°C)
Tristearin	72.93 ± 0.06
Soy PC	231.87 ± 0.16
Curcumin	173.35 ± 0.10
Mix 2	64.21 ± 0.10
Mix 3	64.45 ± 0.14
Mix 4	65.74 ± 0.10
Mix 5	68.01 ± 2.00/119.04 ± 0.76

Values showed as average ± standard deviation.

without evidence of phase separation or crystallization of the single different components.

The homogeneity of the matrix results in a significantly lower melting point with respect to the bulk materials, as listed on Table 2. To note that no significant differences were observed among the melting points of samples obtained with different compositions and prepared under different conditions, namely DMSO feed and room atmosphere/helium processing. These DSC data confirm that the PGSS process allowed for extensive DMSO removal (the peak at the corresponding boiling temperature is missing), without any dragging and segregation of amorphous or crystalline soy PC and curcumin in the particle surface during the expansion step. Furthermore, helium was not affecting the physical structure of the lipid matrix, probably because helium was completely washed out from the lipid mass by CO₂. Instead, in the case of the particle preparation obtained with DMSO feed of 17.5% (Mix 5, Fig. 7g), two endothermic peaks have been observed at 90 and 120 °C which indicates the non-homogeneity of the matrix and possible phase-separation of the components. The literature reports in fact that DMSO mixed to lipids can produce multiple impacted domain growth that, in the DSC thermogram, corresponds to a multiplicity of peaks [44].

The resulting inhomogeneity can be responsible for the particle destabilization, and the increase of size and polydispersity observed in the samples obtained with high DMSO feed by SLS and SEM analysis. It is important to note that, an inhomogeneous matrix such as that of sample SLP 5 may cause undesired biopharmaceutical behaviour such as dissociation of curcumin or lipids components from the matrix upon storage time, and inhomogeneous/unpredictable component dissolution rate, which can dramatically affect the bioavailability of the biologically active molecules.

5. Conclusions

The results reported in the present study show that a few main critical operative conditions dictate the PGSS process for the production of curcumin loaded Solid lipid Particles (SLP). The feed ratio of DMSO used for the preparation of the lipid mass as well as the use of helium were found to be relevant to prepare SLP with suitable biopharmaceutical properties. By using small feed ratios of DMSO and helium during the curcumin/lipid mixture preparation it was possible to obtain dimensionally homogeneous SLP while preventing massive aggregation phenomena. On the other hand, the use of helium preserved the chemical stability of curcumin as no degradation was detected after processing. Interestingly, helium was found to enhance also the drug loading and to participate in the control of the dimensional properties of SLP, indicating that it affects the lipid matrix structure.

The results show that the PGSS process can be properly set-up to produce SLP with pharmaceutical requisites for delivering drugs that, due to their chemical fragility, have not found suitable formulation yet. Furthermore, the process can guarantee the physical stability of the formulation, which is also a crucial for the pharmaceutical exploitation of these products.

Acknowledgements

We would like to thank the FIOCRUZ—Unit CPqGM staff for helping with morphological analysis.

References

- [1] J.M. Witkin, X. Li, Curcumin, an active constituent of the ancient medicinal herb *Curcuma longa* L.: some uses and the establishment and biological basis of medical efficacy, *CNS Neurol. Disord.—Drug Targets* 12 (2013) 487–497.
- [2] B.B. Aggarwal, K.B. Harikumar, Potential therapeutic effects of curcumin, the anti-inflammatory agent, against neurodegenerative, cardiovascular, pulmonary, metabolic, autoimmune and neoplastic diseases, *Int. J. Biochem. Cell Biol.* 41 (2009) 40–59.
- [3] L. Shen, H.-F. Ji, The pharmacology of curcumin: is it the degradation products? *Trends Mol. Med.* 18 (2012) 138–144.
- [4] C. Mohanty, S.K. Sahoo, The in vitro stability and in vivo pharmacokinetics of curcumin prepared as an aqueous nanoparticulate formulation, *Biomaterials* 31 (2010) 6597–6611.
- [5] P. Anand, A.B. Kunnumakkara, R. a Newman, B.B. Aggarwal, Bioavailability of curcumin: problems and promises, *Mol. Pharmaceutics* 4 (2007) 807–818.
- [6] P. Dadhaniya, C. Patel, J. Muchhara, N. Bhadja, N. Mathuria, K. Vachhani, et al., Safety assessment of a solid lipid curcumin particle preparation: acute and subchronic toxicity studies, *Food Chem. Toxicol.* 49 (2011) 1834–1842.
- [7] A. Bernkop-Schnürch, Nanocarrier systems for oral drug delivery: do we really need them? *Eur. J. Pharm. Sci.* 49 (2013) 272–277.
- [8] R. Solaro, F. Chiellini, A. Battisti, Targeted delivery of protein drugs by nanocarriers, *Materials (Basel)* 3 (2010) 1928–1980.
- [9] V. Kakkar, A.K. Mishra, K. Chuttani, I.P. Kaur, Proof of concept studies to confirm the delivery of curcumin loaded solid lipid nanoparticles (C-SLNs) to brain, *Int. J. Pharm.* 448 (2013) 354–359.
- [10] A. Noack, G. Hause, K. Mäder, Physicochemical characterization of curcuminoid-loaded solid lipid nanoparticles, *Int. J. Pharm.* 423 (2012) 440–451.
- [11] S. Kumar, J.K. Randhawa, High melting lipid based approach for drug delivery: solid lipid nanoparticles, *Mater. Sci. Eng., C: Mater. Biol. Appl.* 33 (2013) 1842–1852.
- [12] E. Lepeltier, C. Bourgaux, P. Couvreur, Nanoprecipitation and the “Ouzo effect”: application to drug delivery devices, *Adv. Drug Delivery Rev.* 71 (2014) 86–97.
- [13] S. Chakraborty, D. Shukla, B. Mishra, S. Singh, Lipid—an emerging platform for oral delivery of drugs with poor bioavailability, *Eur. J. Pharm. Biopharm.* 73 (2009) 1–15.
- [14] J. Pietkiewicz, M. Sznitowska, M. Placzek, The expulsion of lipophilic drugs from the cores of solid lipid microspheres in diluted suspensions and in concentrates, *Int. J. Pharm.* 310 (2006) 64–71.
- [15] A. Kovacevic, S. Savic, G. Vuleta, R.H. Müller, C.M. Keck, Polyhydroxy surfactants for the formulation of lipid nanoparticles (SLN and NLC): effects on size, physical stability and particle matrix structure, *Int. J. Pharm.* 406 (2011) 163–172.
- [16] W. Mehnert, K. Mader, Solid lipid nanoparticles: production, characterization and applications, *Adv. Drug Delivery Rev.* 47 (2001) 165–196.
- [17] A. zur Mühlen, C. Schwarz, W. Mehnert, Solid lipid nanoparticles (SLN) for controlled drug delivery—drug release and release mechanism, *Eur. J. Pharm. Biopharm.* 45 (1998) 149–155.
- [18] J. Frenkel, C. Wess, W. Vyverman, G. Pohnert, Chiral separation of a diketopiperazine pheromone from marine diatoms using supercritical fluid chromatography, *J. Chromatogr. B: Anal. Technol. Biomed. Life Sci.* 951–952 (2014) 58–61.
- [19] K. Kalíková, T. Šlechtová, J. Vozka, E. Tesařová, Supercritical fluid chromatography as a tool for enantioselective separation—a review, *Anal. Chim. Acta* 821 (2014) 1–33.
- [20] A. Kemzūraitė, P.R. Venskūtonis, R. Baranauskienė, D. Navikienė, Optimization of supercritical CO₂ extraction of different anatomical parts of lovage (*Levisticum officinale* Koch.) using response surface methodology and evaluation of extracts composition, *J. Supercrit. Fluids* 87 (2014) 93–103.
- [21] M. Rossmann, A. Braeuer, E. Schluecker, Supercritical antisolvent micronization of PVP and ibuprofen sodium towards tailored solid dispersions, *J. Supercrit. Fluids* 89 (2014) 16–27.
- [22] G. Brunner, N.T. Machado, Process design methodology for fractionation of fatty acids from palm fatty acid distillates in countercurrent packed columns with supercritical CO₂, *J. Supercrit. Fluids* 66 (2012) 96–110.
- [23] E. Reverchon, I. De Marco, E. Torino, Nanoparticles production by supercritical antisolvent precipitation: a general interpretation, *J. Supercrit. Fluids* 43 (2007) 126–138.
- [24] E. Reverchon, R. Adami, S. Cardea, G. Della Porta, G. Della Porta, Supercritical fluids processing of polymers for pharmaceutical and medical applications, *J. Supercrit. Fluids* 47 (2009) 484–492.
- [25] A.P. Nayak, W. Tiyaboonchai, S. Patankar, B. Madhusudhan, E.B. Souto, Curcuminoids-loaded lipid nanoparticles: novel approach towards malaria treatment, *Colloids Surf., B: Biointerfaces* 81 (2010) 263–273.
- [26] J. Sun, C. Bi, H.M. Chan, S. Sun, Q. Zhang, Y. Zheng, Curcumin-loaded solid lipid nanoparticles have prolonged in-vitro antitumor activity, cellular uptake and improved in-vivo bioavailability, *Colloids Surf., B: Biointerfaces* 111 (2013) 367–375.
- [27] V. Kakkar, S. Singh, D. Singla, I.P. Kaur, Exploring solid lipid nanoparticles to enhance the oral bioavailability of curcumin, *Mol. Nutr. Food Res.* 55 (2011) 495–503.
- [28] V. Kakkar, S. Bhushan, G.S. Kumar, I.P. Kaur, Enhanced apoptotic effect of curcumin loaded solid lipid nanoparticles, *Mol. Pharm.* 9 (2012) 3411–3421.
- [29] V.R. Yadav, S. Suresh, K. Devi, S. Yadav, Novel formulation of solid lipid microparticles of curcumin for anti-angiogenic and anti-inflammatory activity for optimization of therapy of inflammatory bowel disease, *J. Pharm. Pharmacol.* 61 (2009) 311–321.
- [30] F. Zabihi, N. Xin, S. Li, J. Jia, T. Cheng, Y. Zhao, Polymeric coating of fluidizing nano-curcumin via anti-solvent supercritical method for sustained release, *J. Supercrit. Fluids* 89 (2014) 99–105.
- [31] A. Martín, M.J. Cocero, Micronization processes with supercritical fluids: fundamentals and mechanisms, *Adv. Drug Delivery Rev.* 60 (2008) 339–350.
- [32] S. Salmaso, N. Elvassore, A. Bertucco, P. Caliceti, Production of solid lipid submicron particles for protein delivery using a novel supercritical gas-assisted melting atomization process, *J. Pharm. Sci.* 98 (2009) 640–650.
- [33] S. Salmaso, S. Bersani, N. Elvassore, A. Bertucco, P. Caliceti, Biopharmaceutical characterisation of insulin and recombinant human growth hormone loaded lipid submicron particles produced by supercritical gas micro-atomisation, *Int. J. Pharm.* 379 (2009) 51–58.
- [34] T. Perko, M. Ravber, Z. Knez, M. Skerger, Isolation, characterization and formulation of curcuminoids and in vitro release study of the encapsulated particles, *J. Supercrit. Fluids* 103 (2015) 48–54.
- [35] N. Elvassore, A. Bertucco, P. Caliceti, Production of insulin-loaded poly(ethylene glycol)/poly(L-lactide) (PEG/PLA) nanoparticles by gas antisolvent techniques, *J. Pharm. Sci.* 90 (2001) 1628–1636.
- [36] FDA, International Conference on Harmonisation; Draft Guideline on Impurities: Residual Solvents; Availability; Notice, FDA, 1997.
- [37] Y.K. Han, S.H. Lee, H.J. Jeong, M.H. Yoon, W.M. Kim, Analgesic effects of intrathecal curcumin in the rat formalin test, *Korean J. Pain* 25 (2012) 1–6.
- [38] N. Mittal, R. Joshi, D. Hota, A. Chakrabarti, Evaluation of antihyperalgesic effect of curcumin on formalin-induced orofacial pain in rat, *Phytotherapy Res.* 23 (2009) 507–512.
- [39] K.Y. Yeon, S.A. Kim, Y.H. Kim, M.K. Lee, D.K. Ahn, H.J. Kim, et al., Curcumin produces an antihyperalgesic effect via antagonism of TRPV1, *J. Dent. Res.* 89 (2010) 170–174.
- [40] N. Ahmed, S.A. Baseer, Biotransformation of curcumin to vanillin by *Pseudomonas* species isolated from waste water of Aurangabad, *J. Microbiol. Biotechnol. Res.* 5 (2015) 8–10.
- [41] C. De Jong, H.T. Bading, Determination of free fatty acids in milk and cheese procedures for extraction, clean up, and capillary gas chromatographic analysis, *J. High Resolut. Chromatogr.* 13 (1990) 94–98.
- [42] J.W. King, J.H. Johnson, F.J. Eller, Effect of supercritical carbon dioxide pressurized with helium on solute solubility during supercritical fluid extraction, *Anal. Chem.* 63 (1995) 2288–2291.
- [43] Z. Zhang, J.W. King, The effect of dissolved helium on the density and solvation power of supercritical carbon dioxide, *J. Chromatogr. Sci.* 35 (1997) 483–488.
- [44] S. Tristram-Nagle, T. Moore, H.I. Petrache, Jo.F. Nagle, DMSO produces a new subgel phase in DPPC: DSC and X-ray diffraction study, *Biochim. Biophys. Acta* 1369 (1998) 19–33.
- [45] V.B. Patravale, A new stability-indicating HPLC method for simultaneous determination of curcumin and celecoxib at single wavelength: an application to nanoparticulate formulation, *Pharm. Anal. Acta* 3 (2012) 1–6.
- [46] W. Wichitnithad, N. Jongaroonngamsang, S. Pummangura, P. Rojsitthisak, A simple isocratic HPLC method for the simultaneous determination of curcuminoids in commercial turmeric extracts, *Phytochem. Anal.* 20 (2009) 314–319.
- [47] G.K. Jayaprakasha, L.J.M. Rao, K.K. Sakariah, Improved HPLC method for the determination of curcumin, demethoxycurcumin, and bisdemethoxycurcumin, *J. Agric. Food Chem.* 50 (2002) 3668–3672.
- [48] K. Vezzù, D. Borin, A. Bertucco, S. Bersani, S. Salmaso, P. Caliceti, Production of lipid microparticles containing bioactive molecules functionalized with PEG, *J. Supercrit. Fluids* 54 (2010) 328–334.
- [49] B. Calvignac, Development of characterization techniques of thermodynamic and physical properties applied to the CO₂–DMSO mixture, *Int. J. Chem. Reactor Eng.* 7 (2009) 1–29.
- [50] M. Fraile, Á. Martín, D. Deodato, S. Rodriguez-Rojo, I.D. Nogueira, A.L. Simplicio, M.J. Cocero, C.M.M. Duarte, Production of new hybrid systems for drug delivery by PGSS (particles from gas saturated solutions) process, *J. Supercrit. Fluids* 81 (2013) 226–235.
- [51] K.S. Lindley, N.A. Rowson, Charging mechanisms for particles prior to electrostatic separation, *Magn. Electr. Sep.* 8 (1997) 101–113.
- [52] S. Karner, N. Anne Urbanetz, The impact of electrostatic charge in pharmaceutical powders with specific focus on inhalation-powders, *J. Aerosol Sci.* 42 (2011) 428–445.
- [53] E. Weidner, Z. Knez, Precipitation of solids with dense gases, in: A. Bertucco, G. Vetter (Eds.), *High Pressure Process Technology: Fundamentals and Applications*, Elsevier, Amsterdam, 2001, pp. 587–611.
- [54] J. Li, H.A. Matos, E.G. de Azevedo, Two-phase homogeneous model for particle formation from gas-saturated solution processes, *J. Supercrit. Fluids* 32 (2004) 275–286.

SLN® Production by PGSS and Characterization

1 Size measurement

All SLM samples, after dispersion in distilled water, were submitted to centrifugation at 2500 rpm for 3 min and the supernatants were analyzed by a nanosizer equipment. The intent was to investigate the presence of nanosized populations in the samples not captured by mastersizer analyses. In the supernatants obtained from samples composed of 10.0, 5.0, 2.0 and 1.0% curcumin-loaded SLM, the minimum obscuration required for nanosizer measurements was not achieved. Even after concentration of the sample dispersions, or either test different centrifugation velocities, the measurements could not be performed. Only 0.5 % curcumin samples could be read by nanosizer. A monomodal population of nanoparticles with a homogenous size distribution was found among microparticles as can be proved by a small polydispersion index (PdI) value depicted on Table 8 and also by the typical particle size distribution of the samples showed in Figure 25. This is a very interesting result because the PGSS usually produces microparticles instead of nanoparticles due to the typical high ratio of aggregation during the expansion step. Even in this plant, with an auxiliary N₂ stream to the atomization, it was already proved the increment in aggregation phenomenon caused by the presence of DMSO in the formulation. Despite of this, the current data show the formation of small and homogeneous SLN®. The same tendency was observed for the SLM of the same sample obtained in this work, reinforcing the hypothesis that the applied concentration of DMSO was low enough to not cause an increase in particle aggregation.

Table 8. Size measurement parameters 0.5% curcumin SLN®*

Size	PdI	Zeta potential
118.50 ± 54.34nm	0.62 ± 0.25	-8.97 ± 0.95

*triplicate.

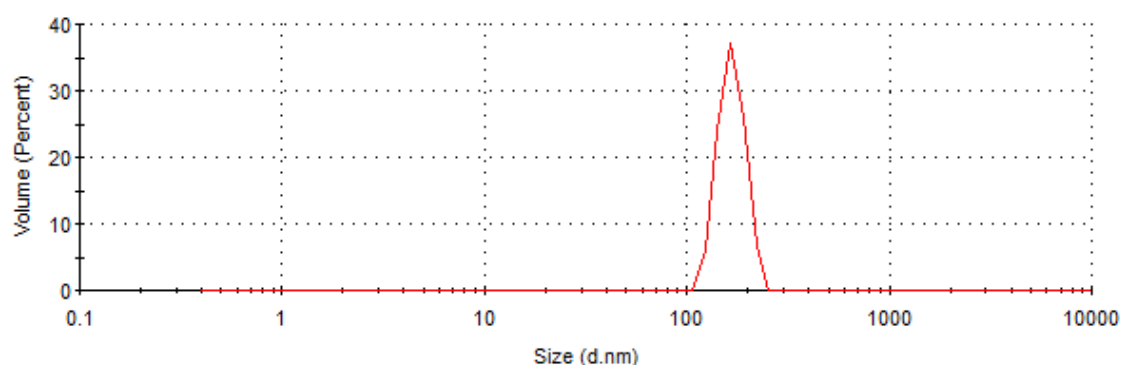


Figure 25. Typical particle size distribution.

2 Morphology

Since the nanoparticle population was collected by dispersion in aqueous media and considering that usual drying methods could affect significantly the morphology of SLN®, the

Transmission Electronic Microscopy (TEM) was selected to analyze the samples. The result is showed in Figure 26.

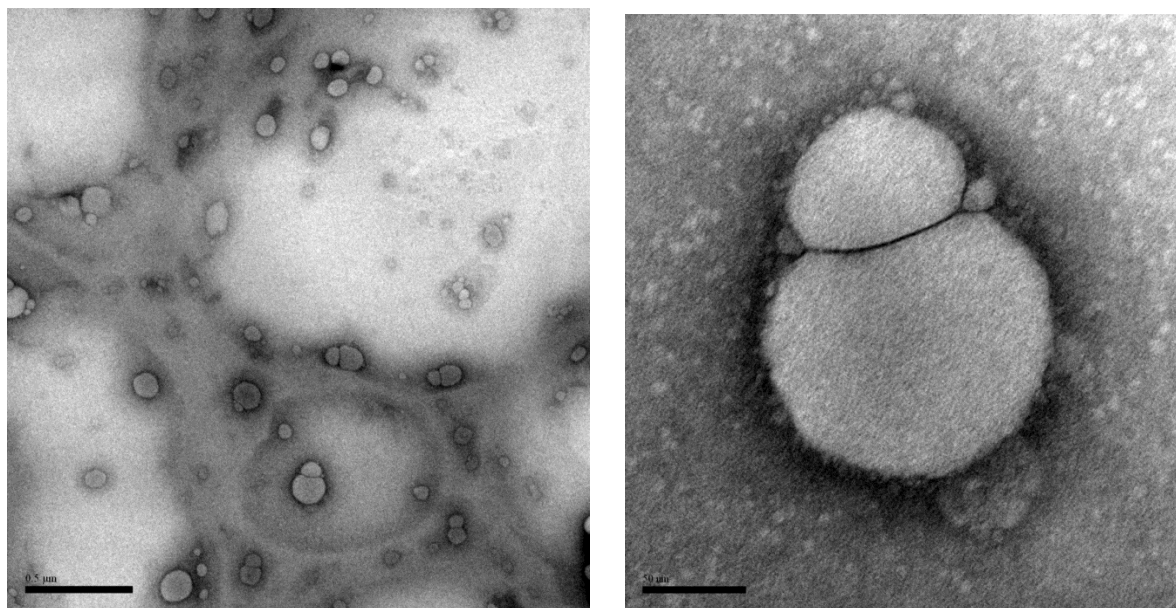


Figure 26. Micrographs of 0.5% curcumin-loaded SLN® obtained by TEM. Scale bar: 500nm

This result is quite surprising because the usual shape of solid lipid particles produced by PGSS is nothing similar to the spherical one (Sampaio De Sousa *et al.*, 2007; Vezzù *et al.*, 2009; Zhu *et al.*, 2010). However, it was already showed that several PGSS operation parameters affect significantly the particle morphology, it means, not only the intrinsic characteristics of the encapsulant material used (Kappler *et al.*, 2003; Pollak *et al.*, 2011). Perhaps, the amount of DMSO in the formulation, which is naturally liquid for both conditions of melting and expansion in the PGSS method, at low concentrations, may act as a glue reinforcing the structural strength of the nanoparticles. Also, since nanoparticles possess a small amount of material associated to a large surface area, they solidify quicker and more homogenously than the microparticles, which favors the maintenance of the original structure just after the droplet formation in the nozzle.

3 Infrared Spectra

The data depicted in Figure 27 were obtained in order to establish a comparison of infrared spectra of free curcumin, empty particles and the 0.5% curcumin-loaded particles. Therefore, the interaction among the curcumin and all the other excipients can be evaluated. The empty particles were prepared by the mixture of only tristearin and Epikuron 200. Table 9 summarizes the main IR bands on the obtained IR spectra and the identification of vibration events was made by comparison with data collected in the literature.

The obtained free-curcumin IR spectrum was very similar to those related in literature. Further, the characteristic bands found showed values very close to those from literature (Mohan *et*

al., 2012; Kundu and Nithiyantham, 2013). As expected, no characteristic band of curcumin was found in IR spectrum of empty particles, which showed to be very similar to those spectra found in literature for PC molecules (Süleymanoglu, 2009; Bridelli *et al.*, 2013). A few number of bands were recognized for tristearin. Since the structure of tristearin is very similar to part of the phospholipid skeletal many of tristearin typical IR bands could be hidden by those for PC. Further, Epikuron 200 is a multi-component product which makes the IR spectrum interpretation more complex.

The curcumin-loaded particles sample provided a IR spectrum very similar to that obtained for empty particles with some typical curcumin bands. All the bands showed to be much sharper than those on the other spectra, but no significant shift or new bands were found. This is a strong indicative that no chemical reaction occurred, which confirms the compatibility among the mixture components. Interestingly, no characteristic sign for DMSO was found on this spectrum, nor even its strongest IR band, the S-O stretching vibration, commonly found in 1014 cm^{-1} (Zazhogin *et al.*, 2008). It was hypothesized that the low DMSO concentration in the sample made its typical bands more difficult to detect.

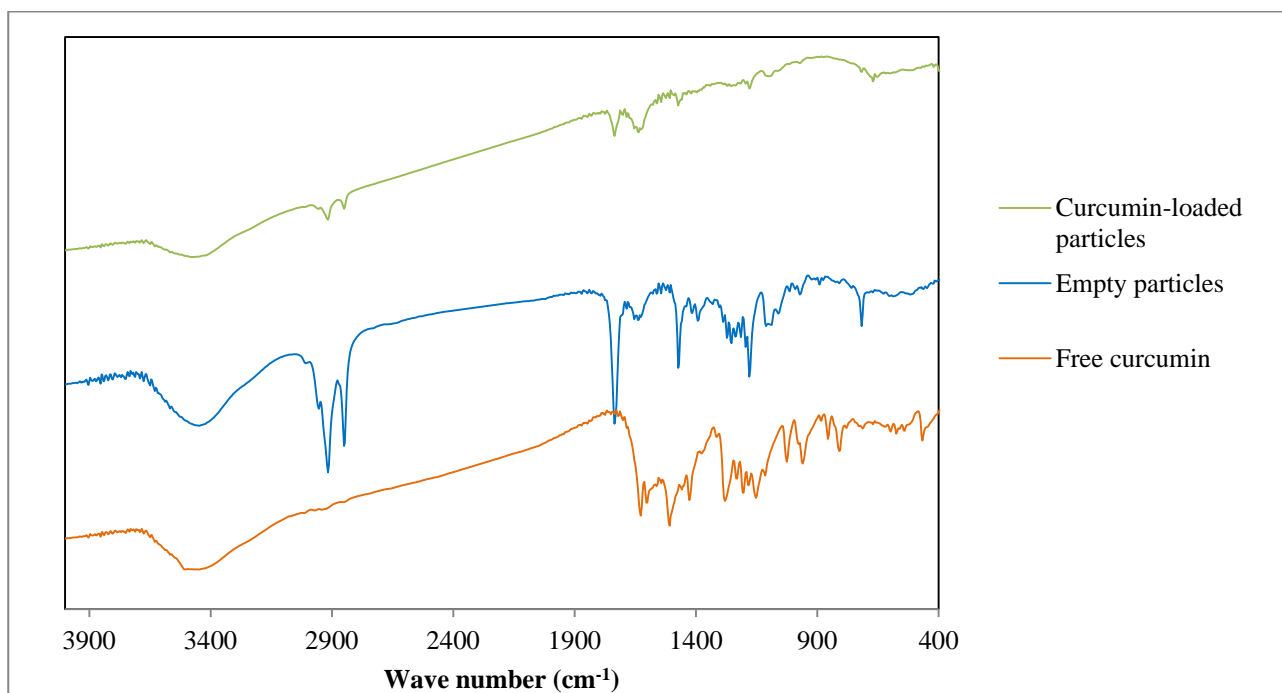


Figure 27. Chemical compatibility evaluation of curcumin and SLN® excipients by IR analysis.

The science of interpretation of structural interactions and composition through IR analysis is based on the assumption that each deformation of the molecule or vibration of a group of atoms will generate a particular band on IR spectrum. However, small steric or electronic effect as well as skeletal vibrations can present an unpredictable behavior after IR exposure, leading to large shifts

on absorbance patterns (Stuart, 2004). In addition, the samples evaluated in this work were prepared with a natural phospholipid - Epikuron 200, which means that it is composed of a complex mixture of fatty-acid-derived components that increment the complexity of inter and intramolecular interactions making the IR interpretation even harder. In this context, only some of the IR bands can be detected or interpreted, and not necessarily the absence or a large shift of an IR band will mean the non compatibility of formulation components.

Table 9. Identification of bands found on obtained IR spectra.

SLN® Components	Vibration events	Sample IR bands (cm ⁻¹)			Literature IR bands (cm ⁻¹)	References
		Free curcumin	Empty particles	Curcumin- loaded particles		
Curcumin	cis aromatic (CH)	709	-	713	713	(Mohan <i>et al.</i> , 2012; Kundu and Nithiyantham, 2013)
	out of plane δ aromatic (CCH)	852	-	864	852	
	benzoate trans (CH)	956	-	-	960	
	ν (C-O-C) / out of plane δ (CH ₃), in plane δ aromatic (CCH)	1022	-	-	1023	
	in plane δ aromatic (CCH)	1423	-	-	1429	
	ν (C=O)	1508	-	1508	1510	
	ν (C=C) aromatic	1600	-	-	1601	
	ν (C=C)	1627	-	1635	1626	
	ν (OH)	3271-3599	-	3278-3606	3200-3600	
	ν (OH) from phenol group	3502	-	-	3508	
Phosphatidylcholine	ν (OH)	-	3603-3305	3614-3352	3600-3200	(Süleymanoglu, 2009; Bridelli <i>et al.</i> , 2013)
	ν (NH ⁺³)	-	3290-3178	3302-3178	3500-3000	
	δ_{as} N ⁺ -[(CH ₃) ₃]	-	972	968	970	
	ν_{as} (C-CH ₃)	-	2916	2912	2920	
	ν_s (C-CH ₃)	-	2846	2846	2850	
	scissoring δ [(CH ₂) _n]	-	1473	1458	1467	
	rocking ν (CH ₂)	-	717	721	722	
	ν (C=O) from R-COOH group	-	1735	1732	1744	
	ν (C=C)	-	1624	1624	1657	
	ν_{as} (PO ₂ ⁻)	-	-	-	1232	
ν_s (PO ₂ ⁻)	-	1087	1072	1085		
Tristearin	ν (C=O) from ester group	-	1735	1735	1736	(Kishore <i>et al.</i> , 2011; Nair <i>et al.</i> , 2012)
	ν_s (C-CH ₃)	-	2846	2846	2849	
	ν_{as} (C-O-C)	-	1176	1180	1176	

* ν = stretching vibrations / δ = bending vibrations / s = symmetric / as = asymmetric.

4 Cytotoxicity test

Only the formulation at 0.5 % curcumin content could be analyzed for cytotoxicity response. After dispersion on culture media, all formulations were dropped into test wells containing pre-incubated cells. However, the samples containing 1.0 - 10.0% curcumin floated and formed aggregates into the wells clogging at the bottom and blocking the access to media nutrients by the

cells, leading to the death of 100% of exposed groups. Once the 0.5% curcumin-loaded sample showed to be composed by the smallest particles, they could be effectively dispersed in culture media using a pipette.

As indicated in Figure 27, the encapsulation of curcumin in the solid lipid particles led to a statistic significant decrease of its cytotoxicity. It can be also observed that there is a larger difference between free and entrapped drug at a concentration of 100 $\mu\text{g/L}$ than that of 10 $\mu\text{g/L}$. This indicates that the protective effect from lipid particles excipients can be dose-related. However, to prove this relation more concentrations must be tested. Higher concentrations were tested, but the increase in particles concentration in culture media led to the problems showed by the afore mentioned samples. Also, it is important to note that from 10 to 100 $\mu\text{g/L}$ of free and encapsulated curcumin, it was observed a maximum cell viability of only 30%. These data bring a concern to the safety profile of the produced SLM/SLN formulation. On the other hand, the full cytotoxicity profile of this formulation cannot be denoted only by this preliminary assay, i.e. much more information must be collected and produced with basis on additional tests.

The use of biocompatible excipients in pharmaceutical formulations plays a pivotal role to the achievement of a safe therapeutic profile. Both tristearin and Epikuron200 are recognized as biocompatible and the fact that this formulation presents the lowest amount of DMSO helps to reach a safer behavior on a biologic environment.

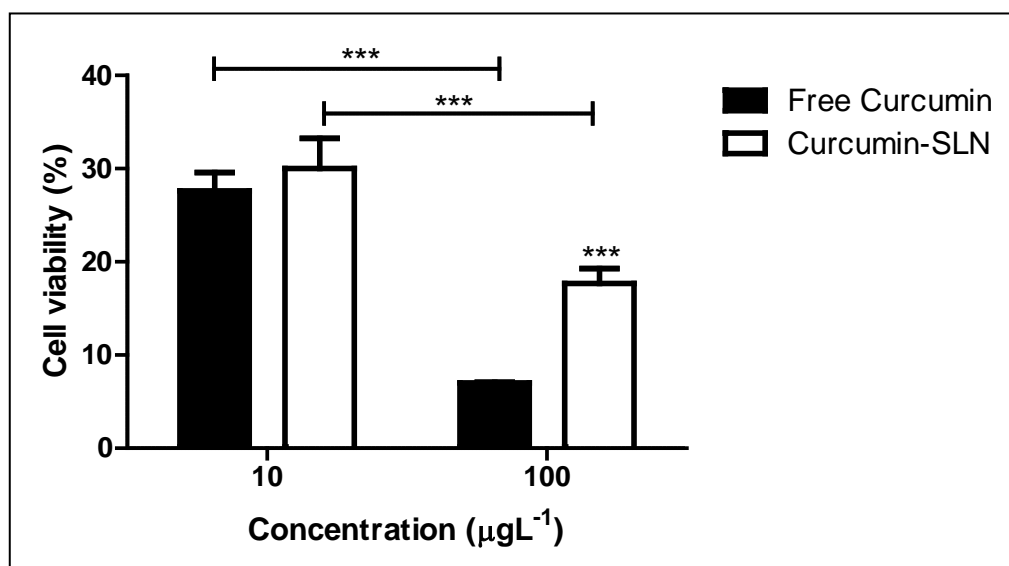


Figure 28. Evaluation of the effect of free and encapsulated curcumin on cell viability. *** $p < 0.0001$

VI

Conclusions

This work has enlighten the interaction among lipid carriers, curcumin and CO₂. The data and discussion brought by this thesis have a great relevance, considering the complexity of the applied system, not only due to the number - five - of components, but also to the nature of components. The large difference of molecular weight among the components, the need of DMSO as co-solvent for dissolving curcumin on the lipid matrix, the natural different crystalline structures that can be present in solid tristearin, as well as the large number of possible structural shifts of unsaturated phospholipids along temperature small changes draw how big was the challenge for understanding the thermal behavior of this system. This complexity also appears as an obstacle for the application of predictive models based on groups contribution methods, since current ones cannot reach the number of intra and intermolecular events involved in these systems. Therefore, experimental data have a pivotal role on this matter. The contribution of this thesis fulfills, at least partially, the huge lack of information concerning the thermodynamic behavior of complex lipids, such as phospholipids, in the context of supercritical fluid processing.

High pressure DSC studies demonstrated in binary lipid mixtures that the higher the natural PC content, the more heterogeneous the mixture with tristearin was showed to be, it means, melting events derived from PC and different crystalline forms of tristearin could be detected. However, when CO₂ is added to the system at 40 bar, the composition shows no effect on the range tested and the homogeneity is detected for all mixtures by obtainment of only one melting peak. It demonstrates that at certain point the plasticization effect of dense CO₂ caused by CO₂ solubilization on the lipid matrix rules the thermal behavior of the system. When curcumin dissolved into DMSO is added to the system, all the range of compositions showed to be homogenous and the dense CO₂ solubilization remarkably reduced the melting point of the system. These data show to be innovative also by the employment of a technique used a few times in literature that allows the association of a very accurate method to detect a phase change event to analysis at high pressure under CO₂ atmosphere.

Solid lipid microparticles and nanoparticles entrapping curcumin were successfully produced by PGSS with a drug loading up to 87% (w/w) and no sign of drug degradation. The obtained drug loading correlates with those obtained by traditional SLN®/SLM preparation methods, but with all natural advantages of supercritical fluid technology. Along with this achievement, the study of operational conditions revealed the importance of structural adaptations of the PGSS plant, as well as of the method the mixture preparation of the lipids and the drug to the production optimization. The auxiliary flow of nitrogen close to the nozzle showed to be essential to reduce the agglomeration improving the atomization of the molten mass derived from the mixing chamber. In addition, the use of helium on the preparation of mixture showed to improve the drug

loading on the particles. Surprisingly the higher the amount of curcumin, the lower the drug loading yield. It was hypothesized that since DMSO has partial solubility in $scCO_2$, the $scCO_2$ can act as an extractor agent leading to a curcumin precipitation avoiding its channeling to the expansion chamber of the PGSS plant. Further, DMSO contributes to the aggregation of particles. This information explained the best result achieved with 0.5% (w/w) curcumin formulation in which the highest values of drug loading and lowest dispersion of size distribution were obtained.

However, the most interesting result obtained in this work was the actual production of SLN®. This is the first time that solid lipid particles of nanometric scale have been obtained by PGSS. All the other works with PGSS have managed to produce lipid microparticles or at most submicroparticles, mainly due to intrinsic limitations of their plants, as well as to the natural aggregation potential of solid lipid material. On the other hand, the SLN® were produced as part of SLM samples, more specifically those of 0.5% (w/w) curcumin. It is also very important to note that the SLM and SLN® produced in this work do not present the conventional structure obtained by traditional methods. Generally, phosphatidylcholine is applied as surfactant and is naturally carried to the surface of the particles stabilizing them on the suspension. In this work, the particles were produced containing the phosphatidylcholine on the interstice of the particle, as a structural component. So, a complete different behavior can be achieved in *in vitro* and *in vivo* tests, due to the unique characteristics of these SLN®/SLM samples produced by PGSS.

The relevance of this find is also intimately related with the advantages of working with PGSS in comparison with other techniques on the context of supercritical fluid technology applied for SLN® production. The direct obtainment of SLN® in powder form, reduces the number of steps, increments the production yield, as well as the use of CO_2 as solute leads to a fewer consumption of gas. Briefly, the method applied in this work showed to be valid, useful and very suitable for the obtainment of homogeneous nano and microsized solid lipid particles.

Future Perspectives

VII

Despite all interesting results obtained in this work, there is so much more to do. A full comprehension of phase equilibrium behavior would be of great value to understand the behavior of curcumin-lipid-DMSO system in PGSS process. This comprehension can lead to achievement of better prediction of optimum operation conditions. The use of a high pressure DSC systems capable of reaching work pressures (above 100 bar) or high pressure equilibrium cells can provide these answers.

Further, not only operation conditions can be altered, but also structural assembly of the plant to grant the production of samples fully composed of nanoparticles. Also, a production of a formulation totally organic solvent free should be achieved, so a new set of experimental runs evolving different component rates can be carried out for this system in order to reach this goal.

In vitro cytotoxicity tests must be conducted in order to provide a better interpretation upon the safety profile of the SLN®/SLM samples obtained in this work. Not only different methods, but also different cell lines must be investigated. *In vitro* drug release tests must be carried out in order to establish the release profile of curcumin from the particles. The selection of correct release media for curcumin obeying the rules of sink conditions as well as the stability profile of curcumin is still a challenge. Meanwhile, *in vivo* tests can be performed with experimental models of acute inflammatory pain and neuropathic pain to finally identify if the proposed formulation in this work is capable of offering an improvement and/or prolonging of analgesic profile of curcumin in different types of chronic pain syndromes.

References. VIII

REFERENCES

AGGARWAL, B. B.; GUPTA, S. C.; SUNG, B. Curcumin: an orally bioavailable blocker of TNF and other pro-inflammatory biomarkers. **British Journal of Pharmacology**, v. 169, n. 8, p. 1672-1692, 2013.

AGGARWAL, B. B.; SURH, Y. J.; SHISHODIA, S. **The Molecular Targets and Therapeutic Uses of Curcumin in Health and Disease**. Springer 2007. 490 ISBN 9780387464015.

AIR PRODUCTS. PolarFit cryogenic grinding/milling system configurations for particle size reduction. Allentown, PA, United States, 2016. Disponível em: <<http://www.airproducts.com/Microsites/grinding-milling/polarfit-system-configurations.aspx>>. Acesso em: June 13th, 2016.

AJI ALEX, M. R.; CHACKO, A. J.; JOSE, S.; SOUTO, E. B. Lopinavir loaded solid lipid nanoparticles (SLN) for intestinal lymphatic targeting. **European Journal of Pharmaceutical Sciences** v. 42, n. 1-2, p. 11-18, 2011.

AKRAM, M.; UDDIN, S.; AHMED, A.; USMANGHANI, K.; HANNAN, A.; MOHIUDDIN, E.; ASIF, M. *Curcuma longa* and curcumin: A review article. **Romanian Journal of Biology - Plant Biology**, v. 55, n. 2, p. 65-70, 2010.

ALESSI, P.; CORTESI, A.; KIKIC, I.; VECCHIONE, F. Plasticization of Polymers with Supercritical Carbon Dioxide: Experimental Determination of Glass-Transition Temperatures. **Journal of Applied Polymer Science**, v. 88, p. 2189-2193, 2003.

ALMEIDA, A. J.; SOUTO, E. Solid lipid nanoparticles as a drug delivery system for peptides and proteins. **Advanced Drug Delivery Reviews**, v. 59, n. 6, p. 478-90, 2007.

ALOMAR, M. J. Factors affecting the development of adverse drug reactions (Review article). **Saudi Pharmaceutical Journal**, v. 22, n. 2, p. 83-94, 2014.

ANAND, P.; THOMAS, S. G.; KUNNUMAKKARA, A. B.; SUNDARAM, C.; HARIKUMAR, K. B.; SUNG, B.; THARAKAN, S. T.; MISRA, K.; PRIYADARSINI, I. K.; RAJASEKHARAN, K. N.; AGGARWAL, B. B. Biological activities of curcumin and its analogues (Congeners) made by man and Mother Nature. **Biochemical Pharmacology**, v. 76, n. 11, p. 1590-1611, 2008.

ASHP. ASHP guidelines on adverse drug reaction monitoring and reporting. American Society of Hospital Pharmacy. **American Journal of Health-System Pharmacy**, v. 52, n. 4, p. 417-419, 1995.

ATTAMA, A. A.; REICHL, S.; MULLER-GOYMANN, C. C. Diclofenac sodium delivery to the eye: in vitro evaluation of novel solid lipid nanoparticle formulation using human cornea construct. **International Journal of Pharmaceutics** v. 355, n. 1-2, p. 307-313, 2008.

BADENS, E. Drug processing using supercritical fluids. Ninth Conference on Supercritical Fluids and Their Applications, 2010, Sorrento, Itália.

BAHRAMI, M.; RANJBARIAN, S. Production of micro- and nano-composite particles by supercritical carbon dioxide. **The Journal of Supercritical Fluids**, v. 40, n. 2, p. 263-283, 2007.

BALASUBRAMANIAN, K. Molecular Orbital Basis for Yellow Curry Spice Curcumin's Prevention of Alzheimer's Disease. **Journal of Agricultural and Food Chemistry**, v. 54, n. 10, p. 3512–3520, 2006.

BALTAZAR, L. M.;KRAUSZ, A. E.;SOUZA, A. C. O.;ADLER, B. L.;LANDRISCINA, A.;MUSAEV, T.;NOSANCHUK, J. D.;FRIEDMAN, A. J. Trichophyton rubrum is Inhibited by Free and Nanoparticle Encapsulated Curcumin by Induction of Nitrosative Stress after Photodynamic Activation. **PLoS ONE**, v. 10, n. 3, p. 1-14, 2015.

BANDYOPADHYAY, D. Farmer to pharmacist: curcumin as an anti-invasive and antimetastatic agent for the treatment of cancer. **Frontiers in Chemistry**, v. 2, n. 113, p. 1-12, 2014.

BARRY, J. J.;SILVA, M. M.;POPOV, V. K.;SHAKESHEFF, K. M.;HOWDLE, S. M. Supercritical carbon dioxide: putting the fizz into biomaterials. **Philosophical Transactions. Series A, Mathematical, Physical, and Engineering Sciences** v. 364, n. 1838, p. 249-261, 2006.

BASNET, P.; SKALKO-BASNET, N. Curcumin: An Anti-Inflammatory Molecule from a Curry Spice on the Path to Cancer Treatment **Molecules** v. 16, n. 6, p. 4567-4598, 2011.

BATTAGLIA, L.;GALLARATE, M.;PANCIANI, P. P.;UGAZIO, E.;SAPINO, S.;PEIRA, E.;CHIRIO, D. Techniques for the Preparation of Solid Lipid Nano and Microparticles. In: SEZER, A. D. (Ed.). **Application of Nanotechnology in Drug Delivery**: InTech, 2014. cap. 2, p.52-75.

BATTAGLIA, L.; TROTTA, M.; CAVALLI, R. Method for the preparation of solid micro and nanoparticles. WIPO Patent. WO2008149215 2008.

BECKMAN, E. J. Supercritical and near-critical CO₂ in green chemical synthesis and processing. **The Journal of Supercritical Fluids**, v. 28 p. 121–191, 2004.

BENKIRANE, R.;PARIENTE, A.;ACHOUR, S.;OUAMMI, L.;AZZOUZI, A.;SOULAYMANI, R. Prevalence and preventability of adverse drug events in a teaching hospital: a cross-sectional study. **Eastern Mediterranean Health Journal**, v. 15, n. 5, p. 1145-1155, 2009.

BENOIT, J.-P.; ROLLAND, H.; THIES, C.; VELDE, V. V. Method of coating particles and coated spherical particles. U.S. Patent. 6087003, 2000.

BERGENSTÄHL, B.; FONTELL, K. Phase equilibria in the system soybean lecithin/water. **Progress in Colloid & Polymer Science** v. 68, n. 8, p. 48-52, 1983.

BERTUCCO, A.; CALICETI, P.; ELVASSORE, N. Process for the production of nano-particles. WIPO Patent. WO 2007/028421 A1, 2007.

BETTS, J.; WAREHAM, D. *In vitro* activity of curcumin in combination with epigallocatechin gallate (EGCG) versus multidrug-resistant *Acinetobacter baumannii*. **BMC Microbiology**, v. 14, n. 1, p. 172-177, 2014.

BHASKAR, K.; ANBU, J.; RAVICHANDIRAN, V.; VENKATESWARLU, V.; RAO, Y. M. Lipid nanoparticles for transdermal delivery of flurbiprofen: formulation, in vitro, ex vivo and in vivo studies. **Lipids Health Dis**, v. 8, p. 6, 2009.

BISWAS, S. K.; MCCLURE, D.; JIMENEZ, L. A.; MEGSON, I. L.; RAHMAN, I. Curcumin Induces Glutathione Biosynthesis and Inhibits NF- κ B Activation and Interleukin-8 Release in Alveolar Epithelial Cells: Mechanism of Free Radical Scavenging Activity. **Antioxidants & Redox Signaling**, v. 7, n. 1-2, p. 32-41, 2005.

BRIDELLI, M. G.; CAPELLETTI, R.; MORA, C. Structural features and functional properties of water in model DMPC membranes: thermally stimulated depolarization currents (TSDCs) and Fourier transform infrared (FTIR) studies. **Journal of Physics D: Applied Physics**, v. 46, p. 1-11, 2013.

BRION, M.; JASPART, S.; PERRONE, L.; PIEL, G.; EVRARD, B. The supercritical micronization of solid dispersions by Particles from Gas Saturated Solutions using experimental design. **The Journal of Supercritical Fluids**, v. 51, n. 1, p. 50-56, 2009.

BUSSANO, R.; CHIRIO, D.; COSTA, L.; TURCI, F.; TROTTA, M. Preparation and Characterization of Insulin-Loaded Lipid-Based Microspheres Generated by Electrospray. **Journal of Dispersion Science and Technology**, v. 32, n. 10, p. 1524-1530, 2011.

CALDERONE, M.; RODIER, E. Method for coating powders. World Intellectual Property Organization Patent. 6056791, 2006.

CALDERONE, M.; RODIER, E.; LETOURNEAU, J.-J.; FAGES, J. Solidification of Precirol® by the expansion of a supercritical fluid saturated melt: From the thermodynamic balance towards the crystallization aspect. **The Journal of Supercritical Fluids**, v. 42, n. 2, p. 189-199, 2007.

CALDERONE, M.; RODIER, E.; LOCHARD, H.; MARCIACQ, F.; FAGES, J. A new supercritical co-injection process to coat microparticles. **Chemical Engineering and Processing: Process Intensification**, v. 47, n. 12, p. 2228-2237, 2008.

CAPITANI, D.; SEGRE, A. L.; DREHER, F.; WALDE, P.; LUISI, P. L. Multinuclear NMR Investigation of Phosphatidylcholine Organogels. **The Journal of Physical Chemistry**, v. 100, p. 15211-15217, 1996.

CHAKRAVARTHI, S. S.; DE, S.; MILLER, D. W.; ROBINSON, D. H. Comparison of anti-tumor efficacy of paclitaxel delivered in nano- and microparticles. **International Journal of Pharmaceutics**, v. 383, n. 1-2, p. 37-44, 2010.

CHARCOSSET, C.; EL-HARATI, A.; FESSI, H. Preparation of solid lipid nanoparticles using a membrane contactor. **Journal of Controlled Release** v. 108, n. 1, p. 112-120, 2005.

CHATTOPADHYAY, P.; HUFF, R.; SHEKUNOV, B. Y. Drug Encapsulation Using Supercritical Fluid Extraction of Emulsions. **Journal of Pharmaceutical Sciences**, v. 95, n. 3, p. 667-678, 2006.

CHATTOPADHYAY, P.; SHEKUNOV, B.; SEITZINGER, J.; GIBSON, A.; HUFF, R. Application of supercritical fluid processing for drug microencapsulation. 15th International Symposium on Microencapsulation, 2005, Parma, Italy. p.21-22.

CHATTOPADHYAY, P.; SHEKUNOV, B. Y.; SEITZINGER, J. S. Method and apparatus for continuous particle production using supercritical fluid. U.S. Patent. 7083748 B2, 2006.

CHATTOPADHYAY, P.; SHEKUNOV, B. Y.; YIM, D.; CIPOLLA, D.; BOYD, B.; FARR, S. Production of solid lipid nanoparticle suspensions using supercritical fluid extraction of emulsions (SFEE) for pulmonary delivery using the AERx system. **Advanced Drug Delivery Reviews**, v. 59, n. 6, p. 444-53, 2007.

CHAUDHARY, A.; NAGAICH, U.; GULATI, N.; SHARMA, V. K.; KHOSA, R. L. Enhancement of solubilization and bioavailability of poorly soluble drugs by physical and chemical modifications: A recent review. **Journal of Advanced Pharmacy Education & Research**, v. 2, n. 1, p. 32-67, 2012.

CHEN, C. C.; TSAI, T. H.; HUANG, Z. R.; FANG, J. Y. Effects of lipophilic emulsifiers on the oral administration of lovastatin from nanostructured lipid carriers: physicochemical characterization and pharmacokinetics. **European Journal of Pharmaceutics and Biopharmaceutics**, v. 74, n. 3, p. 474-82, 2010.

CHIRIO, D.; GALLARATE, M.; PEIRA, E.; BATTAGLIA, L.; SERPE, L.; TROTTA, M. Formulation of curcumin-loaded solid lipid nanoparticles produced by fatty acids coacervation technique. **Journal of Microencapsulation**, v. 28, n. 6, p. 537-548, 2011.

CHO, J.-W.; LEE, K.-S.; KIM, C.-W. Curcumin attenuates the expression of IL-1 β , IL-6, and TNF- α as well as cyclin E in TNF- α -treated HaCaT cells; NF- κ B and MAPKs as potential upstream targets. **International Journal of Molecular Medicine**, v. 19, n. 3, p. 469-474, 2007.

CHUNG, H.; KIM, T.; KWON, I.; JEONG, S. Stability of the oil-in-water type triacylglycerol emulsions. **Biotechnology and Bioprocess Engineering**, v. 6, n. 4, p. 284-288, 2001.

CIFTCI, O. N.; TEMELLI, F. Formation of solid lipid microparticles from fully hydrogenated canola oil using supercritical carbon dioxide. **Journal of Food Engineering**, v. -, n. -, p. . in press, 2016.

COCERO, M. J.; MARTÍN, Á.; MATTEA, F.; VARONA, S. Encapsulation and co-precipitation processes with supercritical fluids: Fundamentals and applications. **The Journal of Supercritical Fluids**, v. 47 p. 546-555, 2009.

CORRIAS, F.; LAI, F. New methods for lipid nanoparticles preparation. **Recent Patents on Drug Delivery and Formulation**, v. 5, n. 3, p. 201-213, 2011.

DA SILVA, E.; BRESSON, S.; ROUSSEAU, D. Characterization of the three major polymorphic forms and liquid state of tristearin by Raman spectroscopy. **Chemistry and Physics of Lipids**, v. 157, n. 2, p. 113-119, 2009.

DAS, L.; VINAYAK, M. Long-term effect of curcumin down-regulates expression of tumor necrosis factor- α and interleukin-6 via modulation of E26 transformation-specific protein and nuclear factor- κ B transcription factors in livers of lymphoma bearing mice. **Leukemia & Lymphoma**, v. 55, n. 11, p. 2627-2636, 2014.

DAVIES, O.; LEWIS, A.; WHITAKER, M.; TAI, H.; SHAKESHEFF, K.; HOWDLE, S. Applications of supercritical CO₂ in the fabrication of polymer systems for drug delivery and tissue engineering. **Advanced Drug Delivery Reviews**, v. 60, p. 373-387, 2008.

DE PAZ-CAMPOS, M. A.; CHAVEZ-PINA, A. E.; ORTIZ, M. I.; CASTANEDA-HERNANDEZ, G. Evidence for the Participation of ATP-sensitive Potassium Channels in the Antinociceptive Effect of Curcumin. **Korean Journal of Pain**, v. 25, n. 4, p. 221-227, 2012.

DE PAZ-CAMPOS, M. A.; ORTIZ, M. I.; CHÁVEZ PIÑA, A. E.; ZAZUETA-BELTRÁN, L.; CASTAÑEDA-HERNÁNDEZ, G. Synergistic effect of the interaction between curcumin and diclofenac on the formalin test in rats. **Phytomedicine**, v. 21, n. 12, p. 1543-1548, 2014.

DEL CURTO, M. D.; CHICCO, D.; D'ANTONIO, M.; CIOLLI, V.; DANNAN, H.; D'URSO, S.; NEUTEBOOM, B.; POMPILI, S.; SCHIESARO, S.; ESPOSITO, P. Lipid microparticles as sustained release system for a GnRH antagonist (Antide). **Journal of Controlled Release**, v. 89, n. 2, p. 297-310, 2003.

DEL POZO-RODRIGUEZ, A.; DELGADO, D.; SOLINIS, M. A.; GASCON, A. R.; PEDRAZ, J. L. Solid lipid nanoparticles for retinal gene therapy: transfection and intracellular trafficking in RPE cells. **International Journal of Pharmaceutics** v. 360, n. 1-2, p. 177-183, 2008.

DEL POZO-RODRIGUEZ, A.; DELGADO, D.; SOLINIS, M. A.; PEDRAZ, J. L.; ECHEVARRIA, E.; RODRIGUEZ, J. M.; GASCON, A. R. Solid lipid nanoparticles as potential tools for gene therapy: in vivo protein expression after intravenous administration. **International Journal of Pharmaceutics** v. 385, n. 1-2, p. 157-162, 2010.

DÍAZ-TRISTE, N. E.; GONZÁLEZ-GARCÍA, M. P.; JIMÉNEZ-ANDRADE, J. M.; CASTAÑEDA-HERNÁNDEZ, G.; CHÁVEZ-PIÑA, A. E. Pharmacological evidence for the participation of NO-cGMP-KATP pathway in the gastric protective effect of curcumin against indomethacin-induced gastric injury in the rat. **European Journal of Pharmacology**, v. 730, n. -, p. 102-106, 2014.

DOUCET, L.; ASCANIO, G.; TANGUY, P. A. Hydrodynamics Characterization of Rotor-Stator Mixer with Viscous Fluids. **Chemical Engineering Research and Design**, v. 83, n. 10, p. 1186-1195, 2005.

EKAMBARAM, P.; ABDUL HASAN SATHALI, A. Formulation and Evaluation of Solid Lipid Nanoparticles of Ramipril. **Journal of Young Pharmacists**, v. 3, n. 3, p. 216-220, 2011.

EKAMBARAM, P.; SATHALI, A. A. H.; PRIYANKA, K. Solid lipid nanoparticles: A Review. **Scientific Reviews & Chemical Communications**, v. 2, n. 1, p. 80-102, 2012.

FDA. **CFR - Code of Federal Regulations Title 21 - Food and Drugs. Chapter 1 - Food and Drug Administration Department Of Health And Human Services. Subchapter D-Drugs For Human Use. Part 312 - Investigational New Drug Application. Subpart B-Investigational New Drug Application (IND)**. US Government. 2015

FRANCESCHI, M.;SCARCELLI, C.;NIRO, V.;SERIPA, D.;PAZIENZA, A.;PEPE, G.;COLUSSO, A.;PACILLI, L.;PILOTTO, A. Prevalence, clinical features and avoidability of adverse drug reactions as cause of admission to a geriatric unit: a prospective study of 1756 patients. **Drug Safety**, v. 31, n. 6, p. 545-556, 2008.

GALANO, A.;ÁLVAREZ-DIDUK, R.;RAMÍREZ-SILVA, M. T.;ALARCÓN-ÁNGELES, G.;ROJAS-HERNÁNDEZ, A. Role of the reacting free radicals on the antioxidant mechanism of curcumin. **Chemical Physics**, v. 363, n. 1–3, p. 13-23, 2009.

GAO, F.;BU, H.;ZHANG, Z.;XIAO, J.;LI, Y. Solid lipid nanoparticles loading candesartan cilexetil enhance oral bioavailability: in vitro characteristics and absorption mechanism in rats. **Nanomedicine: Nanotechnology, Biology and Medicine**. *in press.*, 2011.

GAO, Y.;GU, W.;CHEN, L.;XU, Z.;LI, Y. The role of daidzein-loaded sterically stabilized solid lipid nanoparticles in therapy for cardio-cerebrovascular diseases. **Biomaterials**, v. 29, n. 30, p. 4129-4136, 2008.

GARCÍA-GONZÁLEZ, C. A.;ARGEMÍ, A.;SOUSA, A. R. S. D.;DUARTE, C. M. M.;SAURINA, J.;DOMINGO, C. Encapsulation efficiency of solid lipid hybrid particles prepared using the PGSS® technique and loaded with different polarity active agents. **The Journal of Supercritical Fluids**, v. 54 p. 342–347, 2010.

GARGEYI, P.;SENTHIL, K. K.;HAREESHA, C.;MADHURI, K.;SWATHI, K. V. Curcumin: The Spice for Life. **International Journal of Pharmaceutical, Chemical and Biological Sciences**, v. 1, n. 1, p. 48-56, 2011.

GEREMIAS-ANDRADE, I.; ANDREASSA, D.; PINHO, S. **Influence of the incorporation of curcumin-loaded solid lipid microparticles on the characteristics of mixed whey protein isolate-xanthan gum gels**. 16th Food Colloids Conference. SCHOLTEN, E.;MARTIN, A., *et al.* Wageningen, the Netherlands: 75 p. 2016.

GOKCE, E. H.;SANDRI, G.;BONFERONI, M. C.;ROSSI, S.;FERRARI, F.;GUNERI, T.;CAMELLA, C. Cyclosporine A loaded SLNs: evaluation of cellular uptake and corneal cytotoxicity. **International Journal of Pharmaceutics** v. 364, n. 1, p. 76-86, 2008.

GONÇALVES, V. S. S.;RODRÍGUEZ-ROJO, S.;MATIAS, A. A.;NUNES, A. V. M.;NOGUEIRA, I. D.;NUNES, D.;FORTUNATO, E.;DE MATOS, A. P. A.;COCERO, M. J.;DUARTE, C. M. M. Development of multicore hybrid particles for drug delivery through the precipitation of CO₂ saturated emulsions. **International Journal of Pharmaceutics**, v. 478, n. 1, p. 9-18, 2015.

GONZÁLEZ-ARIAS, S.;VERÓNICO-SÁNCHEZ, F. J.;ELIZALDE-SOLIS, O.;ZÚÑIGA-MORENO, A.;CAMACHO-CAMACHO, L. E. An enhanced “first freezing point” method for solid–liquid–gas equilibrium measurements in binary systems. **The Journal of Supercritical Fluids**, v. 104, p. 301-306, 2015.

GOTA, V. S.;MARU, G. B.;SONI, T. G.;GANDHI, T. R.;KOCHAR, N.;AGARWAL, M. G. Safety and pharmacokinetics of a solid lipid curcumin particle formulation in osteosarcoma patients and healthy volunteers. **Journal of Agricultural and Food Chemistry** v. 58, n. 4, p. 2095-2099, 2010.

GRIFFIN, W. C. Classification of Surface Active Agents by HLB. **Journal of Cosmetic Science**, v. 1, n. 5, p. 311-326, 1949.

GRODOWSKA, K.; PARCZEWSKI, A. Organic solvents in the pharmaceutical industry. **Acta Poloniae Pharmaceutica - Drug Research**, v. 67, n. 1, p. 3-12, 2010.

GUO, Y.; LI, X.; KUANG, C. Antioxidant pathways and chemical mechanism of curcumin. **Advanced Materials Research**, v. 236-238, n. -, p. 2311-2314, 2011.

HAIDER, S.;NAQVI, F.;TABASSUM, S.;SALEEM, S.;BATOOL, Z.;SADIR, S.;RASHEED, S.;SALEEM, D.;NAWAZ, A.;AHMAD, S. Preventive Effects of Curcumin Against Drug- and Starvation-Induced Gastric Erosions in Rats. **Scientia Pharmaceutica**, v. 81, n. 2, p. 549-558, 2013.

HAN, Y. K.;LEE, S. H.;JEONG, H. J.;SUNKIM, M.;YOON, M. H.;KIM, W. M. Analgesic Effects of Intrathecal Curcumin in the Rat Formalin Test. **Korean Journal of Pain**, v. 25, n. 1, p. 1-6, 2012.

HARDY, C. L.;LEMASURIER, J. S.;MOHAMUD, R.;YAO, J.;XIANG, S. D.;ROLLAND, J. M.;O'HEHIR, R. E.;PLEBANSKI, M. Differential uptake of nanoparticles and microparticles by pulmonary APC subsets induces discrete immunological imprints. **The Journal of Immunology**, v. 191, n. 10, p. 5278-5290, 2013.

HART, B. L. The evolution of herbal medicine: behavioural perspectives. **Animal Behaviour**, v. 70, n. 5, p. 975-989, 2005.

HASIMA, N.; AGGARWAL, B. B. Cancer-linked targets modulated by curcumin. **International Journal of Biochemistry and Molecular Biology**, v. 3, n. 4, p. 328-351, 2012.

HAZZAH, H. A.;FARID, R. M.;NASRA, M. M. A.;EL-MASSIK, M. A.;ABDALLAH, O. Y. Lyophilized sponges loaded with curcumin solid lipid nanoparticles for buccal delivery: Development and characterization. **International Journal of Pharmaceutics**, v. 492, n. 1–2, p. 248-257, 2015.

HAZZAH, H. A.;FARID, R. M.;NASRA, M. M. A.;HAZZAH, W. A.;EL-MASSIK, M. A.;ABDALLAH, O. Y. Gelucire-Based Nanoparticles for Curcumin Targeting to Oral Mucosa: Preparation, Characterization, and Antimicrobial Activity Assessment. **Journal of Pharmaceutical Sciences**, v. 104, n. 11, p. 3913-3924, 2015.

- HEINRICH, M. **Ethnopharmacology and Drug Discovery**. Waltham, MA, US: Elsevier, 2013.
- HOLPUCH, A. S.;HUMMEL, G. J.;TONG, M.;SEGHI, G. A.;PEI, P.;MA, P.;MUMPER, R. J.;MALLERY, S. R. Nanoparticles for local drug delivery to the oral mucosa: proof of principle studies. **Pharmaceutical Research**, v. 27, n. 7, p. 1224-36, 2010.
- HOU, D.; XIE, C.; HUANG, K.; ZHU, C. The production and characteristics of solid lipid nanoparticles (SLNs). **Biomaterials** v. 24, p. 1781–1785, 2003.
- HSU, S. H.;WEN, C. J.;AL-SUWAYEH, S. A.;CHANG, H. W.;YEN, T. C.;FANG, J. Y. Physicochemical characterization and in vivo bioluminescence imaging of nanostructured lipid carriers for targeting the brain: apomorphine as a model drug. **Nanotechnology**, v. 21, n. 40, p. 405101, 2010.
- IJSEBAERT, J. C.;GEERSE, K. B.;MARIJNISSEN, J. C. M.;LAMMERS, J.-W. J.;ZANEN, P. Electro-hydrodynamic atomization of drug solutions for inhalation purposes. **Journal of Applied Physiology**, v. 91, n. 6, p. 2735-2741, 2001.
- IRVING, G. R.;KARMOKAR, A.;BERRY, D. P.;BROWN, K.;STEWART, W. P. Curcumin: the potential for efficacy in gastrointestinal diseases. **Best Practice & Research Clinical Gastroenterology**, v. 25, n. 4-5, p. 519-34, 2011.
- IVANOV, S. M.; LAGUNIN, A. A.; POROIKOV, V. V. In silico assessment of adverse drug reactions and associated mechanisms. **Drug Discovery Today**, v. -, n. -, p. -. in press., 2015.
- JÄGER, R.;LOWERY, R. P.;CALVANESE, A. V.;JOY, J. M.;PURPURA, M.;WILSON, J. M. Comparative absorption of curcumin formulations. **Nutrition Journal**, v. 13, n. 1, p. 1-8, 2014.
- JAGETIA, G.; RAJANIKANT, G. Curcumin Stimulates the Antioxidant Mechanisms in Mouse Skin Exposed to Fractionated γ -Irradiation. **Antioxidants**, v. 4, n. 1, p. 25-41, 2015.
- JAIN, A.;AGARWAL, A.;MAJUMDER, S.;LARIYA, N.;KHAYA, A.;AGRAWAL, H.;MAJUMDAR, S.;AGRAWAL, G. P. Mannosylated solid lipid nanoparticles as vectors for site-specific delivery of an anti-cancer drug. **Journal of Controlled Release** v. 148, n. 3, p. 359-367, 2010.
- JAMISON, D. E. High Shear Mixing Apparatus. U.S. Patent. 4900159, 1990.
- JANTARAT, C. Bioavailability enhancement techniques of herbal medicine: a case example of curcumin. **International Journal of Pharmacy and Pharmaceutical Sciences**, v. 5, n. Suppl 1, p. 493-500, 2013.
- JASPART, S.; PIEL, G.; DELATTRE, L.; EVRARD, B. Solid lipid microparticles: formulation, preparation, characterisation, drug release and applications. **Expert Opinion on Drug Delivery**, v. 2, n. 1, p. 75-87, 2005.

JILL, B. C.; RAJ, B.; NICHOLAS, J. M.; VERA, W. Copaxone® in the Era of Biosimilars and Nanosimilars. In: BAWA, R.;AUDETTE, G. F., *et al* (Ed.). **Handbook of Clinical Nanomedicine**: Pan Stanford, v.1, 2016. cap. 28, p.783-826. (Pan Stanford Series on Nanomedicine). ISBN 978-981-4669-20-7.

JOSHI, M. D.; MULLER, R. H. Lipid nanoparticles for parenteral delivery of actives. **European Journal of Pharmaceutics and Biopharmaceutics** v. 71, n. 2, p. 161-72, 2009.

JOURGHANIAN, P.;GHAFFARI, S.;ARDJMAND, M.;HAGHIGHAT, S.;MOHAMMADNEJAD, M. Sustained release Curcumin loaded Solid Lipid Nanoparticles. **Advanced Pharmaceutical Bulletin**, v. 6, n. 1, p. 17-21, 2016.

JURENKA, J. S. Anti-inflammatory Properties of Curcumin, a Major Constituent of *Curcuma longa*: A Review of Preclinical and Clinical Research. **Alternative Medicine Review** v. 14, n. 2, p. 141-153, 2009.

KAEWSAMUT, B.;PINLAOR, S.;BOONMARS, T.;SRISAWANGWONG, T.;YONGVANIT, P. Effect of curcumin on the inducible nitric oxide synthase (iNOS) and antioxidant enzyme expression in hamsters infected with *Opisthorchis viverrini*. **The Southeast Asian Journal of Tropical Medicine and Public Health**, v. 38, n. Suppl 1, p. 66-73, 2007.

KAKKAR, V.; BHUSHAN, S.; KUMAR, G. S.; KAUR, I. P. Enhanced Apoptotic Effect of Curcumin Loaded Solid Lipid Nanoparticles. **Molecular Pharmaceutics**, v. 9, n. 12, p. 3411–3421, 2012.

KAKKAR, V.; KAUR, I. P. Evaluating potential of curcumin loaded solid lipid nanoparticles in aluminium induced behavioural, biochemical and histopathological alterations in mice brain. **Food and Chemical Toxicology**, v. 49, n. 11, p. 2906-2913, 2011.

KAKKAR, V.; MISHRA, A. K.; CHUTTANI, K.; KAUR, I. P. Proof of concept studies to confirm the delivery of curcumin loaded solid lipid nanoparticles (C-SLNs) to brain. **International Journal of Pharmaceutics**, v. 448, n. 2, p. 354-359, 2013.

KAKKAR, V.; MUPPU, S. K.; CHOPRA, K.; KAUR, I. P. Curcumin loaded solid lipid nanoparticles: An efficient formulation approach for cerebral ischemic reperfusion injury in rats. **European Journal of Pharmaceutics and Biopharmaceutics**, v. -, n. -, p. in press, 2013.

KAKKAR, V.; SINGH, S.; SINGLA, D.; KAUR, I. P. Exploring solid lipid nanoparticles to enhance the oral bioavailability of curcumin. **Molecular Nutrition & Food Research**, v. 55, n. 3, p. 495-503, 2011.

KAKKAR, V.;SINGH, S.;SINGLA, D.;SAHWNEY, S.;CHAUHAN, A. S.;SINGH, G.;KAUR, I. P. Pharmacokinetic applicability of a validated liquid chromatography tandem mass spectroscopy method for orally administered curcumin loaded solid lipid nanoparticles to rats. **Journal of chromatography. B, Analytical technologies in the biomedical and life sciences**, v. 878, n. 32, p. 3427-3431, 2010.

KAMBLE, V. A.; JAGDALE, D. M.; KADAM, V. J. Solid lipid nanoparticles as drug delivery system. **International Journal of Pharma and Bio Sciences**, v. 1, n. 3, p. 1-9, 2010.

KANAI, M.; IMAIZUMI, A.; OTSUKA, Y.; SASAKI, H.; HASHIGUCHI, M.; TSUJIKO, K.; MATSUMOTO, S.; ISHIGURO, H.; CHIBA, T. Dose-escalation and pharmacokinetic study of nanoparticle curcumin, a potential anticancer agent with improved bioavailability, in healthy human volunteers. **Cancer Chemotherapy and Pharmacology**, v. 69, n. 1, p. 65-70, 2012.

KAPPLER, P.; LEINER, W.; PETERMANN, M.; WEIDNER, E. Size and morphology of particles generated by spraying polymer-melts with carbon dioxide. Sixth International Symposium on Supercritical Fluids, 2003, Versailles, France. p.1891-1896.

KAUR, I. P.; BHANDARI, R.; BHANDARI, S.; KAKKAR, V. Potential of solid lipid nanoparticles in brain targeting. **Journal of Controlled Release** v. 127, n. 2, p. 97-109, 2008.

KAWABATA, Y.; WADA, K.; NAKATANI, M.; YAMADA, S.; ONOUE, S. Formulation design for poorly water-soluble drugs based on biopharmaceutics classification system: Basic approaches and practical applications. **International Journal of Pharmaceutics**, v. 420, n. 1, p. 1-10, 2011.

KHAN, H.; RAUF, A. Medicinal Plants: Economic Perspective and Recent Developments. **World Applied Sciences Journal**, v. 31, n. 11, p. 1925-1929, 2014.

KHERADMANDNIA, S.; VASHEGHANI-FARAHANI, E.; NOSRATI, M.; ATYABI, F. Preparation and characterization of ketoprofen-loaded solid lipid nanoparticles made from beeswax and carnauba wax. **Nanomedicine**, 2010.

KIM, S.; DIAB, R.; JOUBERT, O.; CANILHO, N.; PASC, A. Core-shell microcapsules of solid lipid nanoparticles and mesoporous silica for enhanced oral delivery of curcumin. **Colloids and Surfaces B: Biointerfaces**, v. 140, p. 161-168, 2016.

KISHORE, N.; RAJA, M. D.; DHANALEKSHMI, U. M.; BHAVANI; SARANYA; REDDY, P. N. Formulation and Evaluation of NSAID - Loaded Tristearin Solid Lipid Nanoparticles. **International Journal of Medicobiological**, v. 1, n. 4, p. 217-233, 2011.

KNEZ; WEIDNER, E. 9.8 Precipitation of solids with dense gases. In: BERTUCCO, A. e VETTER, G. (Ed.). **Industrial Chemistry Library**: Elsevier, v. Volume 9, 2001. p.587-611. ISBN 0926-9614.

KOHANE, D. S. Microparticles and nanoparticles for drug delivery. **Biotechnology Bioengineering**, v. 96, n. 2, p. 203-209, 2007.

KOSTANECKI, K.; MIŁOBĘDZKA, J.; LAMPE, W. Zur Kenntnis des Curcumins. **Berichte der Deutschen Chemischen Gesellschaft**, v. 43, n. 2, p. 2163-2170, 1910.

KOTZ, J. Phenotypic screening, take two. **SciBX - Science Business Exchange**, v. 5, n. 15, p. 1-3, 2012.

KUCHLER, S.;RADOWSKI, M. R.;BLASCHKE, T.;DATHE, M.;PLENDL, J.;HAAG, R.;SCHAFER-KORTING, M.;KRAMER, K. D. Nanoparticles for skin penetration enhancement--a comparison of a dendritic core-multishell-nanotransporter and solid lipid nanoparticles. **European Journal of Pharmaceutics and Biopharmaceutics** v. 71, n. 2, p. 243-250, 2009.

KUMAR, M. N. V. R. Nano and Microparticles as Controlled Drug Delivery Devices. **Journal of Pharmacy & Pharmaceutical Sciences** v. 3, n. 2, p. 234-258, 2000.

KUMARI, A.; DASH, D.; SINGH, R. Lipopolysaccharide (LPS) exposure differently affects allergic asthma exacerbations and its amelioration by intranasal curcumin in mice. **Cytokine**, v. -, n. -, p. -. in press, 2015.

KUNAC, D.; KENNEDY, J.; AUSTIN, N.; REITH, D. Incidence, preventability, and impact of Adverse Drug Events (ADEs) and potential ADEs in hospitalized children in New Zealand: a prospective observational cohort study. **Paediatric Drugs**, v. 11, n. 2, p. 153-160, 2009.

KUNDU, S.; NITHIYANANTHAM, U. In-situ formation of Curcumin Stabilized Shape-selective Ag Nanostructures in aqueous Solution and their pronounced SERS Activity. **RSC Advances**, v. 3, p. 25278-25290, 2013.

KUTAMA, A. S.;DANGORA, I. I.;AISHA, W.;AUYO, M. I.;SHARIF, U.;UMMA, M.;HASSAN, K. Y. An overview of plant resources and their economic uses in Nigeria. **Global Advanced Research Journal of Agricultural Science**, v. 4, n. 2, p. 42-67, 2015.

LAHLOU, M. The Success of Natural Products in Drug Discovery. **Pharmacology & Pharmacy**, v. 4, p. 17-31, 2013.

LEONTI, M.; CASU, L. Traditional medicines and globalization: current and future perspectives in ethnopharmacology. **Frontiers in Pharmacology**, v. 4, n. 92, p. 1-13, 2013.

LEWANDOWSKA, U.;GORLACH, S.;OWCZAREK, K.;HRABEC, E.;SZEWCZYK, K. Synergistic Interactions Between Anticancer Chemotherapeutics and Phenolic Compounds and Anticancer Synergy Between Polyphenols. **Postepy Higieny i Medycyny Doswiadczalnej**, v. 68, p. 528-540, 2014.

LI, J.;RODRIGUES, M.;PAIVA, A.;MATOS, H. A.;AZEVEDO, E. G. D. Binary solid-liquid-gas equilibrium of the tripalmitin/CO₂ and ubiquinone/CO₂ systems. **Fluid Phase Equilibria**, v. 241, n. 1-2, p. 196-204, 2006.

LI, J.;RODRIGUES, M.;PAIVA, A.;MATOS, H. A.;GOMES DE AZEVEDO, E. Modeling of the PGSS process by crystallization and atomization. **AIChE Journal**, v. 51, n. 8, p. 2343-2357, 2005.

LI, R.;QIAO, X.;LI, Q.;HE, R.;YE, M.;XIANG, C.;LIN, X.;GUO, D. Metabolic and pharmacokinetic studies of curcumin, demethoxycurcumin and bisdemethoxycurcumin in mice tumor after intragastric administration of nanoparticle formulations by liquid chromatography coupled with tandem mass spectrometry. **Journal of chromatography. B - Analytical technologies in the biomedical and life sciences**, v. 879, n. 26, p. 2751-2758, 2011.

LI, S.;YUAN, W.;DENG, G.;WANG, P.;YANG, P.;AGGARWAL, B. B. Chemical Composition and Product Quality Control of Turmeric (*Curcuma longa* L.) **Pharmaceutical Crops**, v. 2, n. -, p. 28-54, 2011.

LIEDTKE, S.; WISSING, S.; MULLER, R. H.; MADER, K. Influence of high pressure homogenisation equipment on nanodispersions characteristics. **International Journal of Pharmaceutics**, v. 196, n. 2, p. 183-185, 2000.

LIN, C.-L.; LIN, J.-K. Curcumin: a Potential Cancer Chemopreventive Agent through Suppressing NF- κ B Signaling. **Journal of Cancer Molecules** v. 4, n. 1, p. 11-16, 2008.

LIU, J.;GONG, T.;FU, H.;WANG, C.;WANG, X.;CHEN, Q.;ZHANG, Q.;HE, Q.;ZHANG, Z. Solid lipid nanoparticles for pulmonary delivery of insulin. **International Journal of Pharmaceutics**, v. 356, n. 1-2, p. 333-44, 2008.

LIU, R. **Water-Insoluble Drug Formulation**. 2nd. CRC Press, 2008. 688 ISBN 9781420009552.

LU, B.;XIONG, S. B.;YANG, H.;YIN, X. D.;CHAO, R. B. Solid lipid nanoparticles of mitoxantrone for local injection against breast cancer and its lymph node metastases. **European Journal of Pharmaceutical Sciences** v. 28, n. 1-2, p. 86-95, 2006.

LU, X.;HOWARD, M. D.;MAZIK, M.;ELDRIDGE, J.;RINEHART, J. J.;JAY, M.;LEGGAS, M. Nanoparticles containing anti-inflammatory agents as chemotherapy adjuvants: optimization and in vitro characterization. **The AAPS Journal** v. 10, n. 1, p. 133-140, 2008.

LUO, C. F.;YUAN, M.;CHEN, M. S.;LIU, S. M.;ZHU, L.;HUANG, B. Y.;LIU, X. W.;XIONG, W. Pharmacokinetics, tissue distribution and relative bioavailability of puerarin solid lipid nanoparticles following oral administration. **International Journal of Pharmaceutics** v. 410, n. 1-2, p. 138-144, 2011.

LV, Q.;YU, A.;XI, Y.;LI, H.;SONG, Z.;CUI, J.;CAO, F.;ZHAI, G. Development and evaluation of penciclovir-loaded solid lipid nanoparticles for topical delivery. **International Journal of Pharmaceutics** v. 372, n. 1-2, p. 191-198, 2009.

MA, P.;DONG, X.;SWADLEY, C. L.;GUPTE, A.;LEGGAS, M.;LEDEBUR, H. C.;MUMPER, R. J. Development of idarubicin and doxorubicin solid lipid nanoparticles to overcome Pgp-mediated multiple drug resistance in leukemia. **Journal of Biomedical Nanotechnology**, v. 5, n. 2, p. 151-161, 2009.

MACDONALD, R. L. Nanoparticles and Microparticles. **Neurosurgery**, v. 62, n. -, p. 152-159, 2015.

MÄDER, K. Solid Lipid Nanoparticles as Drug Carriers. In: TORCHILIN, V. P. (Ed.). **Nanoparticulates as Drug Carriers**. London: Imperial College Press, 2006. cap. 9, p.187-212.

MADERUELO, C.; ZARZUELO, A.; LANAO, J. M. Critical factors in the release of drugs from sustained release hydrophilic matrices. **Journal of Controlled Release**, v. 154, n. 1, p. 2-19, 2011.

MANDZUKA, Z.; KNEZ, Z. Influence of temperature and pressure during PGSS(TM) micronization and storage time on degree of crystallinity and crystal forms of monostearate and tristearate. **The Journal of Supercritical Fluids**, v. 45, n. 1, p. 102-111, 2008.

MANTRIPRAGADA, S. DepoFoam Technology. In: RATHBONE, M. J.;HADGRAFT, J., *et al* (Ed.). **Modified-Release Drug Delivery Technology**: Marcel Dekker, Inc., 2003. p.705-712.

MARQUEZ, S.; HERDEIRO, M. T.; RIBEIRO-VAZ, I. An Educational Intervention to Improve Nurses Reporting of Adverse Drug Reactions. **Clinical Therapeutics**, v. 37, n. 8S, p. e57, 2015.

MARTÍN, A.; COCERO, M. J. Micronization processes with supercritical fluids: Fundamentals and mechanisms. **Advanced Drug Delivery Reviews** v. 60, p. 339–350, 2008.

MARTINS, S.; SARMENTO, B.; FERREIRA, D. C.; SOUTO, E. B. Lipid-based colloidal carriers for peptide and protein delivery--liposomes versus lipid nanoparticles. **International Journal of Nanomedicine** v. 2, n. 4, p. 595-607, 2007.

MEHNERT, W.; MADER, K. Solid lipid nanoparticles: production, characterization and applications. **Advanced Drug Delivery Reviews**, v. 47, n. 2-3, p. 165-196, 2001.

MEHTA, U.;DURRHEIM, D. N.;BLOCKMAN, M.;KREDO, T.;GOUNDEN, R.;BARNES, K. I. Adverse drug reactions in adult medical inpatients in a South African hospital serving a community with a high HIV/AIDS prevalence: prospective observational study. **British Journal of Clinical Pharmacology**, v. 65, n. 3, p. 396-406, 2008.

MISHRA, H.;MISHRA, D.;MISHRA, P. K.;NAHAR, M.;DUBEY, V.;JAIN, N. K. Evaluation of Solid Lipid Nanoparticles as Carriers for Delivery of Hepatitis B Surface Antigen for Vaccination Using Subcutaneous Route. **Journal of Pharmaceutical Sciences**, v. 13, n. 4, p. 495 - 509, 2010.

MOFFAT, J. G.; RUDOLPH, J.; BAILEY, D. Phenotypic screening in cancer drug discovery - past, present and future. **Nature Reviews Drug Discovery**, v. 13, p. 588-602, 2014.

MOHAN, P. R. K.; SREELAKSHMI, G.; MURALEEDHARAN, C. V.; JOSEPH, R. Water soluble complexes of curcumin with cyclodextrins: Characterization by FT-Raman spectroscopy. **Vibrational Spectroscopy**, v. 62, p. 77-84, 2012.

MOHANRAJ, V.; CHEN, Y. Nanoparticles – A Review. **Tropical Journal of Pharmaceutical Research**, v. 5, n. 1, p. 561-573, 2006.

MOORTHY, C.; KATHIRESAN, K. Fabrication of highly stable sonication assisted curcumin nanocrystals by nanoprecipitation method. **Drug Invention Today**, v. 5, n. 1, p. 66-69, 2013.

MORIBE, K.; TOZUKA, Y.; YAMAMOTO, K. Supercritical carbon dioxide processing of active pharmaceutical ingredients for polymorphic control and for complex formation. **Advanced Drug Delivery Reviews** v. 60, p. 328-338, 2008.

MULIK, R. S.;MONKKONEN, J.;JUVONEN, R. O.;MAHADIK, K. R.;PARADKAR, A. R. Transferrin mediated solid lipid nanoparticles containing curcumin: enhanced in vitro anticancer activity by induction of apoptosis. **International Journal of Pharmaceutics**, v. 398, n. 1-2, p. 190-203, 2010.

MÜLLER, R. **Colloidal carriers for controlled drug delivery and targeting-modification, characterization and in vivo distribution**. . 1st ed. Boca Raton: Wissenschaftliche Verlagsgesellschaft Stuttgart. CRC Press, 1991. 379

MÜLLER, R. H.; MÄDER, K.; GOHLA, S. Solid lipid nanoparticles (SLN) for controlled drug delivery - a review of the state of the art. **European Journal of Pharmaceutics and Biopharmaceutics** v. 50, p. 161-177, 2000.

MUN, S.-H.;KIM, S.-B.;KONG, R.;CHOI, J.-G.;KIM, Y.-C.;SHIN, D.-W.;KANG, O.-H.;KWON, D.-Y. Curcumin Reverse Methicillin Resistance in *Staphylococcus aureus*. **Molecules**, v. 19, n. 11, p. 18283-18294, 2014.

MUN, S. H.;JOUNG, D. K.;KIM, Y. S.;KANG, O. H.;KIM, S. B.;SEO, Y. S.;KIM, Y. C.;LEE, D. S.;SHIN, D. W.;KWEON, K. T.;KWON, D. Y. Synergistic antibacterial effect of curcumin against methicillin-resistant *Staphylococcus aureus*. **Phytomedicine**, v. 20, n. 8-9, p. 714-718, 2013.

NAIR, R.;KUMAR, A. C. K.;PRIYA, V. K.;YADAV, C. M.;RAJU, P. Y. Formulation and evaluation of chitosan solid lipid nanoparticles of carbamazepine. **Lipids in Health and Disease**, v. 11, n. 72, p. 1-8, 2012.

NALAWADE, S. P.; PICCHIONI, F.; JANSSEN, L. P. B. M. Supercritical carbon dioxide as a green solvent for processing polymer melts: Processing aspects and applications. **Progress in Polymer Science**, v. 31, p. 19-43, 2006.

NALAWADE, S. P.; PICCHIONI, F.; JANSSEN, L. P. B. M. Batch production of micron size particles from poly(ethylene glycol) using supercritical CO₂ as a processing solvent. **Chemical Engineering Science**, v. 62, n. 6, p. 1712-1720, 2007.

NASSIMI, M.;SCHLEH, C.;LAUENSTEIN, H. D.;HUSSEIN, R.;HOYMAN, H. G.;KOCH, W.;POHLMANN, G.;KRUG, N.;SEWALD, K.;RITTINGHAUSEN, S.;BRAUN, A.;MULLER-GOYMAN, C. A toxicological evaluation of inhaled solid lipid nanoparticles used as a potential drug delivery system for the lung. **European Journal of Pharmaceutics and Biopharmaceutics** v. 75, n. 2, p. 107-116, 2010.

NAYAK, A. P.;TIYABOONCHAI, W.;PATANKAR, S.;MADHUSUDHAN, B.;SOUTO, E. B. Curcuminoids-loaded lipid nanoparticles: novel approach towards malaria treatment. **Colloids Surf B Biointerfaces**, v. 81, n. 1, p. 263-73, 2010.

NOACK, A.; HAUSE, G.; MÄDER, K. Physicochemical characterization of curcuminoid-loaded solid lipid nanoparticles. **International Journal of Pharmaceutics**, v. 423, n. 2, p. 440-451, 2012.

OBEIDAT, W. M. Recent Patents Review in Microencapsulation of Pharmaceuticals Using the Emulsion Solvent Removal Methods. **Recent Patents on Drug Delivery & Formulation**, v. 3, p. 178-192, 2009.

PANDEY, M. K.;KUMAR, S.;THIMMULAPPA, R. K.;PARMAR, V. S.;BISWAL, S.;WATTERSON, A. C. Design, synthesis and evaluation of novel PEGylated curcumin analogs as potent Nrf2 activators in human bronchial epithelial cells. **European Journal of Pharmaceutical Sciences**, v. 43, n. 1–2, p. 16-24, 2011.

PAPP, N.;BIRKÁS-FRENDL, K.;BENCSIK, T.;STRANCZINGER, S.;CZÉGÉNYI, D. Survey of traditional beliefs in the Hungarian Csángó and Székely ethnomedicine in Transylvania, Romania. **Brazilian Journal of Pharmacognosy**, v. 24, n. 2, p. 141-152, 2014.

PARHI, R.; SURESH, P. Production of Solid Lipid Nanoparticles-Drug Loading and Release Mechanism. **Journal of Chemical and Pharmaceutical Research**, v. 2, n. 1, p. 211-227, 2010.

PASQUALI, I.; COMI, L.; PUCCIARELLI, F.; BETTINI, R. Swelling, melting point reduction and solubility of PEG 1500 in supercritical CO₂. **International Journal of Pharmaceutics** v. 356, n. -, p. 76-81, 2008.

PASQUALI, I.; BETTINI, R.; GIORDANO, F. Supercritical fluid technologies: An innovative approach for manipulating the solid-state of pharmaceuticals. **Advanced Drug Delivery Reviews** v. 60, p. 399-410, 2008.

PATEL, B. B.; PATEL, J. K.; CHAKRABORTY, S.; SHUKLA, D. Revealing facts behind spray dried solid dispersion technology used for solubility enhancement. **Saudi Pharmaceutical Journal**, v. 23, n. 4, p. 352-365, 2015.

PEDRÓS, C.;QUINTANA, B.;REBOLLEDO, M.;PORTA, N.;VALLANO, A.;ARNAU, J. Prevalence, risk factors and main features of adverse drug reactions leading to hospital admission. **European Journal of Clinical Pharmacology**, v. 70, n. 3, p. 361-367, 2014.

PÉREZ MENÉNDEZ-CONDE, C.; BERMEJO VICEDO, T.; DELGADO SILVEIRA, E.; CARRETERO ACCAME, E. Adverse Drug Reactions Which Provoke Hospital Admission. **Farmacia Hospitalaria**, v. 35, n. 5, p. 236-243, 2011.

PIETKIEWICZ, J.; SZNITOWSKA, M.; PLACZEK, M. The expulsion of lipophilic drugs from the cores of solid lipid microspheres in diluted suspensions and in concentrates. **International Journal of Pharmaceutics**, v. 310, n. 1-2, p. 64-71, 2006.

PLIANBANGCHANG, P.; TUNGPRADIT, W.; TIYABOONCHAI, W. Efficacy and safety of curcuminoids loaded solid lipid nanoparticles facial cream as an anti-aging agent. **Naresuan University Journal**, v. 15, n. 2, p. 73-81, 2007.

PLUTA, R.;BOGUCKA-KOCKA, A.;UŁAMEK-KOZIOŁ, M.;FURMAGA-JABŁOŃSKA, W.;JANUSZEWSKI, S.;BRZOZOWSKA, J.;JABŁOŃSKI, M.;KOCKI, J. Neurogenesis and neuroprotection in postischemic brain neurodegeneration with Alzheimer phenotype: is there a role for curcumin? **Folia Neuropathologica**, v. 53, n. 2, p. 89-99, 2015.

- POLLAK, S.; KARETH, S.; KILZER, A.; PETERMANN, M. Thermal analysis of the droplet solidification in the PGSS-process. **The Journal of Supercritical Fluids** v. 56, p. 299-303, 2011.
- PORTER, C. J.; TREVASKIS, N. L.; CHARMAN, W. N. Lipids and lipid-based formulations: optimizing the oral delivery of lipophilic drugs. **Nature Reviews Drug Discovery**, v. 6, n. 3, p. 231-48, 2007.
- POTHAKAMURY, U. R.; BARBOSA-CANOVAS, G. V. Fundamental aspects of controlled release in foods. **Trends in Food Science and Technology**, v. 6, p. 397-406, 1995.
- PUGLIA, C.; BLASI, P.; RIZZA, L.; SCHOUBBEN, A.; BONINA, F.; ROSSI, C.; RICCI, M. Lipid nanoparticles for prolonged topical delivery: an in vitro and in vivo investigation. **International Journal of Pharmaceutics** v. 357, n. 1-2, p. 295-304, 2008.
- RAHMAN, Z.; ZIDAN, A. S.; KHAN, M. A. Non-destructive methods of characterization of risperidone solid lipid nanoparticles. **European Journal of Pharmaceutics and Biopharmaceutics** v. 76, n. 1, p. 127-37, 2010.
- REIS, P. C.; NEUFELD, R. J.; RIBEIRO, A. J.; VEIGA, F. Nanoencapsulation I. Methods for preparation of drug-loaded polymeric nanoparticles. **Nanomedicine**, v. 2, n. 1, p. 8-21, 2006.
- REITZ, R. D.; BRACCO, F. V. Mechanism of atomization of a liquid jet. **Physics of Fluids**, v. 25, n. 10, p. 1730-1742, 1982.
- REVATHY, S.; ELUMALAI, S.; BENNY, M.; ANTONY, B. Isolation, Purification and Identification of Curcuminoids from Turmeric (*Curcuma longa* L.) by Column Chromatography. **Journal of Experimental Sciences**, v. 2, n. 7, p. 21-25, 2011.
- REVERCHON, E.; ADAMI, R.; CARDEA, S.; PORTA, G. D. Supercritical fluids processing of polymers for pharmaceutical and medical applications. **The Journal of Supercritical Fluids**, v. 47, p. 484-492, 2009.
- RIBEIRO DOS SANTOS, I.; RICHARD, J.; PECH, B.; THIES, C.; BENOIT, J. P. Microencapsulation of protein particles within lipids using a novel supercritical fluid process. **International Journal of Pharmaceutics**, v. 242, n. 1-2, p. 69-78, 2002.
- RIBEIRO DOS SANTOS, I.; RICHARD, J.; THIES, C.; PECH, B.; BENOIT, J. P. A supercritical fluid-based coating technology. 3: preparation and characterization of bovine serum albumin particles coated with lipids. **Journal of Microencapsulation**, v. 20, n. 1, p. 110-28, 2003.
- RIBEIRO DOS SANTOS, I.; THIES, C.; RICHARD, J.; LE MEURLAY, D.; GAJAN, V.; VANDELDE, V.; BENOIT, J. P. A supercritical fluid-based coating technology. 2: solubility considerations. **Journal of Microencapsulation**, v. 20, n. 1, p. 97-109, 2003.
- RIGHESCHI, C.; BERGONZI, M. C.; ISACCHI, B.; BAZZICALUPI, C.; GRATTERI, P.; BILIA, A. R. Enhanced curcumin permeability by SLN formulation: The PAMPA approach. **LWT - Food Science and Technology**, v. 66, p. 475-483, 2016.

RODRIGUES, M.; PEIRIÇO, N.; MATOS, H.; GOMES DE AZEVEDO, E.; LOBATO, M. R.; ALMEIDA, A. J. Microcomposites theophylline/hydrogenated palm oil from a PGSS process for controlled drug delivery systems. **The Journal of Supercritical Fluids**, v. 29, n. 1-2, p. 175-184, 2004.

RODRIGUEZ-ROJO, S.; REGO, D.; NUNES, A. V. M.; NOGUEIRA, I. D.; COCERO, M. J.; DUARTE, C. M. M. Supercritical Fluids (SCF) strategies to produce double walled particles for drug delivery applications. 12th European Meeting on Supercritical Fluids, 2010, Graz, Austria.

SALMASO, S.; BERSANI, S.; ELVASSORE, N.; BERTUCCO, A.; CALICETI, P. Biopharmaceutical characterisation of insulin and recombinant human growth hormone loaded lipid submicron particles produced by supercritical gas micro-atomisation. **International Journal of Pharmaceutics**, v. 379, n. 1, p. 51-58, 2009.

SALMASO, S.; ELVASSORE, N.; BERTUCCO, A.; CALICETI, P. Production of solid lipid submicron particles for protein delivery using a novel supercritical gas-assisted melting atomization process. **Journal of Pharmaceutical Sciences**, v. 98, n. 2, p. 640-650, 2009.

SAMPAIO DE SOUSA, A. R.; CALDERONE, M.; RODIER, E.; FAGES, J.; DUARTE, C. M. M. Solubility of carbon dioxide in three lipid-based biocarriers. **The Journal of Supercritical Fluids**, v. 39, n. 1, p. 13-19, 2006.

SAMPAIO DE SOUSA, A. R.; SIMPLÍCIO, A. L.; DE SOUSA, H. C.; DUARTE, C. M. M. Preparation of glyceryl monostearate-based particles by PGSS®--Application to caffeine. **The Journal of Supercritical Fluids**, v. 43, n. 1, p. 120-125, 2007.

SAMYUKTHA, S. M.; MOUNICA, N.; SIREESHA, R.; PAVANI, K.; M, K. B. Formulation & evaluation of aripiprazole solid lipid nanoparticles for brain targeting. **Indian Journal of Research in Pharmacy and Biotechnology**, v. 2, n. 5, p. 1396-1403, 2014.

SANKAR, P.; TELANG, A. G.; SURESH, S.; KESAVAN, M.; KANNAN, K.; KALAIIVANAN, R.; SARKAR, S. N. Immunomodulatory effects of nanocurcumin in arsenic-exposed rats. **International Immunopharmacology**, v. 17, n. 1, p. 65-70, 2013.

SAUPE, A.; RADES, T. Solid Lipid Nanoparticles. In: MOZAFARI, M. R. (Ed.). **Nanocarrier Technologies: Frontiers of Nanotherapy**. New Zeland: Springer, 2006. cap. 3, p.41-50.

SCALIA, S.; YOUNG, P. M.; TRAINI, D. Solid lipid microparticles as an approach to drug delivery. **Expert Opinion on Drug Delivery**, v. 12, n. 4, p. 583-599, 2015.

SCHMIDTS, T.; SCHLUPP, P.; GROSS, A.; DOBLER, D.; RUNKEL, F. Required HLB Determination of Some Pharmaceutical Oils in Submicron Emulsions. **Journal of Dispersion Science and Technology**, v. 33, n. 6, p. 1-5, 2012.

SEKHON, B. S. Supercritical Fluid Technology: An Overview of Pharmaceutical Applications. **International Journal of PharmTech Research**, v. 2, n. 1, p. 810-826, 2010.

SEYEDZADEH, M. H.;SAFARI, Z.;ZARE, A.;GHOLIZADEH NAVASHENAQ, J.;RAZAVI, S. A.;KARDAR, G. A.;KHORRAMIZADEH, M. R. Study of curcumin immunomodulatory effects on reactive astrocyte cell function. **International Immunopharmacology**, v. 22, n. 1, p. 230-235, 2014.

SHEKUNOV, B. Y.; CHATTOPADHYAY, P.; SEITZINGER, J.; HUFF, R. Nanoparticles of Poorly Water-Soluble Drugs Prepared by Supercritical Fluid Extraction of Emulsions. **Pharmaceutical Research**, v. 23, n. 1, p. 196-204, 2006.

SHIEH, J.-M.;CHEN, Y.-C.;LIN, Y.-C.;LIN, J.-N.;CHEN, W.-C.;CHEN, Y.-Y.;HO, C.-T.;WAY, T.-D. Demethoxycurcumin Inhibits Energy Metabolic and Oncogenic Signaling Pathways through AMPK Activation in Triple-Negative Breast Cancer Cells. **Journal of Agricultural and Food Chemistry**, v. 61, n. 26, p. 6366-6375, 2013.

SHOBA, G.;JOY, D.;JOSEPH, T.;MAJEED, M.;RAJENDRAN, R.;SRINIVAS, P. S. S. R. Influence of Piperine on the Pharmacokinetics of Curcumin in Animals and Human Volunteers. **Planta Medica**, v. 64, n. 4, p. 353-356, 1998.

SIEKMANN, B.; WESTESEN, K. Sub-micron sized parenteral carrier systems based on solid lipids. **Pharmaceutical and Pharmacological Letters**, v. 1, p. 123-126, 1992.

SIMANJUNTAK, P.;PRANA, T. K.;WULANDARI, D.;DHARMAWAN, A.;SUMITO, E.;HENDRIYANTO, M. R. Chemical studies on a curcumin analogue produced by endophytic fungal transformation. **Asian Journal of Applied Sciences**, v. 3, n. 1, p. 60-66, 2010.

SINGH, A.; VAN DEN MOOTER, G. Spray drying formulation of amorphous solid dispersions. **Advanced Drug Delivery Reviews**, v. 100, p. 27-50, 2016.

SINGH, U.;VERMA, S.;GHOSH, H. N.;RATH, M. C.;PRIYADARSINI, K. I.;SHARMA, A.;PUSHPA, K. K.;SARKAR, S. K.;MUKHERJEE, T. Photo-degradation of curcumin in the presence of TiO₂ nanoparticles: Fundamentals and application. **Journal of Molecular Catalysis A: Chemical**, v. 318, n. 1-2, p. 106-111, 2010.

SINHA, V. R.; SRIVASTAVA, S.; GOEL, H.; JINDAL, V. Solid Lipid Nanoparticles (SLN'S) – Trends and Implications in Drug Targeting. **International Journal of Advances in Pharmaceutical Sciences**, v. 1, n. 3, p. 212-238, 2010.

SONAROME. Spray Drying Technology. Bangalore, India, 2014. Disponível em: <<http://sonarome.com/2014/12/02/spray-drying-technology/>>. Acesso em: June 10th, 2016.

SOUTO, E. B.; MÜLLER, R. H. Lipid Nanoparticles: Effect on Bioavailability and Pharmacokinetic Changes Drug Delivery. In: HOFMANN, F. B. (Ed.). **Handbook of Experimental Pharmacology**. Berlin: Springer-Verlag, v.197, 2010. p.115-141. (Handbook of Experimental Pharmacology). ISBN 978-3-642-00477-3.

SREENIVASAN, D.; JAYAKUMAR, C.; GANDHI, N. N. Effect of Hydrotropes on Solubility and Mass Transfer Co-Efficient of Curcuminoids. **Journal of Pharmacy Research** v. 3, n. 9, p. 2170-2171, 2010.

SRIVASTAVA, P.;YADAV, R. S.;CHANDRAVANSI, L. P.;SHUKLA, R. K.;DHURIYA, Y. K.;CHAUHAN, L. K. S.;DWIVEDI, H. N.;PANT, A. B.;KHANNA, V. K. Unraveling the mechanism of neuroprotection of curcumin in arsenic induced cholinergic dysfunctions in rats. **Toxicology and Applied Pharmacology**, v. 279, n. 3, p. 428-440, 2014.

STAUSBERG, J. International prevalence of adverse drug events in hospitals: an analysis of routine data from England, Germany, and the USA. **BMC Health Services Research** v. 14, n. 125, p. 1-9, 2014.

STRUMENDO, M.; BERTUCCO, A.; ELVASSORE, N. Modeling of particle formation processes using gas saturated solution atomization. **The Journal of Supercritical Fluids**, v. 41, n. 1, p. 115-125, 2007.

STUART, B. **Infrared Spectroscopy: Fundamentals and Applications**. Chichester, UK: John Wiley & Sons, Ltd, 2004. ISBN 0-470-85427-8.

SUBEDI, R. K.; KANG, K. W.; CHOI, H. K. Preparation and characterization of solid lipid nanoparticles loaded with doxorubicin. **European Journal of Pharmaceutical Sciences**, v. 37, n. 3-4, p. 508-513, 2009.

SÜLEYMANOĞLU, E. The use of infrared spectroscopy for following drug membrane interactions: probing paclitaxel (taxol)-cell phospholipid surface recognition. **Electronic Journal of Biomedicine**, v. 3, p. 19-35, 2009.

SUN, J.;BI, C.;CHAN, H. M.;SUN, S.;ZHANG, Q.;ZHENG, Y. Curcumin-loaded solid lipid nanoparticles have prolonged in-vitro antitumour activity, cellular uptake and improved in-vivo bioavailability. **Colloids and Surfaces B: Biointerfaces**, v. -, n. -, p. in press, 2013.

TADROS, T. F. **Nanodispersions**. Walter de Gruyter GmbH & Co KG, 2016. 312 ISBN 9783110388794.

TAJIK, H.; TAMADDONFARD, E.; HAMZEH-GOOSHCHI, N. Interaction between curcumin and opioid system in the formalin test of rats. **Pakistan Journal of Biological Sciences**, v. 10, n. 15, p. 2583-2586, 2007.

TAKECHI, C.;KAWAGUCHI, T.;KANEKO, F.;YAMAMURO, O.;AKITA, H.;ONO, M.;SUZUKI, M. Incoherent quasielastic neutron scattering study on the polymorphism of tristearin: dynamical properties of hydrocarbon chains. **Journal of Physical Chemistry B**, v. 111, n. 33, p. 9706-10, 2007.

TANDON, V. R.;KHAJURIA, V.;MAHAJAN, A.;GILLANI, Z.;MAHAJAN, V.;CHANDAIL, V. Fatal adverse drug reactions: Experience of adverse drug reactions in a tertiary care teaching hospital of North India - A case series. **Indian Journal of Critical Care Medicine**, v. 18, n. 5, p. 315-319, 2014.

TELLES, M. V. L.;NOBRE, M. E. P.;ALENCAR, L. P.;SIQUEIRA, K. P. D.;BORGES, A. M. F. S.;TAVARES, M. W. L.;ALVES, I. B.;DUARTE, L. S.;LACERDA, N. K. R. D.;ALCÂNTARA, G. F. T. D.;SCERNI, D. A.;NEVES, K. R. T.;VIANA, G. S. D. B. Prenatal Curcumin

Administration Reverses Behavioral and Neurochemical Effects and Decreases iNOS and COX-2 Expressions in Ischemic Rat Pups. **International Journal of Brain Science**, v. 2014 n. ID 907581, p. 1-10, 2014.

THIES, C.;RIBEIRO DOS SANTOS, I.;RICHARD, J.;VANDEVELDE, V.;ROLLAND, H.;BENOIT, J. P. A supercritical fluid-based coating technology 1: process considerations. **Journal of Microencapsulation**, v. 20, n. 1, p. 87-96, 2003.

TIYABOONCHAI, W.; TUNGPRADIT, W.; PLIANBANGCHANG, P. Formulation and characterization of curcuminoids loaded solid lipid nanoparticles. **International Journal of Pharmaceutics**, v. 337, n. 1-2, p. 299-306, 2007.

TROTTA, M.;CAVALLI, R.;TROTTA, C.;BUSSANO, R.;COSTA, L. Electrospray technique for solid lipid-based particle production. **Drug Development and Industrial Pharmacy**, v. 36, n. 4, p. 431-438, 2010.

ULRICH-MERZENICH, G.;PANEK, D.;ZEITLER, H.;VETTER, E.;WAGNER, H. Drug Development from Natural Products: Exploiting Synergistic Effects. **Indian Journal of Experimental Biology**, v. 48, p. 208-219, 2010.

URBAN-MORLAN, Z.;GANEM-RONDERO, A.;MELGOZA-CONTRERAS, L. M.;ESCOBAR-CHAVEZ, J. J.;NAVA-ARZALUZ, M. G.;QUINTANAR-GUERRERO, D. Preparation and characterization of solid lipid nanoparticles containing cyclosporine by the emulsification-diffusion method. **International Journal of Nanomedicine**, v. 5, p. 611-620, 2010.

UT. High Pressure Homogenization (HPH). Knoxville, 2011. Disponível em: <<http://web.utk.edu/~fede/high%20pressure%20homogenization.html>>. Acesso em: August 19th , 2011.

VACLAVIK, V.; CHRISTIAN, E. W. **Essentials of Food Science**. Third. Springer Science & Business Media, 2007. 590 ISBN 9780387699400.

VAREED, S. K.;KAKARALA, M.;RUFFIN, M. T.;CROWELL, J. A.;NORMOLLE, D. P.;DJURIC, Z.;BRENNER, D. E. Pharmacokinetics of Curcumin Conjugate Metabolites in Healthy Human Subjects. **Cancer Epidemiology, Biomarkers & Prevention**, v. 17, n. 6, p. 1411-1417, 2008.

VEZZÙ, K.;BORIN, D.;BERTUCCO, A.;BERSANI, S.;SALMASO, S.;CALICETI, P. Production of lipid microparticles containing bioactive molecules functionalized with PEG. **The Journal of Supercritical Fluids**, v. 54, n. 3, p. 328-334, 2010.

VEZZÙ, K.; CAMPOLMI, C.; BERTUCCO, A. Production of Lipid Microparticles Magnetically Active by a Supercritical Fluid-Based Process. **International Journal of Chemical Engineering**, v. 2009, n. ID 781247, p. 1-9, 2009.

VOGEL, H.; PELLETIER, J. Curcumin - biological and medicinal properties. **Journal of Pharmaceutical Sciences**, v. 2, n. -, p. 50, 1815.

- WANG, F.;ZHAO, S.;LI, F.;ZHANG, B.;QU, Y.;SUN, T.;LUO, T.;LI, D. Investigation of Antioxidant Interactions between *Radix Astragali* and *Cimicifuga foetida* and Identification of Synergistic Antioxidant Compounds. **PLoS One**, v. 9, n. 1, p. 1-12, 2014.
- WANG, J.;LU, Z.;GAO, Y.;WIEN TJES, M. G.;AU, J. L. S. Improving delivery and efficacy of nanomedicines in solid tumors: Role of tumor priming. **Nanomedicine (London, England)**, v. 6, n. 9, p. 1-24, 2011.
- WANG, W.;ZHU, R.;XIE, Q.;LI, A.;XIAO, Y.;LI, K.;LIU, H.;CUI, D.;CHEN, Y.;WANG, S. Enhanced bioavailability and efficiency of curcumin for the treatment of asthma by its formulation in solid lipid nanoparticles. **International Journal of Nanomedicine**, v. 7, p. 3667-3677, 2012.
- WANG, X.;CHEN, H.;GUO, Y.;SU, Y.;WANG, H.;LI, J. Preparation of ibuprofen/lipid composite microparticles by supercritical fluid technique. **Frontiers of Chemical Engineering in China** v. 2, n. 4, p. 361–367, 2008.
- WEIDNER, E.; KNEZ, Ž.; NOVAK, Z. Process for preparing particles or powders. WIPO Patent. WO 95/21688, 1995.
- WHO. **Safety of Medicines - A guide to detecting and reporting adverse drug reactions - Why health professionals need to take action**. Geneva: World Health Organization 2002.
- WISSING, S. A.; KAYSER, O.; MÜLLER, R. H. Solid lipid nanoparticles for parenteral drug delivery. **Advanced Drug Delivery Reviews** v. 56, p. 1257- 1272, 2004.
- WONG, H. L.; CHATTOPADHYAY, N.; WU, X. Y.; BENDAYAN, R. Nanotechnology applications for improved delivery of antiretroviral drugs to the brain. **Advanced Drug Delivery Reviews** v. 62, n. 4-5, p. 503-517, 2010.
- WU, J.;LI, Q.;WANG, X.;YU, S.;LI, L.;WU, X.;CHEN, Y.;ZHAO, J.;ZHAO, Y. Neuroprotection by curcumin in ischemic brain injury involves the Akt/Nrf2 pathway. **PLoS One**, v. 8, n. 3, p. e59843, 2013.
- XIE, S.;ZHU, L.;DONG, Z.;WANG, X.;WANG, Y.;LI, X.;ZHOU, W. Preparation, characterization and pharmacokinetics of enrofloxacin-loaded solid lipid nanoparticles: influences of fatty acids. **Colloids and Surfaces B: Biointerfaces** v. 83, n. 2, p. 382-387, 2011.
- YADAV, S. K.;SAH, A. K.;JHA, R. K.;SAH, P.;SHAH, D. K. Turmeric (curcumin) remedies gastroprotective action. **Pharmacognosy Reviews**, v. 7, n. 13, p. 42-46, 2013.
- YADAV, V. R.; SURESH, S.; DEVI, K.; YADAV, S. Novel formulation of solid lipid microparticles of curcumin for anti-angiogenic and anti-inflammatory activity for optimization of therapy of inflammatory bowel disease. **Journal of Pharmacy and Pharmacology**, v. 61, n. 3, p. 311-321, 2009.
- YALLAPU, M. M.; JAGGI, M.; CHAUHAN, S. C. Curcumin nanoformulations: a future nanomedicine for cancer. **Drug Discovery Today**, v. 17, n. 1-2, p. 71-80, 2012.

YEO, S.-D.; KIRAN, E. Formation of polymer particles with supercritical fluids: a review. **The Journal of Supercritical Fluids**, v. 34, p. 287-308, 2005.

YUN, J.;ZHANG, S.;SHEN, S.;CHEN, Z.;YAO, K.;CHEN, J. Continuous production of solid lipid nanoparticles by liquid flow-focusing and gas displacing method in microchannels. **Chemical Engineering Science**, v. 64, n. 19, p. 4115-4122, 2009.

ZAZHOGIN, A. P.; KOMYAK, A. I.; UMREIKO, D. S. Infrared spectra and structure of tetravalent uranium chloride nanoclusters in electron-donor solvents. **Journal of Applied Spectroscopy**, v. 75, n. 5, p. 735-738, 2008.

ZHANG, J.;WEI, H.;LIN, M.;CHEN, C.;WANG, C.;LIU, M. Curcumin protects against ischemic spinal cord injury: The pathway effect. **Neural Regeneration Research**, v. 8, n. 36, p. 3391-3400, 2013.

ZHANG, Q.; MO, Z.; LIU, X. Reducing effect of curcumin on expressions of TNF-alpha, IL-6 and IL-8 in rats with chronic nonbacterial prostatitis. **Zhonghua Bing Li Xue Za Zhi. Chinese Journal of Pathology**, v. 16, n. 1, p. 84-88, 2010.

ZHANG, S.-H.;SHEN, S.-C.;CHEN, Z.;YUN, J.-X.;YAO, K.-J.;CHEN, B.-B.;CHEN, J.-Z. Preparation of solid lipid nanoparticles in co-flowing microchannels. **Chemical Engineering Journal**, v. 144, n. 2, p. 324-328, 2008.

ZHANG, S.;YUN, J.;SHEN, S.;CHEN, Z.;YAO, K.;CHEN, J.;CHEN, B. Formation of solid lipid nanoparticles in a microchannel system with a cross-shaped junction. **Chemical Engineering Science**, v. 63, n. 23, p. 5600-5605, 2008.

ZHANG, X. G.;MIAO, J.;LI, M. W.;JIANG, S. P.;HU, F. Q.;DU, Y. Z. Solid lipid nanoparticles loading adefovir dipivoxil for antiviral therapy. **Journal of Zhejiang University Science B**, v. 9, n. 6, p. 506-510, 2008.

ZHAO, X.;XU, Y.;ZHAO, Q.;CHEN, C. R.;LIU, A. M.;HUANG, Z. L. Curcumin exerts antinociceptive effects in a mouse model of neuropathic pain: descending monoamine system and opioid receptors are differentially involved. **Neuropharmacology**, v. 62, n. 2, p. 843-854, 2012.

ZHU, L.;LAN, H.;HE, B.;HONG, W.;LI, J. Encapsulation of Menthol in Beeswax by a Supercritical Fluid Technique. **International Journal of Chemical Engineering**, v. 2010, n. 608680, p. 1-7, 2010.

Attachment I - Method Details

1 Particle Production

1.1 PGSS plant

Figure 29 depicts the scheme of the PGSS plant used in this work, which is installed in the Dipartimento di Principi e Impianti di Ingegneria Chimica at the University of Padova, Italy. Photos of the plant are presented in Figure 30. Prior to feed the plant, CO₂ is subcooled until 5 °C by a WKL 1200 chiller (Lauda, Würzburg, DE), and stored on a reservoir. CO₂ is pumped from this reservoir by a piston pump (DOXE Office Meccaniche Gallaratesi, Milan, IT) to feed the mix chamber and the secondary reservoir. At the same inlet pipeline, a pressure safety valve (V9) is mounted in order to prevent overpressure events. The secondary reservoir is a 73 cm³ cylinder made of AISI 316L stainless steel. The closure is assisted by two flanges externally screwed and the seal is performed by a neoprene gasket (OR 2125). The surge cylinder was designed to keep constant the pressure inside the mix chamber during the expansion step. The temperature is controlled by an on-off regulator connected to a heat tape wrapped around the reservoir.

The mix chamber is a 14 cm³ vertical cylinder made of AISI 316L stainless steel, in which the upper part was adapted to connect a magnetic stirrer, where the seal was performed by a neoprene gasket (OR 2118). Three connections are laterally placed at 120° from each other for connecting the CO₂ pipeline, the temperature probe and the manometer. At the bottom part of the mixer there is one connection for the exit of the CO₂ saturated material. All these connections are mounted to fit to double ferrule fittings NPT 1/8". The mixing in the mix chamber is performed by a magnetic stirrer, model MRK34 (Premex Reactor AG) that works at maximum temperature of 537 °C and maximum pressure of 200 bar. This stirrer is connected to a motor (Eurostar digital Kika Laboetecnik), which runs rotation cycles from 50 to 2000 rpm transmitted by a connection with a gum tube that absorbs the vibrations. The mix chamber is connected to the micronization unit by a needle valve (Swagelock, Lengnau, CH) (V14) that allow transferring the gas saturated mix to the expansion zone. V14 and the pipe where it is connected were maintained heated by the same heat tape.

In the micronization unit there is an atomization nozzle (Figure 31) made of stainless steel with 180 microns convergent-divergent orifice in sapphire and a spray angle of 20°, 1/8" NPT thread, n13 hexagonal head, suitable for maximum work pressure of 200 bar. This unit is maintained heated by ceramic cartridges inserted in cylindrical cavities placed 120° from each other. The gas saturated mass transferred from the mix chamber is submitted to a co-axial inlet of nitrogen (N₂) at high pressure in the micronization unit to improve the atomization of the mass,

which leads to the formation of submicron particles. Further, a low pressure stream of synthetic air is provided to generate a streamline flow upon the expansion chamber walls avoiding the adhesion of the fresh particles formed.

The expansion chamber is constituted by a plexiglass tube where the spray tower is produced. This tube was screwed to the divergent section of the harvest chamber made in PVC. In the harvest chamber a metallic filter is placed in order to retain the obtained particles. The metallic filter is accommodated in the cross section in the harvest chamber sealed by a neoprene gasket.

A design of a new nozzle was done based on the requirements of the plant. The technical design was assisted by the supplier (Gardella srl, Voghera, IT) as depicted in Figure 31.

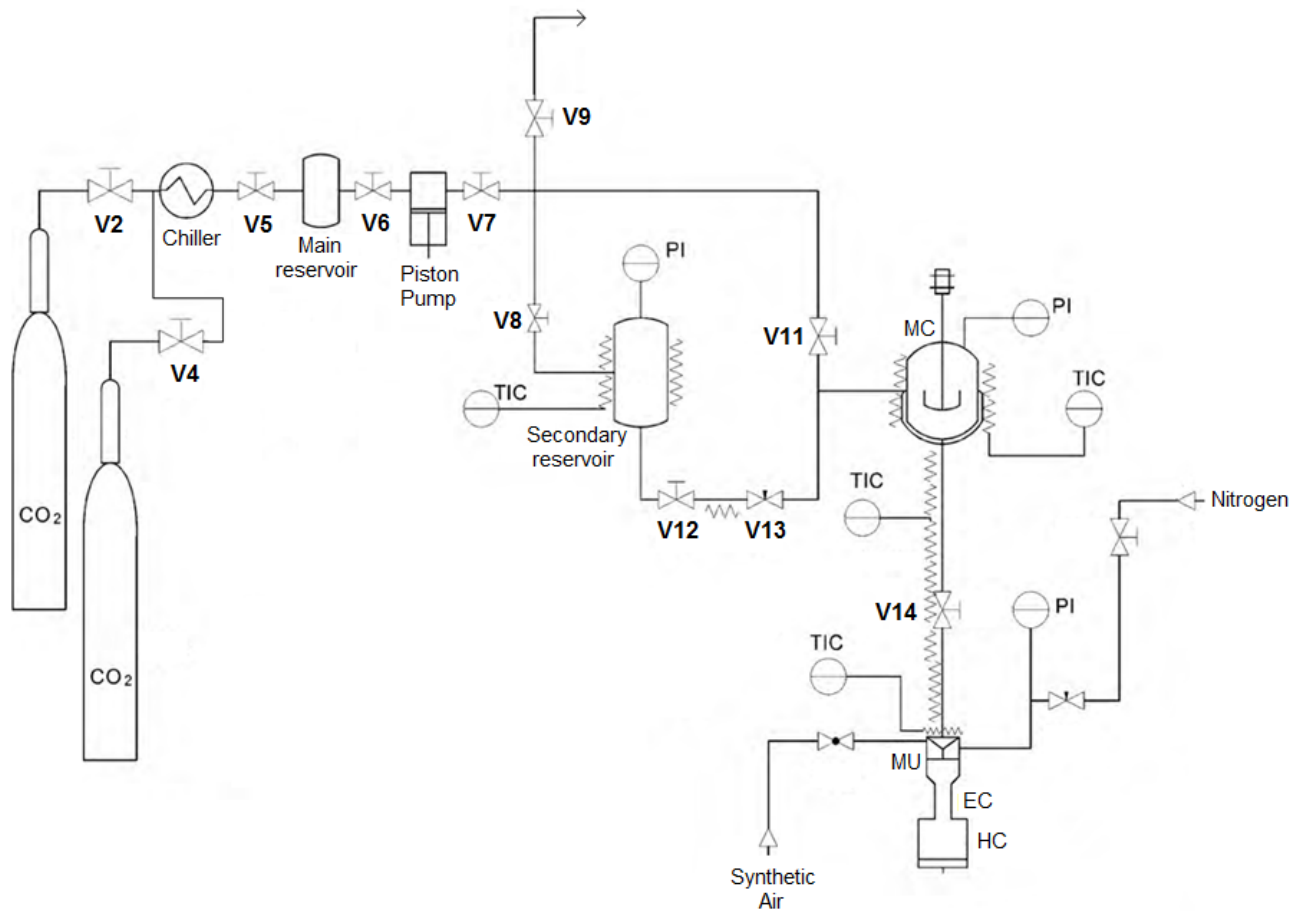


Figure 29. Scheme of PGSS plant used in this work. V2-V14 – valves; PI - Pressure Indicator; TIC – Temperature Indicator – Controller; MC – Mix Chamber; MU – Micronization Unit; EC – Expansion Chamber; HC – Harvest Unit.

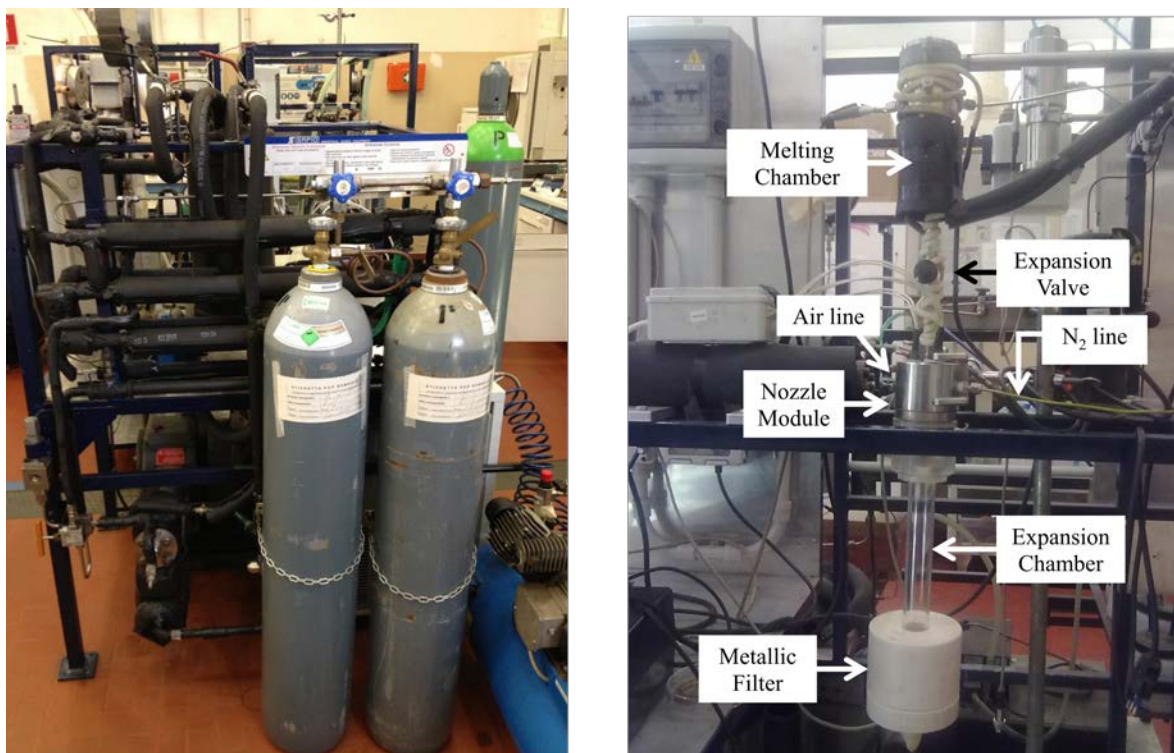


Figure 30. Photos of the PGSS plant used in this work.

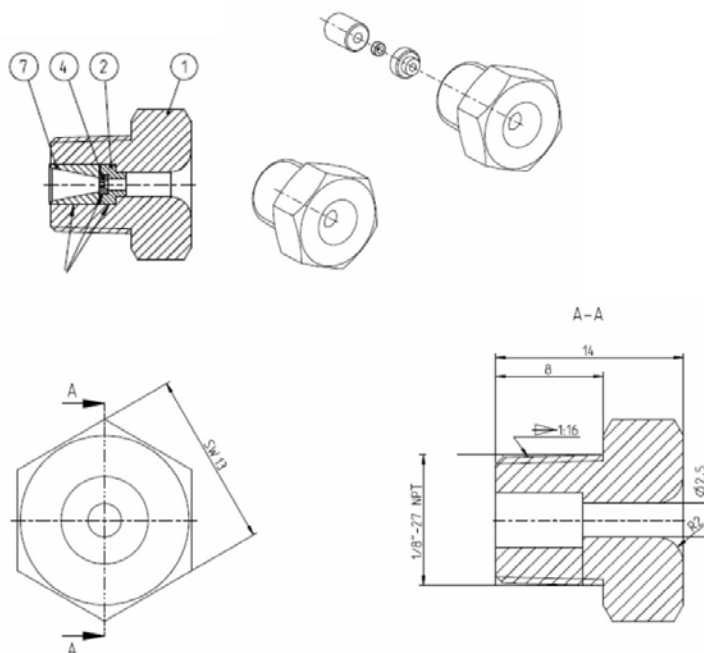


Figure 31. Scheme produced by Gardella srl. under instructions and supervision of customer.

1.2 Mixture preparation

In an amber glass flask, the Epikuron 200 was solubilized in dichloromethane with a ratio of 1.7:1 w/v. This solution was dispersed on melted tristearin at 80 °C. The lipid mixture was stirred under temperature until complete homogenization and expulsion of dichloromethane content. The temperature was decreased to 65 °C. The melted lipid was supplemented with a certain volume of a

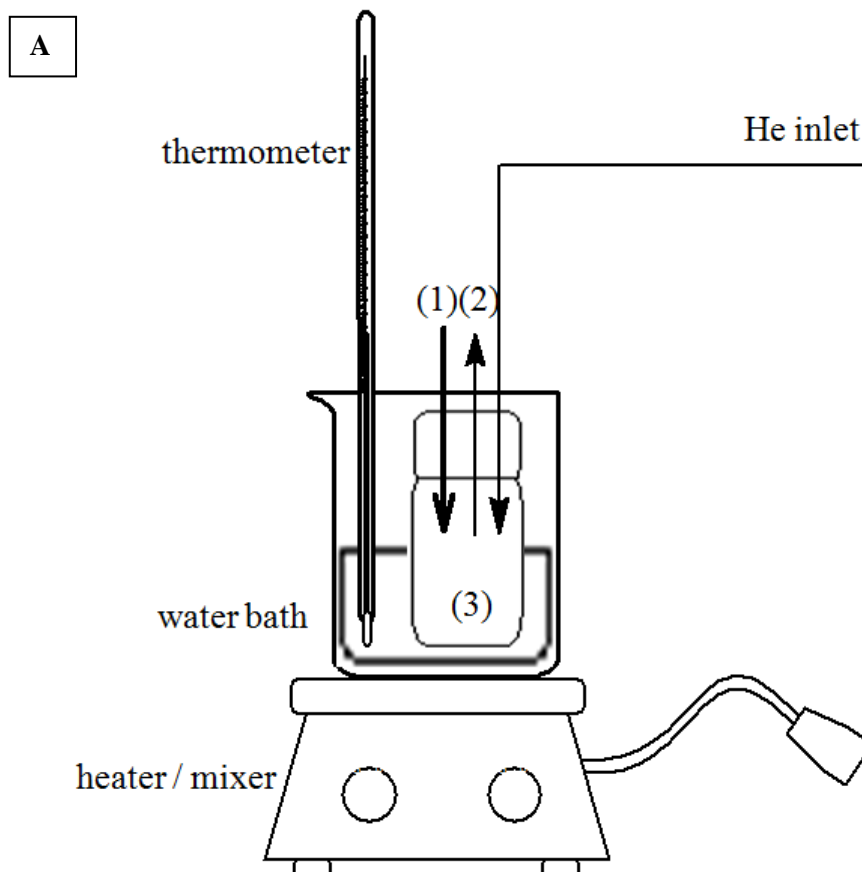
375 mg/mL curcumin solution in DMSO. The composition of the samples is listed on Table 10. The mixture was continuously stirred while the temperature was left to slowly decrease for solidification and subsequently left overnight at vacuum dryer. Further, to evaluate the influence of an inert atmosphere during mixture preparation, a system was assembled as depicted in Figure 32. In an amber glass flask fed by a helium stream continuously flowed through molten lipid mixture under constant stirring, the curcumin solution in DMSO was added by using a glass syringe.

The concentration of curcumin solution in DMSO was empirically chosen based on the achievement of a concentrated solution close to the curcumin solubility coefficient, which allowed working with as minimum as possible amount of DMSO. The lipid ratio between tristearin and phosphatidylcholine was selected according to the results on DSC studies. The initial ratio was chosen based on the results obtained in previous works and on the texture characteristics of the lipid mixture.

Table 10. Compositions tested

Tristearin	Epikuron 200	DMSO	Curcumin
49.5%	24.7%	17.5%	8.3%
54.2%	31.7%	9.6%	4.5%
57.6%	36.5%	4.0%	1.9%
58.7%	38.2%	2.1%	1.0%
59.4%	39.1%	1.0%	0.5%

Minimum load amount of plant reactor: 1.5g



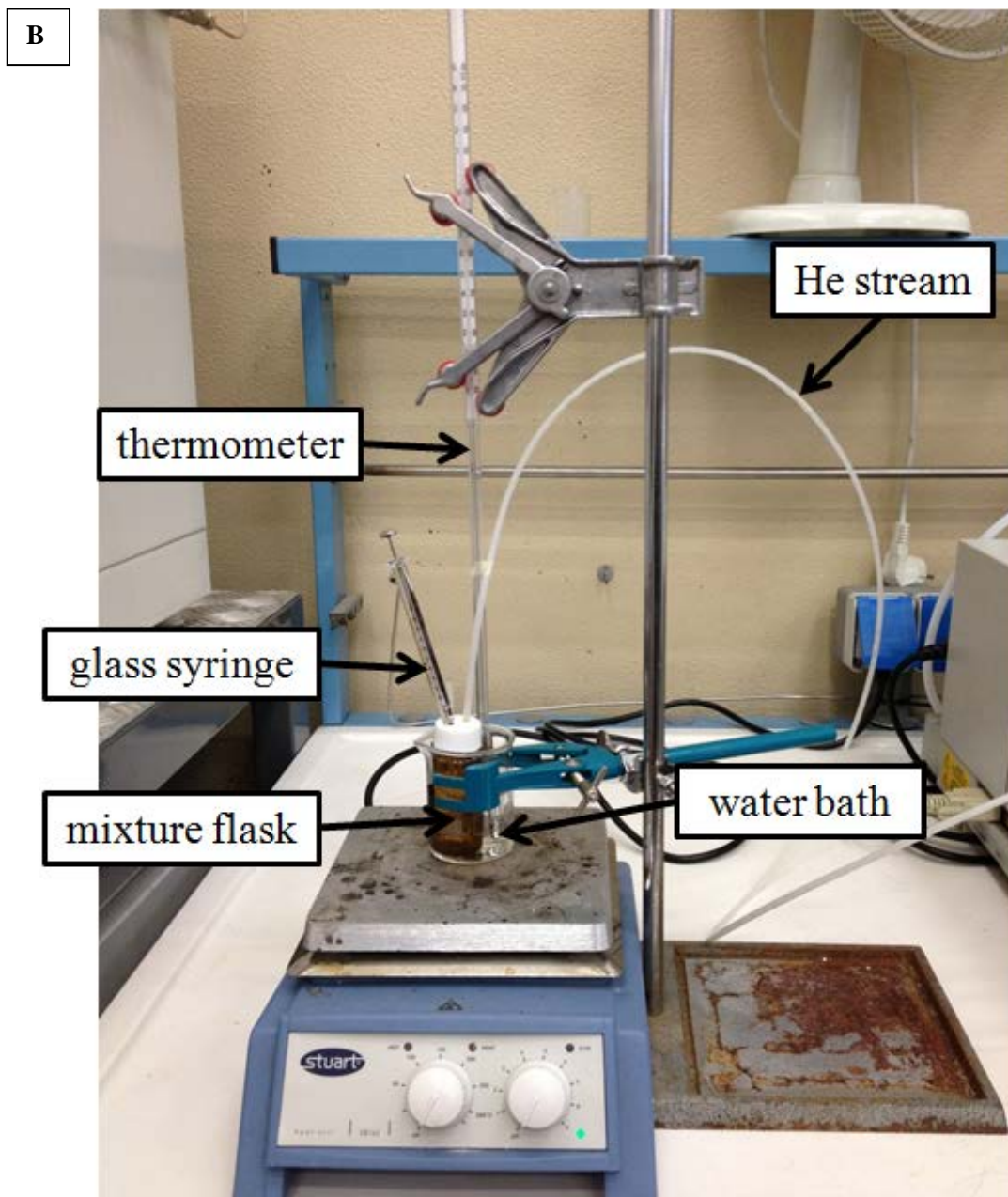


Figure 32. [A]: Scheme for mixture preparation under helium atmosphere - (1) curcumin solution inlet; (2) helium outlet; (3) molten lipid mixture / [B] Photo of the system.

1.3 Particle Production

1.5 g of the mixture was loaded into the mix chamber of the PGSS plant at an initial temperature of 75 °C. The system was pressurized with CO₂ to 150 bar and the temperature decreased to 55 °C. The expansion valve and the nozzle were always maintained 5 °C above the temperature of the mixer. After 30 min, the valve connecting the melting chamber with the collecting vessel was opened and the melted mass was sprayed into the precipitation chamber. Simultaneously, a N₂ flow at 140 bar and a synthetic air flow at 10 bar were co-axially injected. At the end of the run, the dry material was collected from the bottom of the precipitation vessel.

Attachment II - Publication List

1 Presented Conference Proceedings

A. Sao Pedro, S. Dalla Villa, P. Caliceti, S. Salmaso, E. Albuquerque, A. Bertucco. **Curcumin-loaded Lipid Particles produced by Supercritical Fluid Technology**. 6th International Symposium on High Pressure Processes Technology. September 8-11, 2013. Belgrade, Serbia.

Sao Pedro, A.; Dalla Villa, S.; Caliceti, P.; Salmaso, S.; Elvassore, N.; Serena, E.; Fialho, R.; Vieira de Melo, S.; Bertucco, A.; Cabral-Abuquerque, E. **Solid Lipid Nanoparticles Entrapping Curcumin by Supercritical Fluid Technology**. XXI International Conference on Bioencapsulation. August 28-30, 2013. Berlin, Germany.

T. P. P. Freire, A. São Pedro, R. Fialho, E. C. Albuquerque, G. M. Costa. **Modelagem de equilíbrio sólido-líquido envolvendo os lipídios: triestearina e fosfatidilcolina**. XIX Congresso Brasileiro de Engenharia Química. September 9-12, 2012, Búzios, Rio de Janeiro, Brazil.

2 Published journal articles

A. São Pedro, S. Dalla Villa, P. Caliceti, S.A.B. Vieira de Melo, E. Cabral Albuquerque, A. Bertucco, S. Salmaso. **Curcumin-loaded solid lipid particles by PGSS technology**. The Journal of Supercritical Fluids. 2016; 107: 534-541.

A. São Pedro, R. Fernandes, C. Flora Villarreal, R. Fialho, E. Cabral Albuquerque. **Opioid-based micro and nanoparticulate formulations: alternative approach on pain management**. Journal of Microencapsulation. 2016; 33: 18-29.

T. Freire, A. São Pedro, R. Fialho, E. C. Albuquerque, A. Bertucco, G. M. N. Costa. **Measurement and modelling of binary (solid + liquid + vapour) equilibria involving lipids and CO₂**. Journal of Chemical Thermodynamics. 2014; 69: 172-178.

I. Espírito Santo, A. São Pedro, R. Fialho, E. C. Albuquerque. **Supercritical formation of lipid nanoparticles for pharmaceutical application: a review**. Nanoscale Research Letters. 2013; 8: 1-17.